ADVANCES IN INORGANIC CHEMISTRY, VOL. 35

CHEMISTRY OF THIOETHER MACROCYCLIC COMPLEXES

ALEXANDER J. BLAKE and MARTIN SCHRÖDER

Department of Chemistry, University of Edinburgh, Edinburgh EH9 3JJ, Scotland

I. Introduction

In 1981, Murray and Hartley reviewed comprehensively the coordination chemistry of thioether ligands, R_2S (*149*). At that time, relatively few thioether complexes had been prepared compared to the mass of work reported on metal complexes of amines and phosphines. This reflected the general observation that thioethers are poor donors to transition metal ions. Thus, on going from R_3P to R_2S to RCl, the coordinative ability of these ligands to metal centers decreases. This can, in part, be related to the number of available lone pairs on the donor atom. Assuming one lone pair is donated to the metal ion, the number of remaining lone pairs on the donor atom is zero for $R_3P \rightarrow M$, one for $R_2S \rightarrow M$, and two for $RCl \rightarrow M$. Thus, the repulsive term between the lone pairs on the ligand and the metal-based electrons will increase in the order $R_3P \rightarrow M < R_2S \rightarrow M < RCl \rightarrow M$, leading to weaker complexes along this series (*149*).

Tertiary phosphines, R_3P, are generally regarded as good π-acceptor ligands. Thus, synergic bonding involving $P \rightarrow M$ σ-donation and $M \rightarrow P$ π-back-donation is the characteristic Dewar–Chatt model for phosphine binding to metal centers (*142, 143*). For thioethers, R_2S, however, an ambiguity exists. If one lone pair of R_2S is involved in σ-bonding to the metal center (assuming sp^3 hybridization at S), the second lone pair is then capable of π-donation to the metal (Fig. 1). In addition, the S-donor has empty *d* orbitals that may be of the correct symmetry and energy to act as π-acceptor orbitals. In principle, therefore, thioethers are capable of acting as π-acceptors or π-donors(*149*).

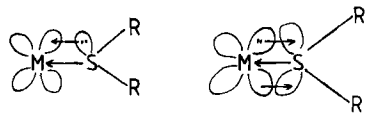

FIG. 1. Metal-thioether bonding assuming sp^3 hybridization at S.

Orpen and Connelly have suggested on the basis of structural evidence that back-donation into a P–X σ^*-orbital (X = substituent on P) is involved in M–P π-bonding (*154*). It remains to be seen whether a similar description of M–S(thioether) bonding is of relevance.

The coordination chemistry of thioether ligands has undergone a renaissance over the past 5 years. This has been primarily due to the observation that *cyclic* thioethers can bind to a range of transition metal ions to form stable metal complexes(*74, 188*). The properties of the M–S(thioether) bond can now be studied with a variety of metal centers, oxidation states, and coordination geometries. The use of cyclic thioether ligands to stabilize and study M–S(thioether) bonding is linked to the thermodynamic macrocyclic effect in which macrocyclic complexes are observed to be of greater stability than their open-chain analogues (*110*). The macrocyclic effect for certain thioether ligands is, however, much diminished (*140*) due to reorganizational energy considerations (*110*). For example, [14]aneS$_4$[1] and [18]aneS$_6$ adopt conformations as metal-free ligands in which the lone pairs of the S atoms are directed out of the ring (*86, 114, 224*). This leads to the formation of complexes in which the thioether donors bind *exo* to the ring, causing bridging between two metal fragments. Early examples of such binding include [Cl$_2$Hg([14]aneS$_4$)HgCl$_2$] (*6, 7*) and [Cl$_5$Nb([14]aneS$_4$)NbCl$_5$] (*85*). The latter is a remarkable example of a thioether ligand bound to a genuinely high-valent, early transition metal center. The formation of *endo* complexes of [14]aneS$_4$ therefore requires reorganization of the metal-free cyclic ligand from an *exo* to an *endo* conformation as observed for the complex [Ni([14]aneS$_4$)]$^{2+}$ (*82, 110, 182, 183*). In contrast, the trithia crown [9]aneS$_3$ requires no such reorganization for facial binding to metal ions; this ligand is preorganized for facial coordination to a metal center(*102, 110*). This, in part, explains the massive current interest in the coordination chemistry of [9]aneS$_3$ and in its N-donor analogues [9]aneN$_3$ and Me$_3$-[9]aneN$_3$ (*67*).

Another impetus for the study of the coordination chemistry of crown thioethers stems from the role of thioether binding in biological systems such as *d*-biotin (involving tetrahydrothiophene) (*145, 208*) and blue copper proteins such as plastocyanin and azurin (involving methionine) (*4, 13, 73, 109, 124, 185*). The binding of Cu(II) and Cu(I) centers to macrocyclic thioethers has led to a greater understanding of Cu–S(thioether) interactions and the stereochemical preferences of these metal centers (*91, 95, 99, 121, 180, 181*).

[1] See list of abbreviations at the end of this chapter.

The binding of cyclic thioethers to metal centers has also led to the isolation of complexes in which the coordinative properties of the ligand do not fit the stereochemical preferences of the metal ion(s) (*188*). Thus, a series of macrocyclic thioether complexes incorporating unusual stereochemistries and/or oxidation states has been generated (*188*). This is linked to the biological activity of the blue copper proteins and model systems in which the coordination geometry about Cu(II) is strained [in an entatic state (*212, 221*)] such that the Cu(II)/(I) couple occurs at a particularly positive potential; that is, the Cu(I) state is stabilized. The ability of cyclic thioethers to modify their coordination properties is inherent in this approach (*76, 108, 111*).

The parallel between the binding of soft, transition metal ions by soft, cyclic thioether ligands and the binding of hard, main-group metal ions (Group IA and IIA) by hard, cyclic oxyether ligands is striking. The Edinburgh group entered the area of thioether coordination chemistry as a route to the synthesis of macrocyclic complexes of the platinum group metal ions, and many of the late second- and third-row metal ions form very stable complexes with a range of thioether crowns (*16, 188*). Interestingly, [9]aneS_3 and its N-donor analogue [9]aneN_3 have quite similar ligand-field strengths, as measured by values of $10Dq$. However, values for the Racah parameter B differ substantially, indicating greater covalency in M–S bonds with [9]aneS_3 compared to M–N bonds with [9]aneN_3 (*175*). This leads to the formation of *low-spin* metal complexes of the first-row transition series with [9]aneS_3 (*219*). A comparative analysis of [9]aneS_3, [9]aneN_3, and [9]aneN_2O using the angular overlap model has been reported (*175*).

The aim of this chapter is to summarize critically the coordination chemistry of homoleptic thioether macrocycles, with emphasis on likely future developments and uses. The chemistry of mixed-donor ligands is not included. The literature is reviewed up to mid-1989 with particular emphasis on the literature since 1980. Some unpublished results, mainly crystallographic data from our own laboratories, are included. Recent reviews on aspects of thioether chemistry include those by Murray and Hartley (*149*), Kuehn and Isied (*125*), Cooper (*74*), Schröder (*188*), and Müller and Diemann (*148*).

II. Synthesis of Ligands

The high-yield syntheses of macrocyclic polyoxoethers are characterized by the strong template effects that arise from oxygen coordination by alkali metal ions during cyclization of polyoxo units (*96, 106, 157,*

158, 159, 160, 161, 162, 168, 214). The low affinity of sulfur for alkali metal ions, however, renders template effects of less consequence in the synthesis of polythia macrocycles. Thus, the competition between cyclization and linear polymerization is more statistically defined, with cyclization kinetically favored only at high dilution (*64, 65, 66*). Consequently, most of the synthetic methods for the synthesis of polythia rings involve high-dilution techniques coupled with relatively long reaction times. Historically, the study of the coordination chemistry of macrocyclic thioethers has been hindered by difficulties in the synthesis of the free ligands. The synthesis of [9]aneS_3, first reported by Ochrymowycz and co-workers in 1977 (*101*), illustrates this well.

Reaction of the disodium salt of 3-thiapentane-1,5-dithiolate with 1,2-dichloroethane (Scheme 1) gave an isolated yield of [9]aneS_3 of only 0.04% (*101*). Glass and co-workers improved the yield to 4.4% by using the benzyltrimethylammonium salt of the dithiolate instead of disodium salt and by performing the reaction under high-dilution conditions (*198*). Although the yield of [9]aneS_3 was still very low, a byproduct of the latter route proved to be the 2 + 2 addition product, [18]aneS_6, in up to 32% yield (*33*). It was not until 1984 that a high-yield synthesis of [9]aneS_3 was reported. Sellmann and Zapf utilized the $Mo(CO)_3$ fragment as a template around which cyclization of the open-chain dithiolate and 1,2-dibromoethane could be achieved (Scheme 2) (*194, 195*). This methodology inhibits the formation of larger ring macrocycles and polymers to give the 1 + 1 condensation product, [9]aneS_3,

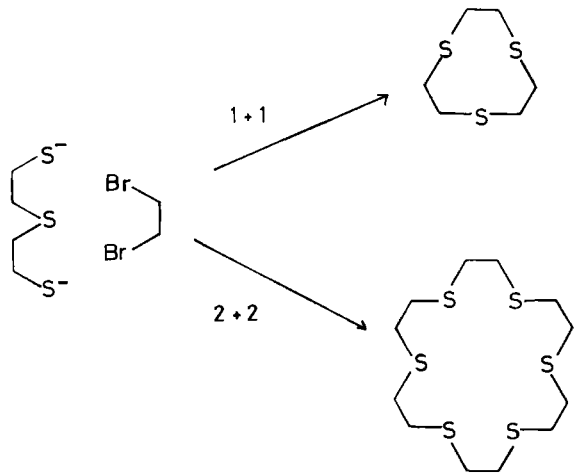

SCHEME 1

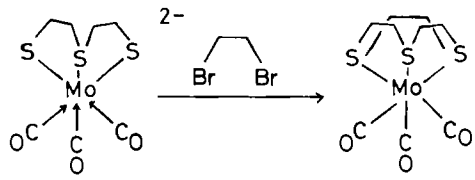

SCHEME 2

in more than 60% yield. Significantly, this synthetic route is simple and reproducible, and can be made catalytic in terms of Mo. More recently, Blower and Cooper have reported a large-scale synthesis of [9]aneS_3 in 50% yield (*54*), which makes use of the Cs_2CO_3-mediated cyclization of thioether macrocycles in dimethylformamide (DMF) first reported by Buter and Kellog (*62, 63*).

Interestingly, a synthesis of [12]aneS_3 in 3% yield was reported by Rosen and Busch as early as 1970 (*184*). This route involved reaction of 1,3-dibromopropane with the dianion of 1,5,9-trithianonane. However, using the Cs_2CO_3/DMF cyclization route, a range of thioether macrocycles of various donacities and ring sizes can now be prepared in good yields (*223*). An alternative route to cyclic sulfides has been developed via hydrolysis of thiouronium salts (*78*).

The syntheses of [12]aneS_4, [13]aneS_4, and [14]aneS_4 were first reported by Rosen and Busch (*182, 183, 184;* see also *107*); Black and McLean (*21, 22*) reported the synthesis of [18]aneS_6 using the procedure first developed by Reid and co-workers (*146, 211*). This latter procedure involves the condensation of dithiolate with the corresponding dibromoalkane (Scheme 3). In 1974 Ochrymowycz and co-workers described the synthesis of 19 S_2-, S_4-, S_5-, and S_6-donor macrocyclic compounds in low to moderate yields (Scheme 4) (*151*). Although the route involved the use of mustard gas or its derivatives, this was an important breakthrough in the synthesis of polythia macrocycles.

By combining the procedures of Ochrymowycz and co-workers (*151*) with the high-dilution Cs_2CO_3/DMF cyclization developed later by

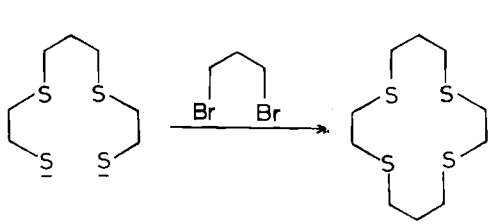

SCHEME 3

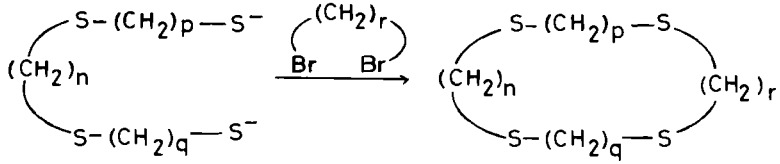

SCHEME 4

Buter and Kellogg (*62, 63*), large-scale synthesis of thioether macrocycles can now be achieved in good yields (*177, 223, 224, 226*). Octathia S_8-donor macrocycles have been synthesized as 2 + 2 products from the cyclization reactions employed to form tetrathia S_4-donor ligands (*59, 61, 83, 147, 209*).

The separation of thioether macrocycles using high-performance liquid chromatography has been reported (*69*). The ligands [9]aneS_3, [12]aneS_4, [14]aneS_4, [16]aneS_4, [15]aneS_5, [18]aneS_6, [24]aneS_8, and [28]aneS_8 are now readily available from commercial suppliers, reflecting the ease of their synthesis and the interest now shown in their chemical and coordinative properties.

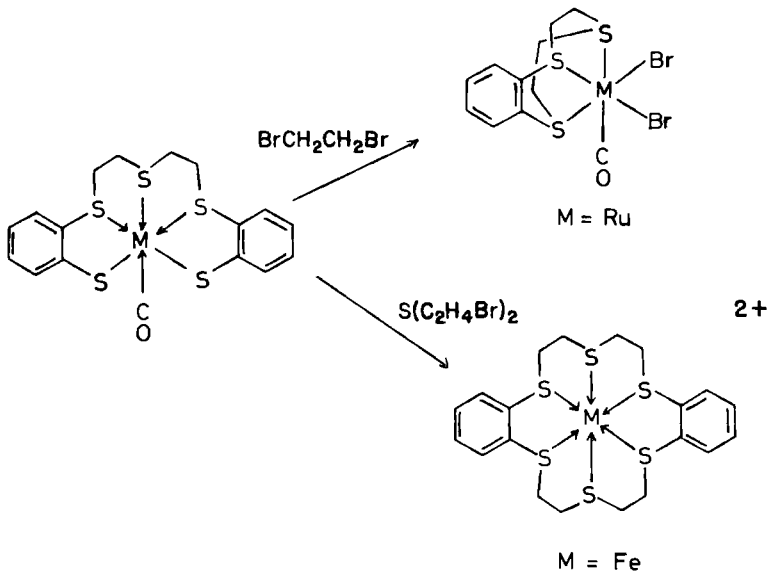

SCHEME 5

A range of mixed-donor thia macrocycles have also been prepared using related techniques (*5, 57, 58, 59, 60, 62, 63, 93, 123, 150, 213*); water-soluble thioether macrocycles incorporating hydroxy-groups on the carbon back-bone have also been reported (*163*).

Sellmann and co-workers have extended their work on the template synthesis of [9]aneS$_3$ and related open-chain thioether ligands at a Mo(CO)$_3$ fragment (*194, 195, 196*) to the template synthesis of Bz$_2$[18]aneS$_6$ and Bz[9]aneS$_3$ about [Fe^{II}(CO)] (*191, 192*) and [Ru^{II}(CO)] (*193*) fragments, respectively (Scheme 5).

Mass spectroscopic (*136, 191*) and ^{13}C NMR spectroscopic (*83*) studies on thioether macrocyclic ligands and related open-chain systems have been reported. The synthesis of thioether macrocyclic compounds incorporating the cycloheptatriene and tropylium ion moieties has been described (*152*).

Very recently, a series of thioether macrocycles containing the thiophene unit was synthesized by Lucas and co-workers (Fig. 2) (*137, 138, 139*).

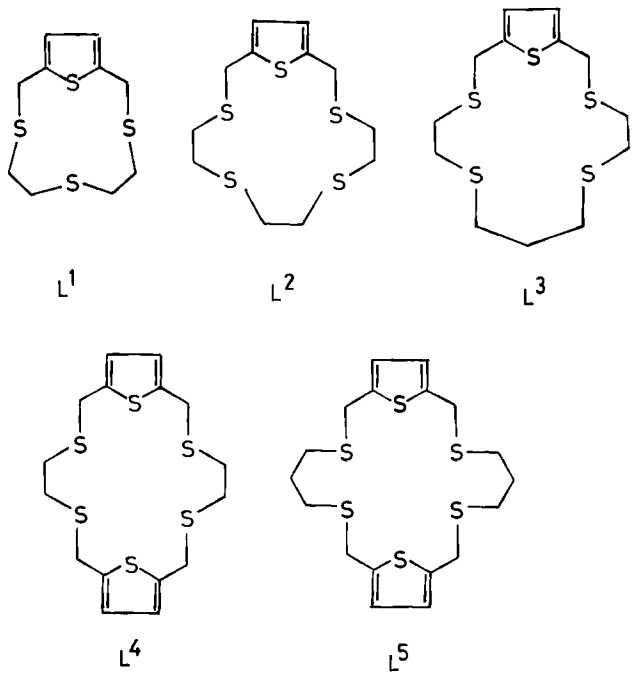

FIG. 2. Thioether macrocycles containing the thiophene unit.

III. [9]aneS$_3$ and Related Trithia Ligands

A. Free Ligands

The single-crystal X-ray structure of [9]aneS$_3$ reported by Glass and co-workers shows (Fig. 3) the compound adopting a [333] (*80*) *endo* conformation (C_3 symmetry) with the S-atoms directed towards the centre of the macrocyclic ring, C–S = 1.820(5), 1.823(5) Å and C–C = 1.510(6) Å (*102*). The transannular S···S distance of 3.451(2) Å is less than 3.70 Å, the sum of the van der Waals radii for S (*156*).

Interestingly, [9]aneO$_3$ adopts an unsymmetrical [234] conformation (*56*). The solid state structure of [9]aneS$_3$ contrasts with those of other polythioether macrocyclic molecules, which generally adopt *exo* conformations with the S-donors pointing out of the macrocyclic cavity (*81, 86, 224*). [9]aneS$_3$ is therefore a unique thioether crown because it is preorganized for facial coordination to metal ion centers; thus, rearrangement from an *exo* to an *endo* conformation as observed in the coordination chemistry of tetra-, penta-, and hexathia crowns (*87, 122, 224*) is not a general feature of the coordination chemistry of [9]aneS$_3$. Conformational analysis of [9]aneS$_3$ using photoelectron spectroscopy suggests retention of the [333] conformation in the gas phase (*197*). Cyclic voltammetry of [9]aneS$_3$ in CH_3CN shows an irreversible oxidation at E_{pa} = +0.99 V vs. Fc^+/Fc to give sulfonium and sulfoxide species (*219*); a return wave is observed at E_{pc} = −0.55 V vs. Fc^+/Fc and is assigned to reduction of the oxidation product rather than of [9]aneS$_3$ itself (*53, 219*). Very recently, the oxidation product of [9]aneS$_3$ was characterized as a bicyclic sulfonium cation (Fig. 4) formed via transannular S–C bond formation and C–H bond cleavage. The resulting bicyclic compound incorporates fused five- and six-membered rings, which leads to the relative stability of this species (*48*).

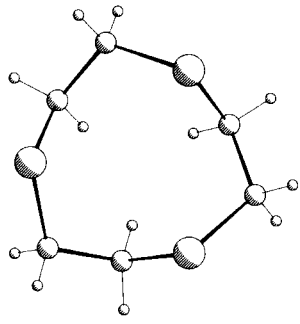

FIG. 3. [9]aneS$_3$.

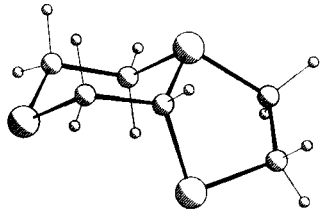

FIG. 4. Bicyclic sulfonium cation formed by oxidation of [9]aneS_3.

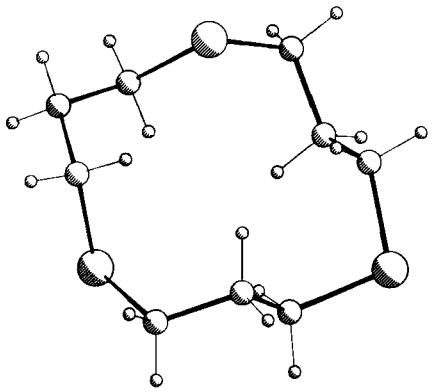

FIG. 5. [12]aneS_3.

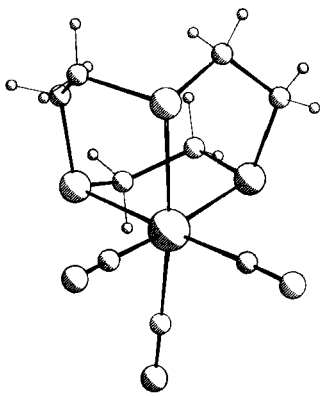

FIG. 6. [$Mo(CO)_3$([9]aneS_3)].

The single-crystal X-ray structure of [12]aneS$_3$ (Fig. 5) shows the molecule to adopt a square conformation similar to that of cyclododecane (*97*) and [12]aneS$_4$ (*178, 224*), with one S atom at a corner and two in side positions (*169*). Four of the six C–S bonds and four of the six C–C bonds in [12]aneS$_3$ lie in gauche placements (*169*).

B. Chromium, Molybdenum, and Tungsten

Reaction of $[Cr(OH_2)_6]Cl_3$ with [9]aneS$_3$ affords $[CrCl_3([9]aneS_3)]$, which can be converted to $[Cr(OSO_2CF_3)_3([9]aneS_3)]$ on treatment with CF_3SO_3H (*126*). Interestingly, reactions of simple Cr(III) salts with two molar equivalents of [9]aneS$_3$ in solution failed to give the bis-sandwich species $[Cr([9]aneS_3)_2]^{3+}$. However, this complex could be prepared by heating solid $[Cr(OH_2)_6](ClO_3)_3$ with solid [9]aneS$_3$. The resultant pink product $[Cr([9]aneS_3)_2](ClO_4)_3$ is highly explosive in the solid state and decomposes in solution. The bonding of [9]aneS$_3$ to Cr(III) is, therefore, weak with a small ligand-field splitting. This can be rationalized in terms of the lack of π-donacity of the hard Cr(III) center to the soft thioether ligands (*126*). The binding of hard metal ions such as Ti(IV) to thioether ligands has been described (*153*).

The template synthesis of [9]aneS$_3$ at a $Mo(CO)_3$ fragment has been reported (*194, 195*) (see Section II, Scheme 2). The single-crystal X-ray structure of $[Mo(CO)_3([9]aneS_3)]$ (Fig. 6) shows facial coordination of [9]aneS$_3$ to the Mo(0) center: Mo–S = 2.512(6), 2.504(6), 2.543(7) Å; Mo–C = 1.94(2), 1.97(2), 1.93(2) Å (*10*). The S–C–C–S torsion angle in $[Mo(CO)_3([9]aneS_3)]$ is 48° (*10*) compared to a value of 58° in metal-free [9]aneS$_3$ (*102*). The reduction in this torsion angle has been ascribed to a decrease in S···S lone-pair repulsions on formation of M–S bonds (*10*).

A structural comparison between $[Mo(CO)_3([9]aneS_3)]$ and $[Mo(CO)_3(L)]$ (L = 2,5,8-trithianonane) indicates that the sulfur-donor orbitals are more favorably directed toward the metal center in the latter, acyclic complex (*9*). Reaction of $[MoCl_3(THF)_3]$ with [9]aneS$_3$ affords $[MoCl_3([9]aneS_3)]$ in high yield as a red/brown product (*195*). Oxidation of $[Mo(CO)_3([9]aneS_3)]$ with 30% H_2O_2 affords the metal-free hexaoxide of [9]aneS$_3$, 1,4,7-trithiacyclononane-1,1,4,4,7,7-hexaoxide (*129*). This compound was prepared previously by direct oxidation of [9]aneS$_3$ with MnO_4^- under acidic conditions (*174*).

Reaction of the Mo(II) dimer $[(CH_3CN)_3Mo(OAc)_2Mo(NCCH_3)_3]^{2+}$ with [9]aneS$_3$ leads to replacement of the coordinated CH_3CN ligands to give $[([9]aneS_3)Mo(OAc)_2Mo(NCCH_3)_3]^{2+}$ and $[([9]aneS_3)MO(OAc)_2Mo([9]aneS_3)]^{2+}$ (*126*). Reaction of $[([9]aneS_3)Mo(OAc)_2Mo(NCCH_3)_3]^{2+}$ with L affords the neutral species

[([9]aneS$_3$)Mo(OAc)$_2$Mo(L)$_3$] (L = SCN, OCN, Cl, Br) (*126*).

No complexes of [9]aneS$_3$ with W have been reported, although it seems likely that [W(CO)$_3$([9]aneS$_3$)] and [WCl$_3$([9]aneS$_3$)] might be prepared by similar routes to their Mo analogues.

C. Manganese and Rhenium

Reaction of [MnX(CO)$_5$] with [9]aneS$_3$ affords the complexes [Mn(CO)$_3$([9]aneS$_3$)]X (X = Cl, Br, I) (*98*). The kinetics of this reaction were found to be zero-order in [9]aneS$_3$; a limiting dissociative mechanism in which loss of a CO ligand *cis* to X in [MnX(CO)$_5$] was proposed as the rate-determining step. Activation parameters for these ligand substitution reactions have been measured. The single-crystal X-ray structure of [Mn(CO)$_3$([9]aneS$_3$)]$^+$ shows [9]aneS$_3$ bound facially to the Mn(I) center with Mn–S = 2.321(3), 2.338(5) Å; Mn–C = 1.810(10) Å (*98*). Treatment of [Mn(CO)$_3$([9]aneS$_3$)]$^+$ with N_2H_4 gives [Mn(NCO)(CO)$_2$([9]aneS$_3$)], which reacts with HCl to afford [MnCl(CO)$_2$([9]aneS$_3$)] and reacts with $NOBF_4$ to give [Mn(CO)$_2$(OH$_2$)([9]aneS$_3$)]$^+$ (*98*). Similar reactivity of [MnBr(CO)$_5$] with the N-donor ligands [9]aneN$_3$ and Me$_3$[9]aneN$_3$ to afford [Mn(CO)$_3$([9]aneN$_3$)]Br and [Mn(CO)$_3$(Me$_3$[9]aneN$_3$)]Br, respectively, has been reported (*164*).

Reaction of [ReBr(CO)$_5$] with [9]aneS$_3$ yields [Re(CO)$_3$([9]aneS$_3$)]Br as a white, air-stable product (*164*). The single-crystal X-ray structure of the complex confirms a stereochemistry similar to that observed for the Mn(I) analogue, with facial binding of [9]aneS$_3$ and mutually *cis* CO ligands, Re–S = 2.459(3), 2.461(3), 2.466(3) Å (*164*). The IR spectrum of [Re(CO)$_3$([9]aneS$_3$)]Br shows C≡O stretching-vibrations, ν_{CO}, at 2010 and 1940 cm^{-1}, compared to values of 2000 and 1870 cm^{-1} for [Re(CO)$_3$([9]aneN$_3$)]Br. Since [9]aneN$_3$ would not be expected to show significant π-interactions with metal centers, these data suggest that the thioether donors in [Re(CO)$_3$([9]aneS$_3$)]Br are acting as π-acceptor ligands. This is supported by crystallographic evidence that shows the average Re–C distances in [Re(CO)$_3$([9]aneS$_3$)]$^+$ to be 0.025 Å longer than in [Re(CO)$_3$([9]aneN$_3$)]$^+$ (*164*).

No complexes of [9]aneS$_3$ with Tc have been reported. Thioether complexes of Tc may have uses in radiopharmaceutical applications and would complement the chemistry of Tc-phosphine complexes (*90*).

D. Iron, Ruthenium, and Osmium

Reaction of [Fe(OH$_2$)$_6$](ClO$_4$)$_2$ or FeCl$_2$·4H$_2$O with two molar equivalents of [9]aneS$_3$ in refluxing CH$_3$OH affords the bis-sandwich complex

$[Fe([9]aneS_3)_2]^{2+}$ as a purple product (*219*). This complex is a low-spin Fe(II) species with $10Dq = 20{,}670\ cm^{-1}$ and $B = 387\ cm^{-1}$ (*219*); for $[Fe([9]aneN_3)_2]^{2+}$ $10Dq = 18{,}940\ cm^{-1}$ and $B = 575\ cm^{-1}$ (*55, 219, 220*). The single-crystal X-ray structure of $[Fe([9]aneS_3)_2]^{2+}$ shows hexathia coordination to Fe(II) with facial binding of both $[9]aneS_3$ ligands, Fe–S = 2.241(1), 2.251(1), 2.259(1) Å (*219*).

The complex $[Fe([9]aneS_3)_2]^{2+}$ shows a reversible one-electron oxidation at $E_{1/2} = +0.98$ V vs. Fc^+/Fc in CH_3CN assigned to an Fe(II)/(III) couple (*219*). Chemical oxidation of $[Fe([9]aneS_3)_2]^{2+}$ with PbO_2 in 1 M H_2SO_4 affords the green Fe(III) species $[Fe([9]aneS_3)_2]^{3+}$, which is stable for ca. 5 min at pH 6 and for ca. 1 h at pH 1 (*129*). This unstable complex has been characterized by electronic and Mössbauer spectroscopy as a low-spin Fe(III) species. Enhanced stability of the 3+ cation was noted in concentrated acidic solutions (*31*) and crystals of the unstable $[Fe([9]aneS_3)_2]^{3+}$ were obtained from concentrated aqueous $HClO_4$. The single-crystal X-ray structure of $[Fe([9]aneS_3)_2]^{3+}$ (Fig. 7) shows a centrosymmetric cation with Fe–S = 2.280(3), 2.2846(25), 2.276(3) Å (*43*). Significantly, the Fe–S bond lengths in $[Fe([9]aneS_3)_2]^{3+}$ are *longer* than those for $[Fe([9]aneS_3)_2]^{2+}$, giving clear structural evidence for the π-acidity of the thioether donors in the 2+ complex. The stabilization of high-valent cationic complexes of $[9]aneS_3$ under highly acidic conditions is attributed to the inhibition of deprotonation and ring-opening reactions of coordinated thioethers (*39*) (see

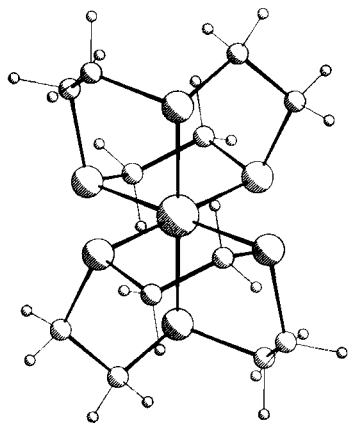

FIG. 7. $[Fe([9]aneS_3)_2]^{3+}$.

Section III, E). $[Fe([9]aneS_3)_2]^{3+}$ is a strong one-electron oxidant that oxidizes Cl^- to Cl_2 and H_2O_2 to O_2 [Eq. (1) and (2)] (*129*).

$$2[Fe([9]aneS_3)_2]^{3+} + 2Cl^- \rightarrow Cl_2 + 2[Fe([9]aneS_3)_2]^{2+} \quad (1)$$

$$2[Fe([9]aneS_3)_2]^{3+} + H_2O_2 \rightarrow O_2 + 2[Fe([9]aneS_3)_2]^{2+} + 2H^+ \quad (2)$$

Oxidation of $[Fe([9]aneS_3)_2]^{2+}$ with $Na_2S_2O_8$ in aqueous solution affords an orange Fe(II) complex in which one of the coordinated S-donors has been oxidized to a sulfoxide (*129*). The single-crystal X-ray structure of $[Fe([9]aneS_3)([9]aneS_2(SO))]^{2+}$ (Fig. 8) shows Fe(II) coordinated to six S-donors. The average Fe–S(thioether) bond length of 2.258(1) Å is similar to that observed for $[Fe([9]aneS_3)_2]^{2+}$ [2.246(1) Å], whereas the Fe–S(sulfoxide) bond is shortened to 2.207(1) Å, S–O = 1.498(7) Å (*129*). The S = O stretching vibration, ν_{SO}, is observed at 1090 cm^{-1}, while COSY ^1H NMR spectroscopic data are consistent with the solid state structure. Thus, depending on the oxidant used, metal- or ligand-based oxidation of $[Fe([9]aneS_3)_2]^{2+}$ is observed (*129*).

Reaction of $[Fe(C_5H_5)I(CO)_2]$ with one molar equivalent of $[9]aneS_3$ affords the mixed-sandwich complex $[Fe(C_5H_5)([9]aneS_3)]^+$, the single-crystal X-ray structure of which shows (Fig. 9) facial binding of both the carbocyclic cyclopentadienyl ligand, Fe–C = 2.007(12)–2.112(12) Å, and the thioether macrocycle, Fe–S = 2.2100(18), 2.2053(19), 2.2078(19) Å (*24*). $[Fe(C_5H_5)([9]aneS_3)]^+$ shows a reversible Fe(II)/(III) couple at $E_{1/2}$ = +0.44 V vs. Fc^+/Fc in CH_3CN (*24*).

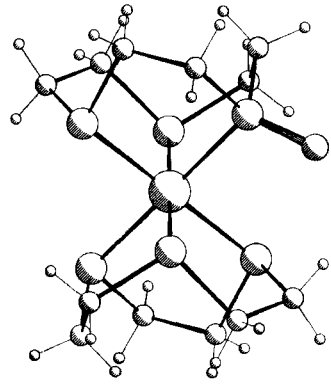

FIG. 8. $[Fe([9]aneS_3)([9]aneS_2(SO))]^{2+}$.

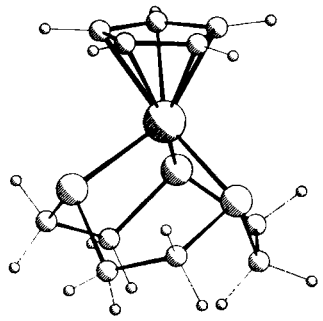

FIG. 9. $[Fe(C_5H_5)([9]aneS_3)]^+$.

Reaction of $[RuCl_2(arene)]_2$ (arene = 4-$MeC_6H_4{}^iPr$, C_6Me_6, C_6H_6) with two molar equivalents of [9]$aneS_3$ or [12]$aneS_3$ affords the homoleptic thioether complexes $[Ru([9]aneS_3)_2]^{2+}$ (Fig. 10) (*18, 170, 172*) and $[Ru([12]aneS_3)_2]^{2+}$ (Fig. 11) (*170, 172*), respectively. The Ru–S distances of 2.3272(14), 2.3357(14), 2.3331(14) Å for $[Ru([9]aneS_3)_2]^{2+}$ (*18*) are on average 0.03 Å shorter than those of 2.3676(4), 2.3772(4), 2.3736(4) Å for $[Ru([12]aneS_3)_2]^{2+}$ (*172*). These complexes can be prepared directly from $RuCl_3$ by reaction with [9]$aneS_3$ or [12]$aneS_3$ in Me_2SO (*18*). Interestingly, the crystal structure of $[Ru([9]aneS_3)_2](BPh_4)_2$ includes two molecules of Me_2SO per Ru cation; the O-atoms of the Me_2SO molecules approach the outer faces of the coordinated [9]$aneS_3$ ligands and interact with their methylene H-atoms (O···H = 2.201(8), 2.419(8), 2.790(8), 3.291(8) Å) (Fig. 12) (*18*).

$[Ru([9]aneS_3)_2]^{2+}$ shows a one-electron oxidation at particularly anodic potential, $E_{1/2}$ = +1.4 V vs. Fc^+/Fc. The redox stability of $[Ru([9]aneS_3)_2]^{2+}$ is remarkable and reflects the matching of the electronic and stereochemical preferences of d^6 Ru(II) with the soft, facially binding tridentate crown (*18*). Interestingly, oxidation of $[Ru([9]aneS_3)_2]^{2+}$ occurs at a potential that is 0.33 V more anodic than for $[Ru([12]aneS_3)_2]^{2+}$, reflecting the tighter fit of [9]$aneS_3$ with Ru(II) (*74, 172*). For $[Ru([9]aneS_3)_2]^{2+}$, $10Dq$ = 30,760 cm^{-1} and B = 291 cm^{-1}; for $[Ru([12]aneS_3)_2]^{2+}$ $10Dq$ = 29,570 cm^{-1} and B = 207 cm^{-1} (*172*). The synthesis of $[Ru([10]aneS_3)_2]^{2+}$ has also been reported (*172*).

Reaction of $[RuCl_2(C_6Me_6)]_2$ with one molar equivalent of [9]$aneS_3$ affords the mixed-sandwich species $[Ru(C_6Me_6)([9]aneS_3)]^{2+}$ (*14, 19, 188*); reaction of $[RuCl_2(arene)]_2$ (arene = C_6H_6, 4–$MeC_6H_4{}^iPr$) with one molar equivalent of [9]$aneS_3$, however, tends to form the bis sandwich complex $[Ru([9]aneS_3)_2]^{2+}$ together with unreacted Ru(II) starting material (*14*).

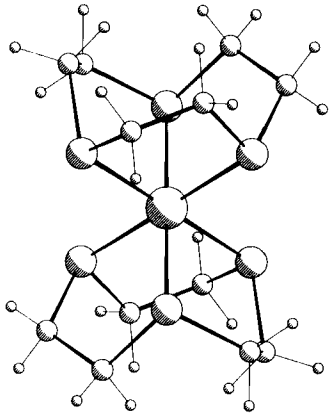

FIG. 10. $[Ru([9]aneS_3)_2]^{2+}$.

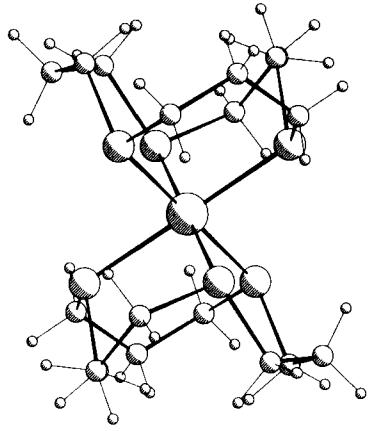

FIG. 11. $[Ru([12]aneS_3)_2]^{2+}$.

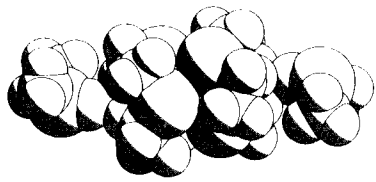

FIG. 12. $[Ru([9]aneS_3)_2]^{2+}.2$ DMSO.

A series of piano-stool complexes of Ru(II) with [9]aneS$_3$ has also been synthesized (*70*). Treatment of [9]aneS$_3$ with RuCl$_3$ in Me$_2$SO affords [RuCl([9]aneS$_3$)(Me$_2$SO)$_2$]$^+$ (*18*). Reaction of [RuX$_2$(PR$_3$)$_3$] (X = Cl, Br; PR$_3$ = PPh$_3$, PEtPh$_2$) with [9]aneS$_3$ affords [RuX$_2$(PR$_3$)([9]aneS$_3$)] or [RuX(PR$_3$)$_2$([9]aneS$_3$)]$^+$ depending on conditions, whereas reaction of [RuCl$_3$(PR$_3$)$_3$] (PR$_3$ = PEt$_2$Ph, PMe$_2$Ph) with [9]aneS$_3$ under reducing conditions gives [RuCl(PR$_3$)$_2$([9]aneS$_3$)]$^+$ (*70*). The single-crystal X-ray structure of [RuCl(PEtPh$_2$)$_2$([9]aneS$_3$)]$^+$ (Fig. 13) shows facial binding of [9]aneS$_3$ to the Ru(II) center with Ru–S(*trans* to Cl) = 2.294(4) Å; Ru–S(*trans* to P) = 2.387(4), 2.369(4) Å; Ru–P = 2.378(4), 2.383(4) Å; Ru–Cl = 2.453(4) Å (*23, 70*). Removal of Cl$^-$ from [RuCl$_2$(PPh$_3$)([9]aneS$_3$)] using TlPF$_6$ in CH$_3$CN affords the chiral species [RuCl(NCCH$_3$)(PPh$_3$)([9]aneS$_3$)]$^+$, the structure of which shows (Fig. 14) Ru–S(*trans* to P) = 2.348(16) Å, Ru–S(*trans* to Cl) = 2.248(14) Å, Ru–S(*trans* to NCCH$_3$) = 2.332(15) Å, Ru–P = 2.360(14) Å, Ru–N = 2.10(4) Å, Ru–Cl = 2.439(13) Å (*23, 70*).

Reaction of [RuCl$_2$(NCCH$_3$)$_4$] with [9]aneS$_3$ under CO affords [RuCl(CO)(NCCH$_3$)([9]aneS$_3$)]$^+$; the structure of this complex shows (Fig. 15) Ru–S(*trans* to Cl) = 2.3139(11) Å, Ru–S(*trans* to N) = 2.3115(13) Å, Ru–S(*trans* to C) = 2.3923(13) Å, Ru–C = 1.884(4) Å, Ru–Cl = 2.4150(14) Å, Ru–N = 2.072(4) Å (*52*). The shortening of the Ru–S distance *trans* to Cl$^-$ can be ascribed to π-donation from Cl → Ru and across to the S-donor; this together with the lengthening of M–S(*trans* to P) is consistent with [9]aneS$_3$ acting as an overall π-acceptor with Ru(II) (*23, 70*). The isolobal analogy between the 6-electron donor arene ligands and [9]aneS$_3$ (and also [9]aneN$_3$ and Me$_3$[9]aneN$_3$) is clear and suggests that the synthesis and development of organometallic half-sandwich complexes of these macrocycles are important synthetic targets.

The template synthesis of Bz[9]aneS$_3$ has been achieved by condensation of bis(2-bromoethyl)sulfide with [Ru(dpttd)(CO)] [dpttd^{2-} = 2,2′-[thiobis(ethylenethio)]bis(thiophenolate)] (*193*). The single-crystal X-ray structure of [RuBr$_2$(CO)(Bz[9]aneS$_3$)] (Fig. 16) shows facial binding of the trithioether macrocycle to Ru(II) with Ru–S(average, *trans* to Br) = 2.303(4) Å, Ru–S(*trans* to C) = 2.426(4) Å (*193*).

Reaction of [OsCl$_2$(4-MeC$_6$H$_4$^{i}Pr)]$_2$ with two molar equivalents of [9]aneS$_3$ in refluxing EtOH affords the homoleptic thioether complex [Os([9]aneS$_3$)$_2$]$^{2+}$, the single-crystal X-ray structure of which shows a centrosymmetric cation, Os–S = 2.3313(18), 2.3380(19), 2.3408(20) Å (*15, 70*). The complex [Os([9]aneS$_3$)$_2$]$^{2+}$ shows a reversible Os(II)/(III) couple at $E_{1/2}$ = +1.16 V vs. Fc$^+$/Fc in CH$_3$CN (*15, 70*). The interme-

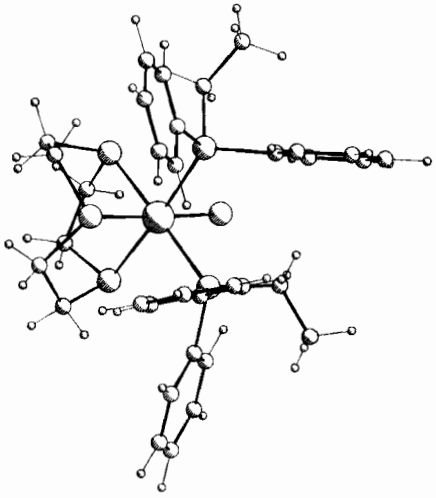

FIG. 13. $[RuCl(PEtPh_2)_2([9]aneS_3)]^+$.

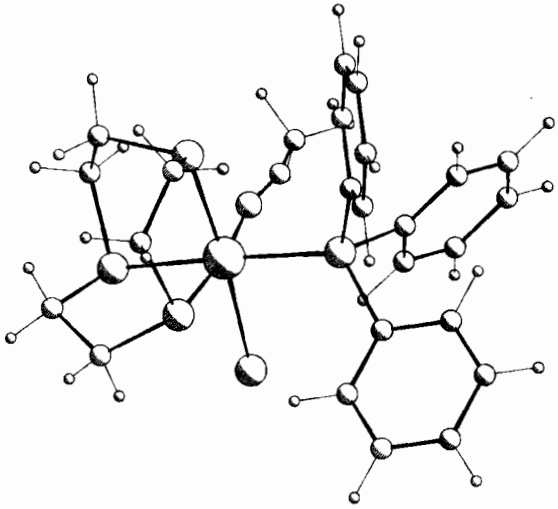

FIG. 14. $[(RuCl(NCCH_3)(PPh_3)([9]aneS_3)]^+$.

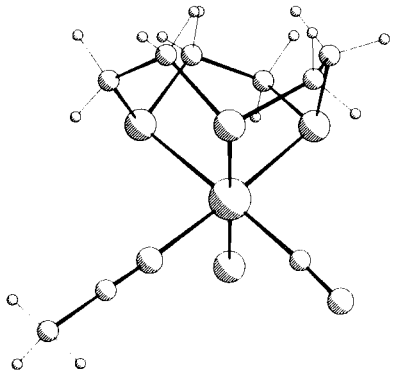

FIG. 15. $[RuCl(CO)(NCCH_3)([9]aneS_3)]^+$.

diate mixed-sandwich complex $[Os(4\text{-}MeC_6H_4{}^iPr)([9]aneS_3)]^{2+}$ can also be isolated (*14, 19, 188*), and a single-crystal X-ray structure determination shows (Fig. 17) Os–S = 2.3207(14), 2.3594(14), 2.3439(14) Å; Os–C = 2.223(5)–2.281(5) Å (*14, 188*).

Reaction of $[OsH_2(CO)_2(PPh_3)_2]$ with $[9]aneS_3$ affords the chiral complex cation $[OsH(CO)(PPh_3)([9]aneS_3)]^+$, the structure of which shows (Fig. 18) Os–S(*trans* to P) = 2.369(3) Å, Os–S(*trans* to H) = 2.402(3) Å, Os–S(*trans* to C) = 2.377(3) Å, Os–C = 1.868(11) Å, Os–H = 1.60(9) Å, Os–P = 2.3344(24) Å (*15, 70*).

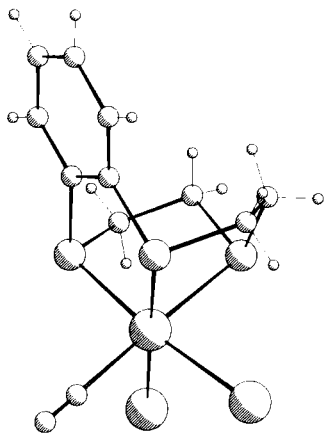

FIG. 16. $[RuBr_2(CO)(Bz[9]aneS_3)]$.

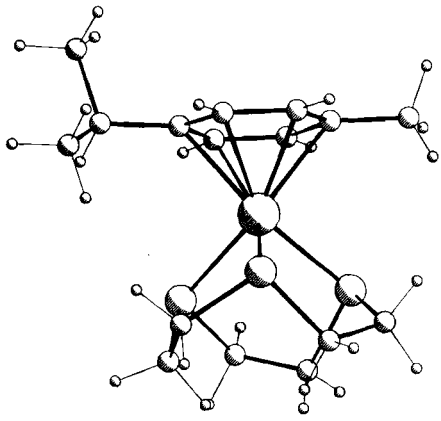

FIG. 17. $[Os(4\text{-}MeC_6H_4{}^iPr)([9]aneS_3)]^{2+}$.

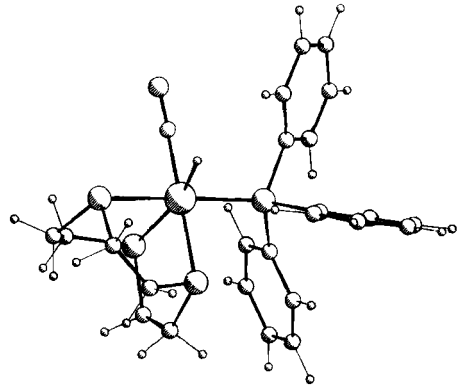

FIG. 18. $[OsH(CO)(PPh_3)([9]aneS_3)]^+$.

E. COBALT, RHODIUM, AND IRIDIUM

The syntheses and structures of $[M([9]aneS_3)_2]^{2+}$ (M = Co, Ni, Cu) were reported by Glass and co-workers in 1983 (*198*). Significantly, this was the first report of $[9]aneS_3$ binding to transition-metal ions. $[Co([9]aneS_3)_2]^{2+}$ is violet and is a rare example of a low-spin Co(II) complex, with a magnetic susceptibility μ_{eff} = 1.82 BM between 100 and 298 K (*219, 222*). ESR spectroscopy shows the expected eight-line spectrum (^{59}Co, I = 7/2, 100%) for the complex with g_{av} = 2.067 (*175, 222*).

The single-crystal X-ray structure of $[Co([9]aneS_3)_2]^{2+}$ shows hexathia coordination about Co(II) with a tetragonally compressed octahedral stereochemistry. The Co–S distances of 2.240(7), 2.356(6), 2.367(5) Å compared to the sum of the covalent radii of Co and S (2.360 Å) (*198*). Interestingly, the structure of $[Co([18]aneS_6)]^{2+}$, which is also low-spin, shows a tetragonally elongated octahedral stereochemistry with Co–S = 2.251(1), 2.292(1), 2.479(1) Å (*113*), whereas the N_6 analogue $[Co([9]aneN_3)_2]^{2+}$ is a high-spin species with μ_{eff} = 4.8 BM (*55, 219, 220*). The overall formation constant for $[Co([9]aneS_3)_2]^{2+}$ has been estimated as 8×10^{13}, indicating that $[9]aneS_3$ is an excellent ligand for Co(II) (*222*). Interestingly, the complexes $[M([12]aneS_3)_2]^{2+}$ (M = Fe, Co, Ni) show much-diminished stability relative to their $[9]aneS_3$ analogues; for example, unlike $[M([9]aneS_3)_2]^{2+}$, the complexes $[M([12]aneS_3)_2]^{2+}$ (M = Fe, Co, Ni) decompose instantly on contact with water (*74, 75*). The preorganization of $[9]aneS_3$ for facial binding to metal centers is the basis for the increase in complex stability with this ligand (*102, 110*).

Cyclic voltammetry of $[Co([9]aneS_3)_2]^{2+}$ shows reversible Co(III)/(II), Co(II)/(I), and Co(I)/(0) couples at $E_{1/2}$ = +0.57, −0.29, and −1.0 V vs. SHE, respectively, in CH_3CN (*219, 222*). The Co(II)/(III) couple for $[Co([9]aneN_3)_2]^{2+/3+}$ occurs at a potential 830 mV more cathodic than for $[Co([9]aneS_3)_2]^{2+/3+}$, reflecting the stability of Co(II) with hexathia coordination (*127*). Oxidation of $[Co([9]aneS_3)_2]^{2+}$ with $Na_2S_2O_8$ under aqueous conditions affords $[Co([9]aneS_3)_2]^{3+}$ as an orange product. The single-crystal X-ray structure of $[Co([9]aneS_3)_2]^{3+}$ shows a regular octahedral geometry consistent with a d^6 Co(III) complex, Co–S = 2.249(1), 2.253(1), 2.258(1) Å (*127*).

The electron-transfer self-exchange rate constant for the $[Co([9]aneS_3)_2]^{2+/3+}$ couple has been determined as 1.3×10^4 $M^{-1}sec^{-1}$ at 25°C (I = 0.2 M) by studying the cross-reaction between $[Co([9]aneS_3)_2]^{3+}$ and $[Co(phen)_3]^{2+}$ (*127*). Using ^1H NMR line-broadening techniques, the self-exchange rate constant has been estimated as 1.6×10^5 $M^{-1}sec^{-1}$ at 25°C (I = 0.2 M) (*130*).

Treatment of $[CoCl_3([9]aneN_3)]$ with $AgNO_3$ followed by addition of $[9]aneS_3$ affords the mixed-sandwich species $[Co([9]aneN_3)([9]aneS_3)]^{3+}$, the single-crystal X-ray structure of which shows Co–S = 2.237(4), 2.248(4), 2.255(5) Å; Co–N = 1.957(13), 1.957(12), 1.970(12) Å (*130*). The electron-transfer self-exchange rate constant for the $[Co([9]aneN_3)([9]aneS_3)]^{2+/3+}$ couple has been determined as 4.2×10^4 $M^{-1}sec^{-1}$ at 25°C (I = 0.2 M) by studying the cross-reaction with $[Ru(NH_3)_6]^{2+}$. The Co(II)/(III) redox couples for $[Co([9]aneN_3)_2]^{2+/3+}$, $[Co([9]aneN_3)([9]aneS_3)]^{2+/3+}$, and [Co-

$([9]aneS_3)_2]^{2+/3+}$ were measured as −0.41, +0.01, and +0.42 V vs. NHE, respectively (*130*).

Reaction of $[Rh(OH_2)_6]^{3+}$ or Rh(III) triflate with two molar equivalents of [9]$aneS_3$ affords $[Rh([9]aneS_3)_2]^{3+}$ as a colorless product (*30, 42, 173, 188*). The single-crystal X-ray structure of $[Rh([9]aneS_3)_2]^{3+}$ shows a symmetrical octahedral stereochemistry about d^6 Rh(III) with Rh–S = 2.3316(14), 2.3335(12), 2.3335(12) Å (*30, 173*).

The complex $[Rh([9]aneS_3)_2]^{3+}$ shows two reversible, one-electron reductions at $E_{1/2}$ = −0.71 V and −1.08 V vs. Fc^+/Fc assigned to Rh(III)/(II) and Rh(II)/(I) couples, respectively. The monomeric d^7 Rh(II) species can be generated by controlled potential electrolysis and shows a strong ESR signal with g = 2.085, 2.042, 2.009 measured at 77 K as a frozen glass (*30, 173*). This is a rare example of a genuine, mononuclear Rh(II) complex. Thus, the trithia crown is capable of conforming to the stereochemical requirements of coordinated d^6, d^7, and d^8 metal centers. The stereochemistry about Rh(II) in $[Rh([9]aneS_3)_2]^{2+}$ has not been confirmed by diffraction studies but is probably tetragonally elongated octahedral as observed for related d^7 Pd(III) complexes (*27, 42*). The geometry of $[Rh([9]aneS_3)_2]^+$ is unknown; although Rh(I) prefers a square planar geometry, weak interaction of the apical S-donors to the $[RhS_4]^+$ plane to give a 4 + 2 coordination appears likely. Similar apical interations have been observed in the related d^8 hexathia complexes $[M([9]aneS_3)_2]^{x+}$ (M = Pd(II) (*41, 218*), Pt(II) (*29*), x = 2; M = Au(III) (*26*), x = 3). Very recently, however, the single crystal X-ray structures of $[Rh([9]aneS_3)(C_2H_4)_2]^+$ and $[Rh([9]aneS_3)(COD)]^+$ (COD = 1,5-cyclooctadiene) have shown these complexes to be five coordinate in the solid state (*37*).

The Rh(III)/(II) and Rh(II)/(I) redox couples shift anodically on going from $[Rh([9]aneS_3)_2]^{3+}$ to $[Rh([12]aneS_3)_2]^{3+}$ (*74*). Thus, Rh(I) is destabilized more by [9]$aneS_3$ than by [12]$aneS_3$, presumably due to the greater apical interaction of [9]$aneS_3$ with Rh(I). Likewise, the Rh–S bond lengths in $[Rh([12]aneS_3)_2]^{3+}$ are on average 0.03 Å longer than in $[Rh([9]aneS_3)_2]^{3+}$; similarly, the corresponding Rh(II) and Rh(I) cations would be expected to show shorter Rh–S bond lengths for the complexes of [9]$aneS_3$.

Reaction of [9]$aneS_3$ with a series of dirhodium(II) carboxylates $[Rh_2(OOCR)_4]$ (R = Me, Et, ^{n}Pr) yields polymeric adducts of stoichiometry $\{[Rh_2(OOCR)_4]_3([9]aneS_3)_2\}_n$ (*118*).

Treatment of $[M(C_5Me_5)Cl_2]_2$ (M = Rh, Ir) with one molar equivalent of [9]$aneS_3$ affords the mixed-sandwich complexes $[M(C_5Me_5)([9]aneS_3)]^{2+}$ (*14, 19, 188*).

The complex cation $[Ir([9]aneS_3)_2]^{3+}$ can be prepared in low yield *via* $[IrCl_3([9]aneS_3)]$ by extended reflux of $IrCl_3$ with $[9]aneS_3$ in ethylene glycol (*188*). A better synthetic route involves reaction of $[IrCl(COT)_2]_2$ (COT = cyclooctene) with four molar equivalents of $[9]aneS_3$ in EtOH (*44, 188*). This yields $[IrH([9]aneS_3)_2]^{2+}$, which can be converted to $[Ir([9]aneS_3)_2]^{3+}$ by treatment with HNO_3. The single-crystal X-ray structure of $[Ir([9]aneS_3)_2]^{3+}$ shows the expected octahedral stereochemistry about Ir(III) with Ir–S = 2.338(3), 2.341(3), 2.342(3) Å (*44*). The intermediate $[IrH([9]aneS_3)_2]^{2+}$ shows a characteristic ^1H NMR spectrum with a resonance at $\delta = -13.4$ ppm assigned to a metal-hydride proton; asymmetric resonances from the methylene protons of two coordinated $[9]aneS_3$ ligands are also observed. The single-crystal X-ray structure of the complex $[IrH([9]aneS_3)_2]^{2+}$ (Fig. 19) confirms an octahedral geometry at Ir(III), with one $[9]aneS_3$ being tridentate and the other $[9]aneS_3$ bidentate to the metal center: Ir–H = 1.58(6) Å; Ir–S(*trans* to H) = 2.476(5) Å; Ir–S = 2.298(5), 2.319(5), 2.321(5), 2.344(5) Å (*44*). The formation of $[IrH([9]aneS_3)_2]^{2+}$ occurs presumably *via* oxidative addition of H^+ to $[Ir([9]aneS_3)_2]^+$ or a related species. Addition of protic acids to $[IrH([9]aneS_3)_2]^{2+}$ gives $[Ir([9]aneS_3)_2]^{3+}$ in good yield (*44*).

The complex $[Ir([9]aneS_3)_2]^{3+}$ shows a reduction at -1.38 V vs. Fc^+/Fc tentatively assigned to an Ir(III)/(II) couple. Dimerization of $[M([9]aneS_3)_2]^{2+}$ (M = Rh, Ir) is a likely route for decomposition of these paramagnetic monomers (*44*). *In situ* electrochemical reduction of

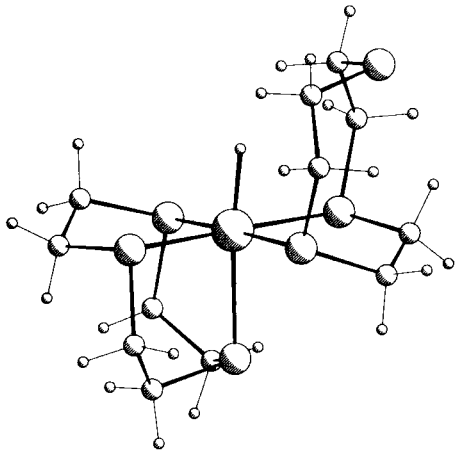

FIG. 19. $[IrH([9]aneS_3)_2]^{2+}$.

$[Rh([9]aneS_3)_2]^{3+}$ at −25°C using a UV/vis optically transparent thin-layer electrode confirms the isosbestic interconversion of 3+, 2+, and 1+ cations with loss of intensity of the S → M charge-transfer bands at 270 nm (*44*).

Addition of one molar equivalent of Et_3N to solutions of the complexes $[Co([9]aneS_3)_2]^{3+}$ (M = Co, Rh, Ir) in CH_3CN or CH_3NO_2, or dissolution of $[M([9]aneS_3)_2]^{3+}$ in water at pH > 4 leads to a rapid change in color of the solutions: from orange to green (λ_{max} = 685 nm) for Co, from colorless to red (λ_{max} = 474 nm) for Rh, and from colorless to yellow (λ_{max} = 379 nm) for Ir. Importantly for M = Co, this process is reversed under aqueous conditions at pH < 2, and the interconversion of orange to green species can be cycled readily by control of pH (*39*).

The ^1H NMR spectra of the basic solutions each show resonances near δ_1 = 6.6 ppm (doublet of doublets, 1H) with a multiplet near δ_2 = 6.2 ppm (2H) assigned to olefinic protons. In addition, a series of multiplets is observed in the range 2.8–4.0 ppm (20H) and is assigned to the methylene protons of coordinated $[9]aneS_3$. Selective decoupling experiments show that the resonances δ_1 and δ_2 are coupled to one another but not to any other proton; these data contrast with the ^1H NMR spectra for the parent 3+ cations that show symmetric multiplets in the δ = 3.6 ppm (24H) region (*127*). The ^{13}C NMR spectra of the products confirm that symmetric binding of $[9]aneS_3$ to M(III) has been perturbed. The NMR data establish that the complexes $[M([9]aneS_3)_2]^{3+}$ (M = Co, Rh, Ir) react under basic conditions to give the same type of products (*39*).

The single-crystal X-ray structure of the red complex derived from the reaction of $[Rh([9]aneS_3)_2]^{3+}$ with Et_3N shows (Fig. 20) hexathia coordination about Rh(III). One $[9]aneS_3$ ligand is intact and bound facially to Rh(III) with Rh–S = 2.315(4), 2.344(4), 2.323(4) Å. The second $[9]aneS_3$, however, has undergone a ring-opening *via* C–S bond cleavage to afford a coordinated vinyl thioether moiety with a terminal thiolate donor: Rh–S = 2.350(4), 2.325(4), 2.356(4) Å; C–C = 1.289(21) Å (*39*). Scheme 6 gives the proposed mechanism for the formation of this species. Deprotonation at a methylene carbon α to a coordinated thioether donor followed by M–C bond formation has been reported previously (*20;* see also *202*).

These results show that thioether crowns can be activated when coordinated to electropositive metal centers. The first step involves deprotonation at an α-methylene carbon center. It seems likely that this type of reactivity will be general for other thioethers since the complexes $[M([9]aneS_3)_2]^{2+}$ (M = Pd, Pt), $[Pd([15]aneS_4)]^{2+}$, $[M([18]aneS_6)]^{n+}$ (M = Co, Rh, n = 3; M = Pd, Pt, n = 2), and

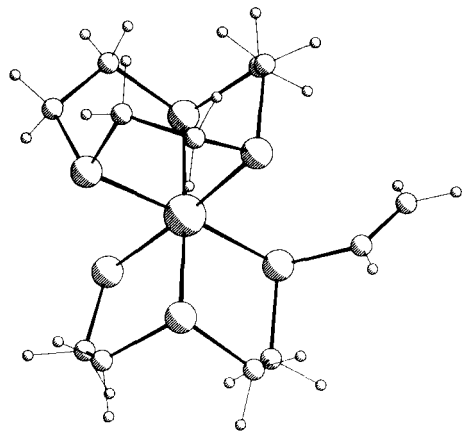

FIG. 20. $[Rh([9]aneS_3)(SCH_2CH_2SCH_2CH_2SCH = CH_2)]^{2+}$.

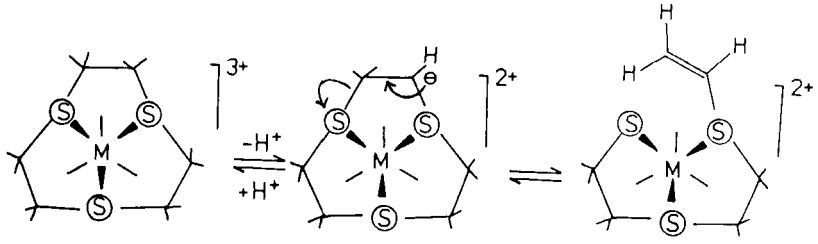

SCHEME 6

$Rh([12]aneS_4)Cl(AsPh_3)]^{2+}$ react similarly (*39*). The stabilization of high-valent complexes of Pd(III) (*42*). Ag(II) (*31*), Au(III) (*26*), Fe(III) (*31, 43*), and Ni(III) (*31*) with $[9]aneS_3$ at low pH involves inhibition of this deprotonation/ring-opening process. Deprotonation of $[9]aneS_3$ and related crowns followed by reaction with electrophiles represents a possible route for the C-functionalization of thioether macrocycles.

F. NICKEL, PALLADIUM, AND PLATINUM

The single-crystal X-ray structure of $[Ni([9]aneS_3)_2]^{2+}$ shows (Fig. 21) octahedral coordination about Ni(II) with Ni–S = 2.377(1), 2.380(1), 2.400(1) Å (*198*). The magnetic susceptibility, μ_{eff} = 3.05 BM for $[Ni([9]aneS_3)_2]^{2+}$ with values for $10Dq$ and B of 12,760 cm^{-1} and 680 cm^{-1}, respectively (*219*); this compares with values for $10Dq$ and B of 12,500 and 853 cm^{-1} for $[Ni([9]aneN_3)_2]^{2+}$ (*225*). Therefore, $[9]aneS_3$ exerts only a slightly stronger ligand-field than $[9]aneN_3$ (*219*).

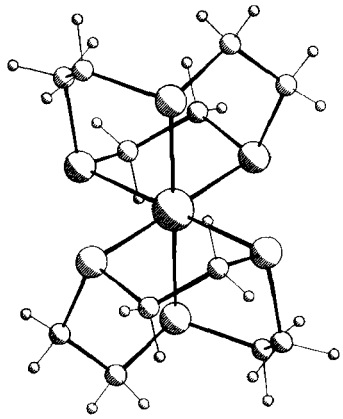

FIG. 21. $[Ni([9]aneS_3)_2]^{2+}$.

The complex $[Ni([9]aneS_3)_2]^{2+}$ shows a one-electron oxidation at $E_{1/2} = +0.97$ V vs. Fc^+/Fc (*219*) and a one-electron reduction at -1.11 V vs. Fc^+/Fc (reversible at $-25°C$) in CH_3CN (*117*). No unequivocal assignment for these being metal- or ligand-based processes has been made (*117, 219*), although ^{61}Ni labelling experiments suggest that the oxidation is metal based (*117*). The role of Ni–S bonds and the interconversion of Ni(I)/(II)/(III) states in Ni hydrogenase enzymes are the subjects of much current interest (*133*); the characterization of the redox products of $[Ni([9]aneS_3)_2]^{2+}$ provides a model for the study of NiS_6 chromophores.

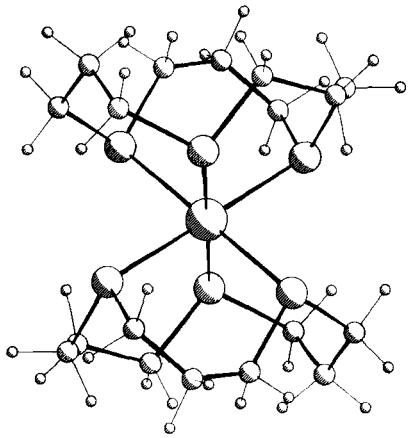

FIG. 22. $[Ni([12]aneS_3)_2]^{2+}$.

The synthesis and crystal structure of $[Ni([12]aneS_3)_2]^{2+}$ have been reported (*75, 184*). The Ni–S bond lengths for this cation (Fig. 22) are 2.409(1), 2.421(2), 2.435(1) Å, significantly longer than for $[Ni([9]aneS_3)_2]^{2+}$ (*75*). $[Ni([12]aneS_3)_2]^{2+}$ has a magnetic susceptibility μ_{eff} = 3.19 BM with $10Dq$ = 11,240 cm^{-1} (*75, 184*).

Reaction of $[NiCl_2(diphos)]$ with $[9]aneS_3$ in the presence of $TlPF_6$ affords $[Ni(diphos)([9]aneS_3)]^{2+}$, the single-crystal X-ray structure of which shows (Fig. 23) a five-coordinate Ni(II) complex with Ni–S = 2.225(3), 2.248(3), 2.381(3) Å; Ni–P = 2.193(3), 2.195(3) Å (*38*).

Reaction of $[PdCl_4]^{2-}$ with two molar equivalents of $[9]aneS_3$ yields a green product, $[Pd([9]aneS_3)_2]^{2+}$ (*41, 218*). The single-crystal X-ray structure of this diamagnetic complex shows (Fig. 24) each $[9]aneS_3$ bound in a bidentate manner to Pd(II) to give a $[PdS_4]^{2+}$ square plane, $Pd–S_{equ}$ = 2.332(3), 2.311(3) Å, $<S_{equ}PdS_{equ}$ = 88.63(11)° (*41, 218*). Interestingly, the two remaining thioether donors are situated at apical sites and are involved in long-range interactions with the Pd(II) center: $Pd\cdots S_{ap}$ = 2.952(4) Å, $<S_{ap}PdS_{equ}$ = 83.13(10)°, 83.24(11)°. The stereochemistry of $[Pd([9]aneS_3)_2]^{2+}$ is therefore a compromise between the preference for Pd(II) to be square planar and for $[9]aneS_3$ to bind facially to a metal center (*41, 218*).

The complex $[Pd([9]aneS_3)_2]^{2+}$ shows a reversible, one-electron oxidation at $E_{1/2}$ = +0.605 V vs. Fc^+/Fc in CH_3CN. Oxidation of $[Pd([9]aneS_3)_2]^{2+}$ either chemically or electrochemically affords the

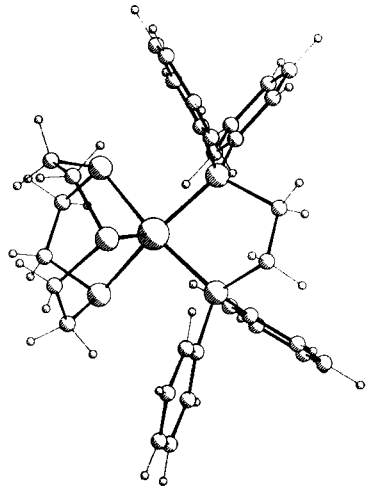

FIG. 23. $[Ni(diphos)([9]aneS_3)]^{2+}$.

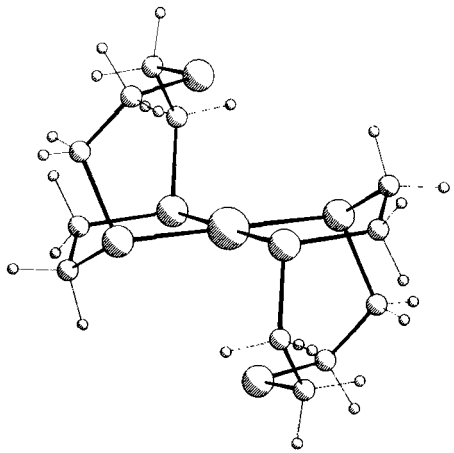

FIG. 24. $[Pd([9]aneS_3)_2]^{2+}$.

highly unusual monomeric Pd(III) species $[Pd([9]aneS_3)_2]^{3+}$, the single-crystal X-ray structure of which shows (Fig. 25) a tetragonally distorted, octahedral stereochemistry, as expected for a low-spin d^7 complex: Pd–S = 2.5448(15), 2.3558(14), 2.3692(15) Å; <SPdS = 87.33(5)°, 87.17(5)°, 88.88(5)° (*27, 41, 42, 188*). Thus, on going from $[Pd([9]aneS_3)_2]^{2+}$ to $[Pd([9]aneS_3)_2]^{3+}$ the Pd–S_{ap} distance contracts from 2.952(4) to 2.5448(15) Å, consistent with the increase in nuclear charge at the metal center and the stereochemical preference of d^7

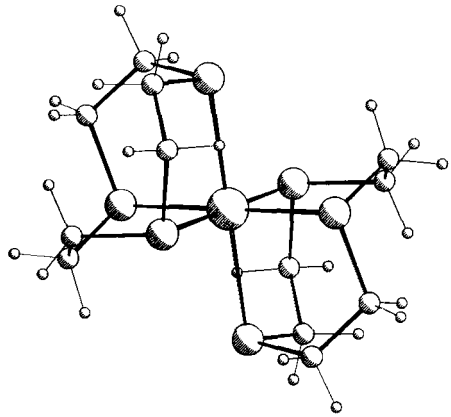

FIG. 25. $[Pd([9]aneS_3)_2]^{3+}$.

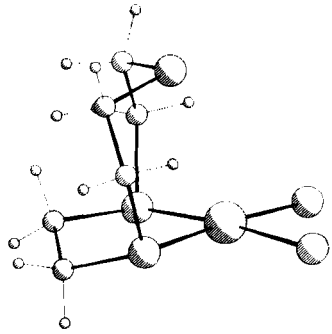

FIG. 26. *cis*-[$PdCl_2$([9]aneS_3)].

metal ions. The oxidation of [Pd([9]aneS_3)$_2$]$^{2+}$ to [Pd([9]aneS_3)$_2$]$^{3+}$ occurs isosbestically and reversibly (*42, 188*). The Pd(III)/(IV) couple is observed near +1.0 V vs. Fc^+/Fc; this is an ill-defined oxidation process with [Pd([9]aneS_3)$_2$]$^{4+}$ decomposing in solution, presumably *via* deprotonation at the coordinated thioether (see Section III,E).

A series of half-sandwich complexes [Pd([9]aneS_3)X_2]$^{x+}$ have been synthesized. These include *cis*-[PdX_2([9]aneS_3)] [X = Cl (*46*) (Fig. 26), Br (*218*)] and *cis*-[PdX_2([9]aneS_3)]$^{2+}$ [X = PPh_3 (Fig. 27), ½bipy, ½phen

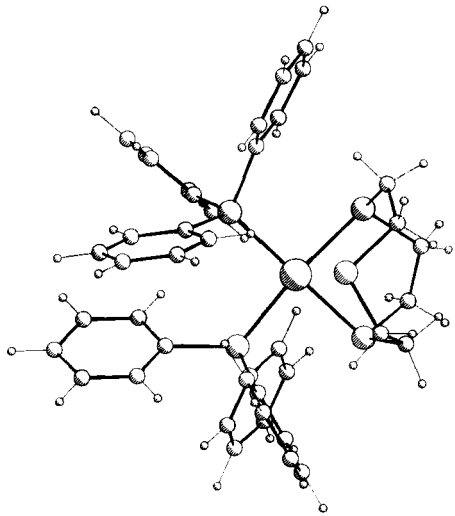

FIG. 27. *cis*-[$Pd(PPh_3)_2$([9]aneS_3)]$^{2+}$.

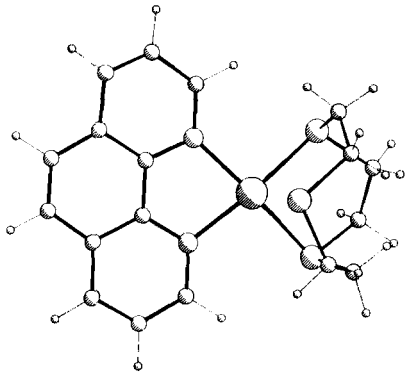

FIG. 28. *cis*-[Pd(phen)([9]aneS$_3$)]$^{2+}$.

(Fig. 28) (*47*)]. All of these complexes show square planar coordination to Pd(II) with an additional long-range interaction of the third thioether donor of [9]aneS$_3$ at an apical site; Pd···S$_{ap}$ = 3.1400(21) Å (X = Cl), 3.125(1) Å (X = Br), 2.877(3) Å (X = PPh$_3$), 2.906(13) Å (X = ½bipy), 2.948(3) Å (X = ½phen).

Reaction of $[PtCl_4]^{2-}$ with two molar equivalents of [9]aneS$_3$ affords [PtCl$_2$([9]aneS$_3$)] (*41*), which reacts further to give $[Pt([9]aneS_3)_2]^{2+}$ as a yellow-orange product (*29*). The single-crystal structure of $[Pt([9]aneS_3)_2]^{2+}$ (Fig. 29) shows that this complex is *not* isostructural with $[Pd([9]aneS_3)_2]^{2+}$. The complex $[Pt([9]aneS_3)_2]^{2+}$ has a square-based pyramidal structure in the solid state with Pt–S$_{equ}$ = 2.246(8),

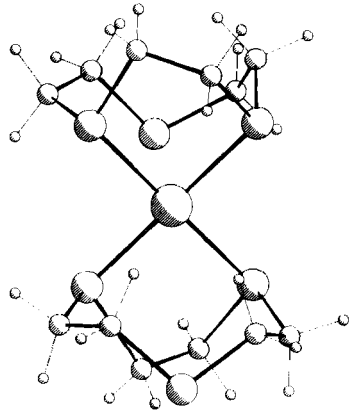

FIG. 29. $[Pt([9]aneS_3)_2]^{2+}$.

2.261(7), 2.293(8), 2.305(8) Å and Pt···S_{ap} = 2.885(7) Å. The sixth thioether donor is 4.04 Å from the Pt(II) center and is noninteracting (*29*).

Cyclic voltammetry of $[Pt([9]aneS_3)_2]^{2+}$ shows a chemically reversible oxidation centered at $E_{1/2}$ = +0.39 V vs. Fc^+/Fc. Controlled potential electrolysis of $[Pt([9]aneS_3)_2]^{2+}$ affords the mononuclear Pt(III) species $[Pt([9]aneS_3)_2]^{3+}$ that has been characterized by ESR and UV/vis spectroscopy (*29, 188*). The complex $[Pt([9]aneS_3)_2]^{3+}$ can be generated reversibly and isosbestically by chemical and electrochemical oxidation. Exhaustive electrolysis or further chemical oxidation of $[Pt([9]aneS_3)_2]^{3+}$ affords the d^6 Pt(IV) cation $[Pt([9]aneS_3)_2]^{4+}$ isosbestically; this species is stabilized under acidic conditions (*28, 188*). The oxidation of $[Pt([9]aneS_3)_2]^{2+}$ at $E_{1/2}$ = +0.39 V is therefore an overall two-electron process.

The stabilization of paramagnetic d^7 Rh(II), Ir(II), Pd(III), and Pt(III) centers as mononuclear $[M([9]aneS_3)_2]^{x+}$ complexes requires comment. The ability of $[9]aneS_3$ to reversibly alter its mode of coordination between 6-, 4-, and 2-electron donation and, most important, its ability to take up *intermediate* donacities as in the case of Pd(II), Pd(III), Au(III), Au(II), and Au(I) (see Section III,G) is central to this work. Additionally, $[9]aneS_3$ stabilizes otherwise highly reactive oxidation states by encapsulation, thus protecting the metal center by leaving no coordination sites available for reaction. The ligand $[9]aneN_3$ has been found to behave similarly with Pd(II), Pd(III), and Pd(IV) centers (*25, 141*).

Ring-opening reactions of $[M([9]aneS_3)_2]^{2+}$ (M = Pd, Pt) are discussed in Section III,E.

Reaction of $[PtClMe_3]_4$ with $[9]aneS_3$ affords the Pt(IV) alkyl complex $[PtMe_3([9]aneS_3)]^+$, the structure of which shows (Fig. 30) Pt–

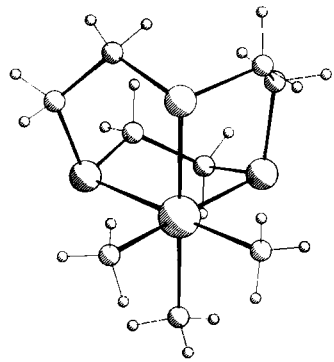

FIG. 30. $[PtMe_3([9]aneS_3)]^+$.

S(av) = 2.407 Å (*1, 2*). The ^{1}H and ^{13}C NMR spectra of $[PtMe_3([9]aneS_3)]^+$ show this complex to be nonfluxional in solution in contrast to $[PtMe_3([12]aneS_4)]^+$ (*1, 2*).

G. Copper, Silver, and Gold

The single-crystal X-ray structure of $[Cu([9]aneS_3)_2]^{2+}$ confirms a tetragonally elongated octahedral stereochemistry at Cu(II), with Cu–S = 2.419(3), 2.426(3), 2.459(3) Å (*198*). The ESR spectrum of $[Cu([9]aneS_3)_2]^{2+}$ shows $g = 2.059$, $A(^{63,65}Cu) = 0.00625$ cm^{-1} (CH_3NO_2 solution at 293 K), $g_{\parallel} = 2.120$, $g_{\perp} = 2.029$, $A_{\parallel} = 0.015$ cm^{-1} (frozen solution at 77 K) (*111, 174*). $[Cu([9]aneS_3)_2]^{2+}$ exhibits a quasi-reversible Cu(II)/(I) couple at $E_{1/2} = +0.61$ V vs. SCE; this value is 120 mV more cathodic than the Cu(II)/(I) couple for $[Cu([18]aneS_6)]^{2+}$ ($E_{1/2} = +0.72$ V vs. SCE), suggesting that [18]aneS$_6$ stabilizes Cu(I) more than [9]aneS$_3$ (*111*). Recently, the synthesis and structure of $[Cu_2([9]aneS_3)_3]^{2+}$ was reported (*71*). This species shows one [9]aneS$_3$ bridging two $[Cu([9]aneS_3)]^+$ moieties to give two tetrahedral Cu(I) centers (*71*).

The structure of $[CuCl_2([12]aneS_3)_2]$ (Fig. 31) shows a distorted octahedral stereochemistry with Cu–Cl = 2.2054(8) Å, Cu–S = 2.4474(9), 3.0504(6) Å (*169*). Significantly, the conformation of [12]aneS$_3$ in $[CuCl_2([12]aneS_3)_2]$ is almost identical to that of the free ligand; this is consistent with the general observation that the kinetic product of thioether coordination involves *exo* coordination to the metal center.

Reaction of CuI with [9]aneS$_3$ in a 1 : 1 molar ratio affords the complex $[CuI([9]aneS_3)]$, the single-crystal X-ray structure of which shows tetrahedral Cu(I) with Cu–I = 2.490(1) Å, Cu–S = 2.329(1), 2.331(1), 2.343(1) Å (*131*). Treatment of $[Cu(NCCH_3)_4]^+$ with one molar equivalent of [9]aneS$_3$ affords $[Cu(NCCH_3)([9]aneS_3)]^+$; replacement of co-

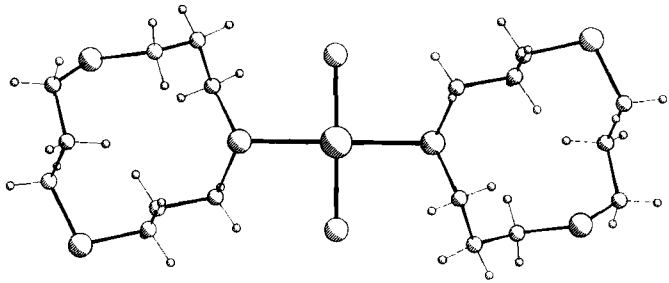

FIG. 31. $[CuCl_2([12]aneS_3)_2]$.

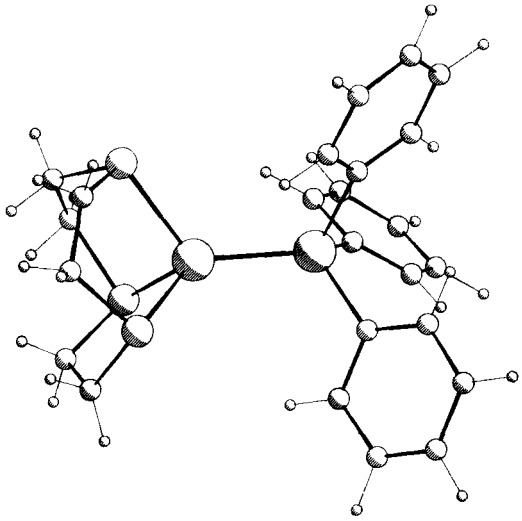

FIG. 32. $[Cu(AsPh_3)([9]aneS_3)]^+$.

ordinated CH_3CN with PPh_3 and $AsPh_3$ has been achieved to give $[Cu(PPh_3)([9]aneS_3)]^+$ and $[Cu(AsPh_3)([9]aneS_3)]^+$ (*32, 117*). The single-crystal X-ray structure of $[Cu(AsPh_3)([9]aneS_3)]^+$ (Fig. 32) shows tetrahedral stereochemistry about Cu(I): Cu–S = 2.315(6) Å, Cu–As = 2.297(4) Å (*32, 117*).

Reaction of $AgNO_3$ with two molar equivalents of $[9]aneS_3$ affords the bis-sandwich Ag(I) complex $[Ag([9]aneS_3)_2]^{2+}$, which shows a centrosymmetric $[AgS_6]^+$ cation with Ag–S = 2.697(5), 2.753(4) Å (*72, 131*). $[Ag([9]aneS_3)_2]^+$ shows a reversible oxidation at +1.30 V vs. NHE assigned to an Ag(I)/(II) couple (*72*). The Ag(II) species can be generated in MeOH and gives a deep blue solution that is stable at −70°C but not at room temperature (*72*). Stabilization of the Ag(II) species, $[Ag([9]aneS_3)_2]^{2+}$, has been achieved in aqueous, acidic media and has been characterized by ESR and UV/vis spectroscopy (*31*). Wieghardt and co-workers have isolated a fascinating trimeric Ag(I) complex $[Ag_3([9]aneS_3)_3]^{3+}$ (*131*). This species involves tetrahedral Ag(I) centers bridged by $[9]aneS_3$ ligands, Ag–S = 2.724(2), 2.595(4), 2.613(4), 2.480(2) Å (Fig. 33) (*131*).

A unique series of bis-sandwich complexes of d^{10} Au(I), d^9 Au(II), and d^8 Au(III) with $[9]aneS_3$ has been synthesized and structurally characterized (*26, 34*). Reaction of $[AuCl_4]^-$ with two molar equivalents of $[9]aneS_3$ under reducing conditions affords the Au(I) complex, $[Au([9]aneS_3)_2]^+$, in low yield. The single-crystal X-ray structure of [Au-

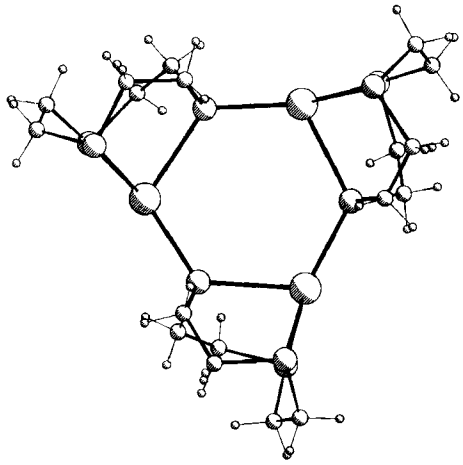

FIG. 33. $[Ag_3([9]aneS_3)_3]^{3+}$.

$([9]aneS_3)_2]^+$ (Fig. 34) shows an unusual distorted tetrahedral stereochemistry at Au(I) with one $[9]aneS_3$ bound as a monodentate ligand, Au–S = 2.302(6) Å, and the second bound asymmetrically through three S-donors, Au–S = 2.350(7), 2.733(8), 2.825(8) Å. The stereochemistry at the metal center is therefore a compromise between the facial binding of $[9]aneS_3$ and the preference of Au(I) for linear coordination. Oxidation of $[Au([9]aneS_3)_2]^+$ affords the d^8 Au(III) complex, $[Au([9]aneS_3)_2]^{3+}$, which adopts (Fig. 35) a tetragonally elongated octahedral stereochemistry similar to the d^8 Pd(II) analogue $[Pd([9]aneS_3)_2]^{2+}$: Au–S = 2.348(4), 2.354(4) Å, Au···S = 2.926(4) Å (*26*).

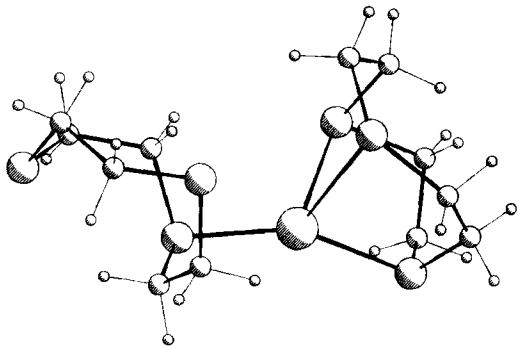

FIG. 34. $[Au([9]aneS_3)_2]^+$.

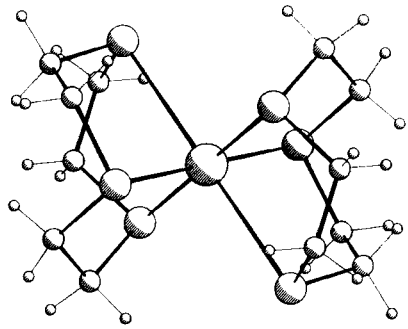

FIG. 35. $[Au([9]aneS_3)_2]^{3+}$.

The intermediate Au(II) species $[Au([9]aneS_3)_2]^{2+}$ has been isolated; the ESR spectrum of this complex at 77 K in frozen CH_3CN shows a strong four-line signal at $g_{av} = 2.010$ with hyperfine coupling to ^{197}Au ($I = 3/2$) ($A = 57.3$ G) (Fig. 36) (*26, 34*). The single-crystal X-ray structure of $[Au([9]aneS_3)_2]^{2+}$ confirms binding of two $[9]aneS_3$ macrocycles to d^9 Au(II) and shows (Fig. 37) a tetragonally elongated stereochemistry with Au–S = 2.452(5), 2.462(5) Å, Au···S = 2.839(5) Å (*34*). Mononuclear Au(II) complexes are particularly rare and $[Au([9]aneS_3)_2]^{2+}$ is the first such complex to have been structurally characterized.

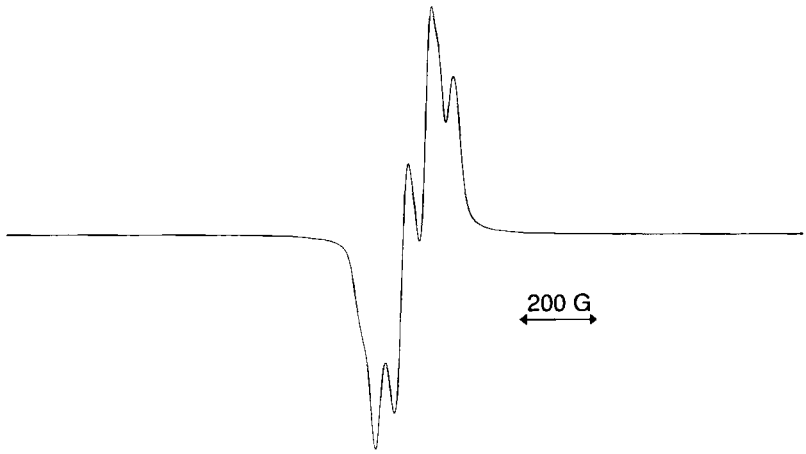

FIG. 36. ESR spectrum of Au(II) species $[Au([9]aneS_3)_2]^{2+}$.

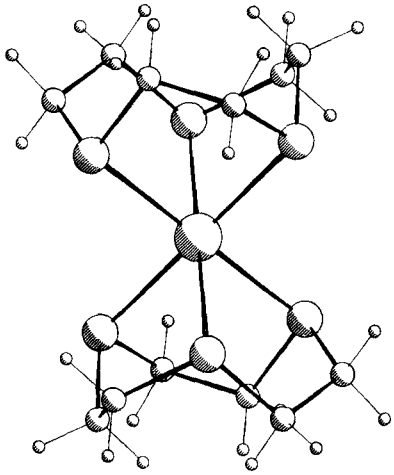

FIG. 37. $[Au([9]aneS_3)_2]^{2+}$.

H. ZINC, CADMIUM, AND MERCURY

Reaction of M(II) salts with two molar equivalents of [9]aneS$_3$ affords the d^{10} sandwich complexes $[M([9]aneS_3)_2]^{2+}$ [M = Zn, Cd (*128*), Hg (*40*)]. The crystal structures of $[M([9]aneS_3)_2]^{2+}$ (M = Zn, Hg) each exhibit octahedral stereochemistries at the metal centers, Zn–S = 2.491(3), 2.494(3), 2.497(3) Å (*128*). Interestingly, the Hg(II) complex shows a significant tetragonal compression, Hg–S = 2.638(3), 2.712(3), 2.728(3) Å (*40*); these structures are similar to that reported for $[Ag([9]aneS_3)_2]^+$, which also shows hexathia coordination (*72, 131*). A structure analogous to the Zn(II) complex is proposed for $[Cd([9]aneS_3)_2]^{2+}$ (*128*). Significantly, the d^{10} Au(I) complex $[Au([9]aneS_3)_2]^+$ (*26*) is not isostructural with the related d^{10} Ag(I), Zn(II), or Hg(II) complexes.

Although cyclic voltammetry of $[Hg([9]aneS_3)_2]^{2+}$ in CH_3CN shows a reversible reduction at $E_{1/2} = -0.15$ V vs. Fc^+/Fc assigned to a Hg(II)/(0) couple, no stable reduction product could be isolated (*40*).

I. INDIUM AND THALLIUM

Treatment of $InCl_3$ with [9]aneS$_3$ affords $[InCl_3([9]aneS_3)]$ (*217*). Reaction of $TlPF_6$ with [9]aneS$_3$ gives the Tl(I) complex

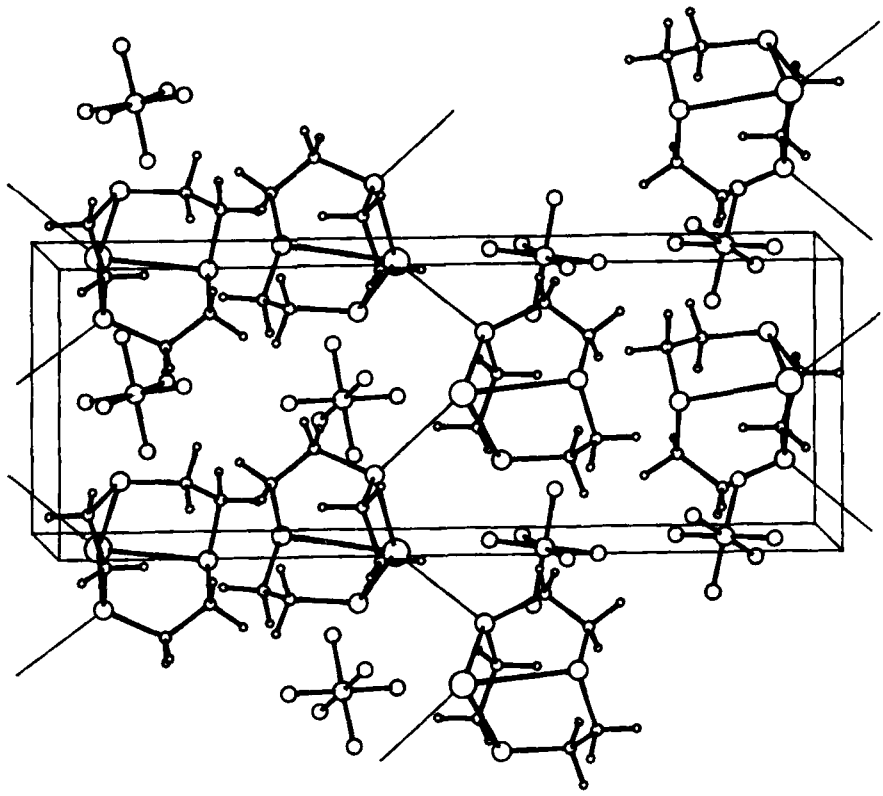

FIG. 38. Packing diagram of [Tl([9]aneS$_3$)]PF$_6$.

[Tl([9]aneS$_3$)](PF$_6$) (*35*). The single-crystal X-ray structure of this complex shows [9]aneS$_3$ bound facially to the metal center, Tl–S = 3.092(3), 3.110(3), 3.114(3) Å, with particularly small <STlS angles of 67.31(7)°, 67.52(7)°, 67.57(7)°. Additional long-range interactions to an S-atom of another [Tl([9]aneS$_3$)]$^+$ cation, Tl···S = 3.431(3) Å, and to four F$^-$ atoms from PF_6^- counter-ions, Tl···F = 3.228(8), 3.246(8), 3.272(9), 3.389(8) Å, are also observed (Fig. 38) (*35*). Similar Tl···F interactions have been observed in the structure of [Tl(Me$_3$-[9]aneN$_3$)]PF$_6$ (*216*).

J. LEAD

Reaction of Pb(ClO$_4$)$_2$ with two molar equivalents of [9]aneS$_3$ affords the complex [Pb(ClO$_4$)$_2$([9]aneS$_3$)$_2$] (*128*). This species has a distorted square antiprismatic structure with Pb(II) bound to all six S-

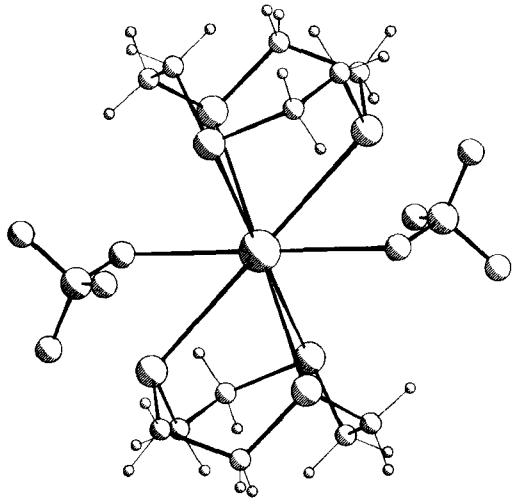

FIG. 39. $[Pb(ClO_4)_2([9]aneS_3)_2]$.

donors of two [9]aneS$_3$ ligands, Pb–S = 3.015(5), 3.084(4), 3.129(5) Å (Fig. 39). The coordination sphere is completed by two mutually *trans* O-bound ClO_4^- ligands, Pb–O = 2.719(15), 2.720(15) Å (*128*). Very few other thioether complexes of Pb(II) have been reported (*153*).

IV. [12–16]aneS$_4$ and Related Tetrathia Ligands

A. FREE LIGANDS

The single-crystal X-ray structure of [12]aneS$_4$ (Fig. 40) shows the macrocycle adopting a conformation with the S-atoms at the corners of a square (*178, 224*). All eight C–S bonds of [12]aneS$_4$ assume mutually gauche placements, consistent with the generally observed conformations of metal-free thioether macrocycles: By maximizing the number of gauche C–S bonds, S···S repulsions are minimized (*178, 224*). Similar solid state features have been found previously by DeSimone and Glick for [14]aneS$_4$, which crystallizes in three conformations, the α, β_1, and β_2; all incorporate *exo* conformations with the S-atoms pointing out of the macrocyclic ring [Fig. 41a (α form) and 41b (β_1 form)] (*86*). These observations explain the tendency for tetrathia macrocycles to bind to metal ions in an *exo* manner. *Endo* complexation

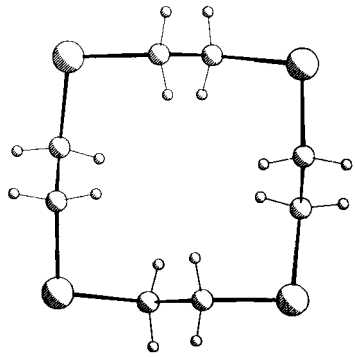

FIG. 40. [12]aneS$_4$.

in which the metal ion is complexed within the macrocyclic hole requires reorganization of the ligand (*86*).

Radical cations of [12]aneS$_4$ and [14]aneS$_4$ have been generated and their possible structures discussed (*11*). [14]aneS$_4$ has been found to be an effective antioxidant for the stabilization of natural rubber (*104*).

The structure of the thiophenophane L^1 (L^1 = 2, 5, 8-trithia[9](*2, 5*)thiophenophane) (see Fig. 2) has been determined crystallographically and shows the thiophene moiety to be placed at an angle of 60° to the plane of the three thioether donors; all the S-donors lie in *exo*cyclic positions with respect to the macrocyclic hole (*138*).

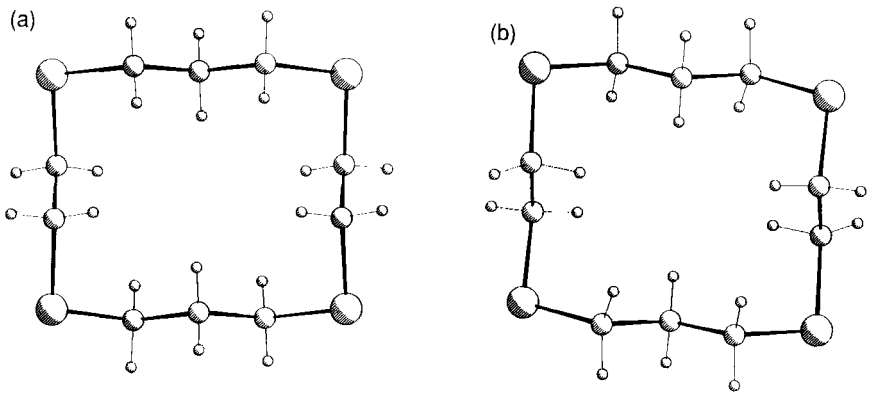

FIG. 41. (a) α-[14]aneS$_4$; (b) β_1-[14]aneS$_4$.

B. Aluminium

Robinson and co-workers have reported the synthesis and structure of the adducts of $[Al(CH_3)_3]$ with [12]aneS_4 (*178*) and [14]aneS_4 (*179*). Reaction of an excess of $[Al(CH_3)_3]$ with [14]aneS_4 affords the tetramer, $[Al(CH_3)_3]_4$[14]aneS_4, in which each thioether S-donor of the macrocycle is bound in an *exo* manner to one $[Al(CH_3)_3]$ moiety (Fig. 42): Al–S = 2.512(2), 2.531(2) Å; Al–C(average) = 1.954(6) Å (*179*). $[Al(CH_3)_3]_4$[14]aneS_4 is under investigation as a catalyst for the formation of liquid clathrates (*179*).

The product isolated from the reaction of $[Al(CH_3)_3]$ with [12]aneS_4 was the complex $[Al(CH_3)_3$([12]aneS_4)] (Fig. 43), which shows [12]aneS_4 bridging $[Al(CH_3)_3]$ moieties: Al–S = 2.718(3), 3.052(3) Å; Al–C = 1.943(8)–1.953(8) Å with an unusual trigonal bipyramidal stereochemistry at Al(III) (*178*).

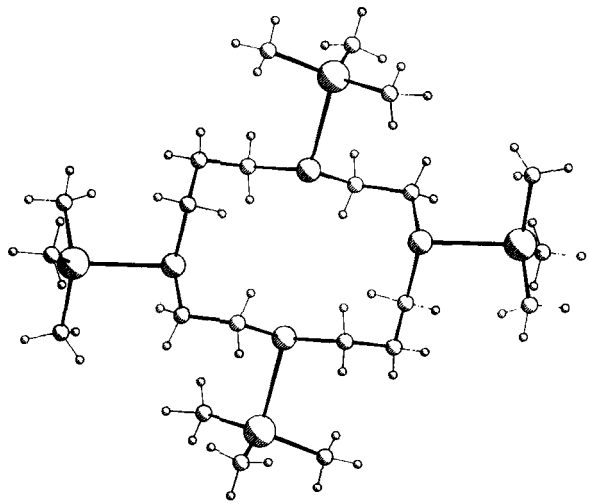

FIG. 42. $[Al(CH_3)_3]_4$[14]aneS_4.

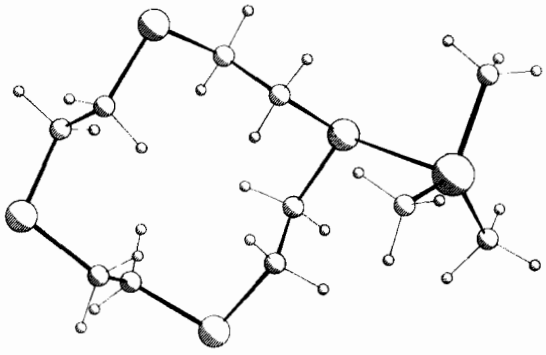

FIG. 43. $[Al(CH_3)_3([12]aneS_4)]$.

C. NIOBIUM

Reaction of $[NbCl_5]$ with a series of tetrathia macrocycles affords the dimeric adducts $[NbCl_5]_2(L)$ (L = $[14]aneS_4$, $[16]aneS_4$, $[20]aneS_4$) (*85, 89*). These highly reactive complexes involve *exo* binding of the macrocyclic ligands to $[NbCl_5]$ moieties. The single-crystal X-ray structure of $[NbCl_5]_2[14]aneS_4$ (Fig. 44) shows each octahedral Nb(V) center bound to five Cl^- ligands, Nb–Cl = 2.31(1) Å, and to one S-donor of $[14]aneS_4$, Nb–S = 2.71(1) Å, leaving two of the S-dnors of $[14]aneS_4$ uncoordinated (*85*). The 4:1 complexes $[NbCl_5]_4(L)$ (L = $[14]aneS_4$, $[16]aneS_4$, $[20]aneS_4$) have also been prepared (*89*).

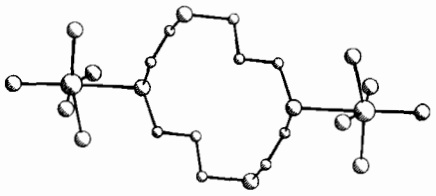

FIG. 44. $[NbCl_5]_2[14]aneS_4$.

D. Molybdenum and Tungsten

Sevdić and co-workers have reported the reaction of $M(CO)_6$ with [14]aneS_4 to afford the monomeric species $[M(CO)_3([14]aneS_4)]$ (M = Mo, W), in which [14]aneS_4 is proposed to act as a tridentate ligand (*200*). Oxidation of $[M(CO)_3([14]aneS_4)]$ with I_2 gives the seven coordinate M(II) species $[MI_2(CO)_3([14]aneS_4)]$ (M = Mo, W) (*200*). The synthesis and characterization of a series of Mo(III) complexes such as $[MoCl_3([14]aneS_4)THF]$ and $[MoCl_3([14]aneS_4)]$, in which the [14]aneS_4 bridges Mo(III) centers, have been described (*202*). Ring-opening reactions of coordinated [14]aneS_4 to yield vinyl thioether complexes have been studied (see Section III,E) (*202*). Reaction of $[MoOCl_3(THF)_2]$ with [14]aneS_4 gives $[MoOCl_3(THF)]_2$[14]aneS_4 with [14]aneS_4 acting as a monodentate ligand to each $[MoOCl_3(THF)]$ moiety (*144, 201*). The synthesis of the complexes $[MoO_2Cl_2(L)]$, $[MoOCl_3(L)]$, $[(MoCl_4)_2(L)]$, and $[MoOCl_4(L)]$ (L = [14]aneS_4) has been reported (*201*).

Treatment of $[Mo_2(O_3SCF_3)_2(OH_2)_4]^{2+}$ with [16]aneS_4 affords a series of complexes including the Mo(II) complex $[Mo_2(SH)_2([16]aneS_4)_2]^{2+}$, and the Mo(IV) species $[Mo_2O_2(OEt)([16]aneS_4)]^{3+}$ and $[MoO(SH)([16]aneS_4)]^+$ (*77, 84, 88*). The single-crystal X-ray structure of $[Mo_2(SH)_2([16]aneS_4)_2]^{2+}$ (Fig. 45) shows a binuclear structure with one S-donor from each [16]aneS_4 ligand bridging the two Mo(II) centers: Mo–S(bridge) = 2.320(1), 2.380(1) Å; Mo–S = 2.461(2) –2.537(2) Å, with terminal –SH groups on each Mo center:

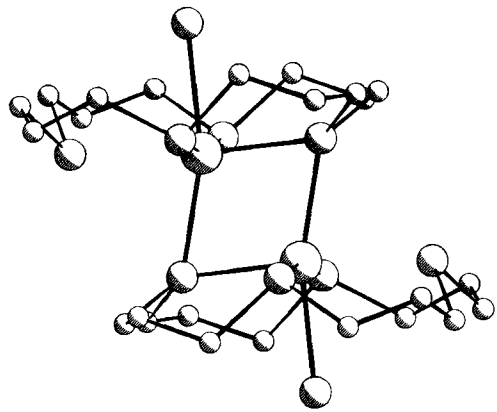

FIG. 45. $[Mo_2(SH)_2([16]aneS_4)_2]^{2+}$.

Mo–SH = 2.471(2) Å; the Mo–Mo distance is 2.823(1) Å (*77*). The structure of $[Mo_2O_2(OEt)([16]aneS_4)]^{3+}$ shows a linear EtO–Mo═O···Mo═O group with [16]aneS$_4$ bound equatorially to the Mo(IV) centers (*84*). The structure of $[MoO(SH)([16]aneS_4)]^+$ (Fig. 46) shows terminal oxo and HS^- ligands mutually *trans* to one another, Mo═O = 1.667(3) Å, Mo–SH = 2.486(1) Å, with [16]aneS$_4$ occupying the equatorial sites, Mo–S = 2.469(1)–2.483(2) Å, at the octahedral Mo(IV) center (*88*).

Yoshida and co-workers have synthesized a series of important Mo(0)/(II)/(III) complexes incorporating Me$_8$[16]aneS$_4$ (*3, 227, 228, 229, 230*). Reaction of $[MoCl_4(NCCH_3)_2]$ with Me$_8$[16]aneS$_4$ and Zn dust (as a reducing agent) affords *fac*-$[MoCl_3(Me_8[16]aneS_4)]$. Treatment of $[MoBr_2(CO)_4]$ and $[MoCl_2(CO)_4]$ with Me$_8$[16]aneS$_4$ gives *trans*-$[MoBr_2(Me_8[16]aneS_4)]$ and *fac*-$[MoCl_3(Me_8[16]aneS_4)]$, respectively; *trans*-$[MoCl_2(Me_8[16]aneS_4)]$ can be prepared by treatment of $[MoCl_2(NCCH_3)_4)]$ with Me$_8$[16]aneS$_4$ (*230*). Cyclic voltammetry of $[MoX_2(Me_8[16]aneS_4)]$(X = Cl, Br) shows highly anodic Mo(II)/(III) and Mo(I)/(III) redox couples, suggesting that Me$_8$[16]aneS$_4$ might stabilize low-valent Mo complexes. This was confirmed by reduction of $[MoX_2(Me_8[16]aneS_4)]$ in the presence of CO to afford the Mo(0) species $[Mo(CO)_2(Me_8[16]aneS_4)]$. The single-crystal X-ray structure of *trans*-$[Mo(CO)_2(Me_8[16]aneS_4)]$ (Fig. 47) confirms the *trans*-placement of the CO ligands, Mo–C = 1.979(8), 2.002(8) Å, with Me$_8$[16]aneS$_4$ occupying the equatorial sites at the octahedral Mo(0) center, Mo–S = 2.432(2), 2.434(2), 2.438(2), 2.439(2) Å (*230*). Reaction of

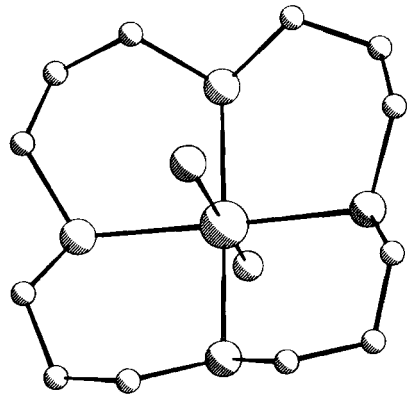

FIG. 46. $[MoO(SH)([16]aneS_4)]^+$.

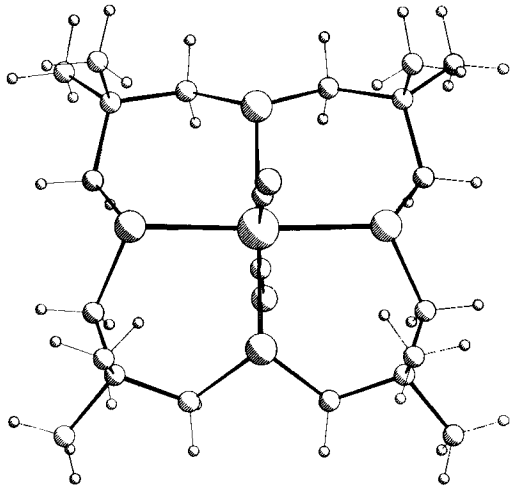

FIG. 47. *trans*-[$Mo(CO)_2(Me_8[16]aneS_4)$].

[$MoBr_2(Me_8[16]aneS_4)$] with Na/Hg in THF under N_2 affords a unique Mo(0)–N_2–thioether complex *trans*-[$Mo(N_2)_2(Me_8[16]aneS_4)$], the single-crystal X-ray structure of which shows (Fig. 48) Mo–S = 2.424(2), 2.428(2), 2.419(2), 2.424(2) Å; Mo–N = 1.991(5), 2.008(5) Å; N≡N = 1.105(7), 1.108(7) Å (*227*).

The Mo center in *trans*-[$Mo(N_2)_2(Me_8[16]aneS_4)$] is particularly electron-rich in comparison to that in *trans*-[$Mo(N_2)_2(dppe)_2$], the result

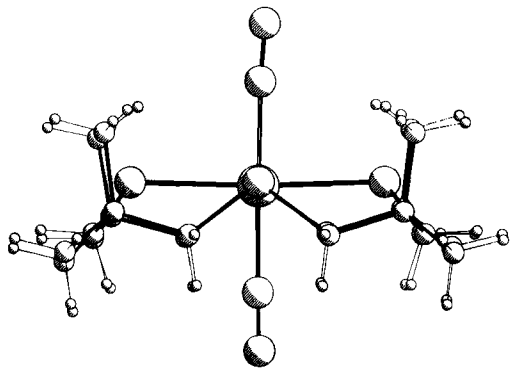

FIG. 48. *trans*-[$Mo(N_2)_2(Me_8[16]aneS_4)$].

of strong $p\pi(S) \rightarrow d\pi(Mo)$ donation; this is reflected in (i) the value of the Mo(0)/(I) couple (−0.52 V vs. SCE compared to −0.16 V for *trans*-$[Mo(N_2)_2(dppe)_2]$), (ii) the low-frequency $\nu_{N\equiv N}$ stretching vibrations at 1955 and 1890 cm^{-1} compared to 2020 and 1970 cm^{-1} for *trans*-$[Mo(N_2)_2(dppe)_2]$, and (iii) the reaction of $[Mo(N_2)_2(Me_8[16]aneS_4)]$ with CH_3Br to give the dimethylhydrazido complex *trans*-$[MoBr(N_2Me_2)(Me_8[16]aneS_4)]Br$ (*227*). The N-arylation and N,N-dibenzylation of *trans*-$[Mo(N_2)_2(Me_8[16]aneS_4)]$ has been described (*229*). Reaction of *trans*-$[Mo(N_2)_2(Me_8[16]aneS_4)]$ with L affords the complexes *trans*-$[Mo(L)_2(Me_8[16]aneS_4)]$ (L = C_2H_2, C_2H_4, ^tBuNC, PhNC) (*228*). The complex $[Mo(PhNC)_2(Me_8[16]aneS_4)]$ incorporates bent and linear PhNC ligands, <CNC = 139° and 167°; dealkylation of the ^tBuNC complex affords $[Mo(CN)_2(Me_8[16]aneS_4)]$ (*3, 228*).

E. Rhenium

Reaction of $[ReBr(CO)_5]$ with $[12]aneS_4$ in THF yields $[Re(CO)_3([12]aneS_4)]^+$, the single-crystal X-ray structure of which shows (Fig. 49) $[12]aneS_4$ acting as a tridentate ligand: Re–S = 2.442(5), 2.476(4), 2.493(5) Å; Re–C = 1.900(20), 1.904(16), 1.907(20) Å (*36*). In contrast, treatment of $[ReBr(CO)_5]$ with $[14]aneS_4$ in THF affords the neutral complex $[ReBr(CO)_3([14]aneS_4)]$ (Fig. 50), which shows bidentate $[14]aneS_4$: Re−S = 2.4954(24), 2.4973(24) Å; Re−Br = 2.6213(12) Å; Re−C = 1.891(11), 1.916(11), 1.920(11) Å (*36*).

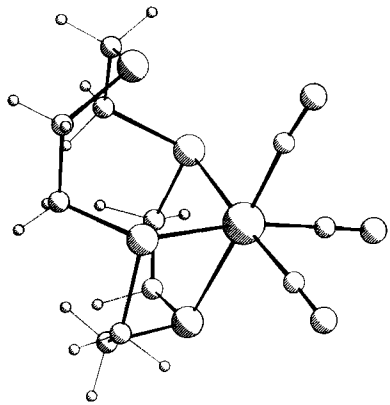

FIG. 49. $[Re(CO)_3([12]aneS_4)]^+$.

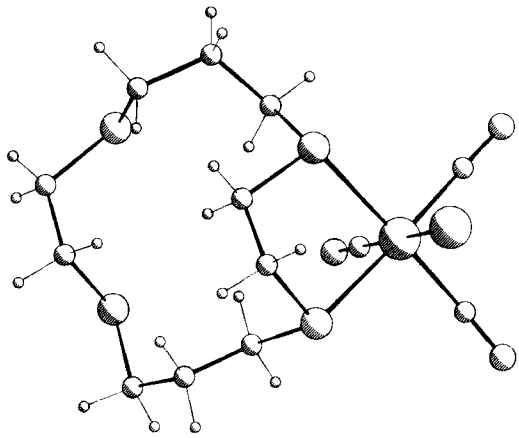

FIG. 50. [$ReBr(CO)_3$([14]$aneS_4$)].

F. IRON, RUTHENIUM, AND OSMIUM

Surprisingly few tetrathioether complexes of Fe, Ru, and Os have been reported.

The Mössbauer spectrum of [$Fe(NCCH_3)_2$([14]$aneS_4$)]$^{2+}$ has been measured (δ = 0.48, ΔEq = ca. 0 mm·sec^{-1}). These parameters are consistent with a low-spin octahedral Fe(II) complex (*79*).

On refluxing $K_2[RuCl_5(OH_2)]$ with L (L = [13]$aneS_4$, [14]$aneS_4$, Bz[15]$aneS_4$) in $EtO_2C_2H_4OH$ for two days the neutral complexes [$RuCl_2$(L)] can be isolated (*132, 165, 166, 167*). The single-crystal X-ray structure of [$RuCl_2$([14]$aneS_4$)] (Fig. 51) confirms *cis*-placement of the

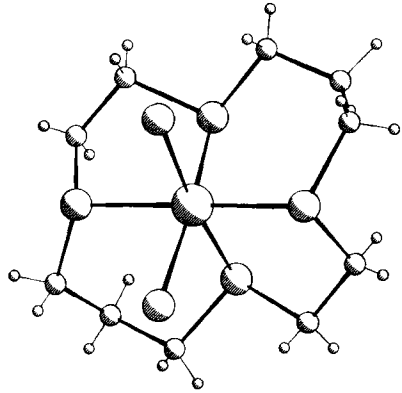

FIG. 51. *cis*-[$RuCl_2$([14]$aneS_4$)].

Cl^- ligands, Ru–Cl = 2.471(1) Å; significantly, the Ru–S distances *trans* to Cl^- [2.262(1) Å] are shorter than those *trans* to S [2.333(1) Å], indicating that Ru → S π-back-donation is occurring (*132*). A range of Ru(II) and Ru(III) complex derivatives of type $[RuXY([14]aneS_4)]^{x+}$ (X,Y = Br, I, NCS, NO_2, N_3, OH_2; x = 0, 1) have been prepared and the Ru(II)/(III) couples related to the stereochemical and electronic properties of the complexes (*132, 165, 166, 167*).

Reaction of $[RuCl_2(PPh_3)_3]$ with $[12]aneS_4$ affords *cis*-$[RuCl(PPh_3)([12]aneS_4)]^+$; removal of Cl^- with $TlPF_6$ in CH_3CN gives *cis*-$[Ru(NCCH_3)(PPh_3)([12]aneS_4)]^{2+}$, the single-crystal X-ray structure of which shows (Fig. 52) Ru–S(*trans* to N) = 2.303(3) Å; Ru–S(*trans* to P) = 2.372(3) Å; Ru–S = 2.362(4), 2.376(3) Å; Ru–N = 2.077(9) Å; Ru–P = 2.357(3) Å (*49*). Treatment of $[RuCl_2(CO)_2DMF(PPh_3)]$ with $[12]aneS_4$ gives *cis*-$[RuCO(PPh_3)([12]aneS_4)]^{2+}$, the structure of which shows (Fig. 53) Ru–S(*trans* to P) = 2.3757(11) Å; Ru–S(*trans* to C) = 2.3986(10) Å; Ru–S = 2.3819(10), 2.3913(10) Å; Ru–P = 2.3880(10) Å; Ru–C = 1.889(4) Å (*49*).

Reaction of $RuCl_3 \cdot 3H_2O$ with $[14]aneS_4$ in EtOH affords $[RuCl_3([14]aneS_4)]$, which is proposed to involve tridentate $[14]aneS_4$ (*8*); treatment of this complex with LiBr gives $[RuBr_3([14]aneS_4)]$(*8*). The ESR spectra of $[RuX_3([14]aneS_4)]$ show signals at g_{av} = 1.957 (X = Cl) and 1.993 (X = Br) (*8*).

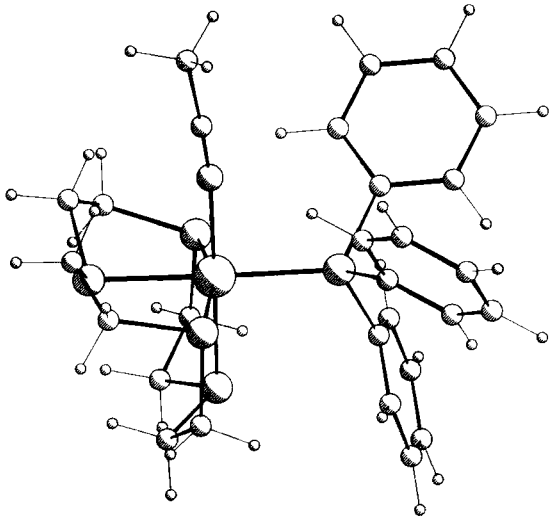

FIG. 52. *cis*-$[Ru(NCCH_3)(PPh_3)([12]aneS_4)]^{2+}$.

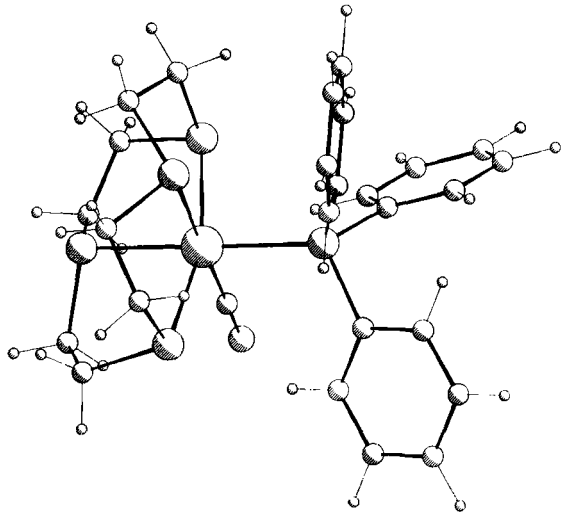

FIG. 53. *cis*-[RuCO(PPh$_3$)([12]aneS$_4$)]$^{2+}$.

The complex [OsCl$_4$([14]aneS$_4$)] has been prepared as a dark green product (*8*).

G. COBALT, RHODIUM, AND IRIDIUM

A series of Co(III) complexes [CoX$_2$([14]aneS$_4$)]$^+$ (X = Cl, Br, NCS, NO$_2$, $\frac{1}{2}$C$_2$O$_4$) and [CoX$_2$(Bz[15]aneS$_4$)]$^+$ (X = Cl, Br) have been prepared (*210*). The complexes of [14]aneS$_4$ were assigned as *cis*-species with the macrocycle coordinated to the metal center in a folded manner. These complexes were characterized by IR and electronic spectroscopy, and by magnetic and conductivity measurements (*210*).

A range of analogous Rh(III) complexes with [12]aneS$_4$, [14]aneS$_4$, and [16]aneS$_4$ has been synthesized (*51, 134, 210*). The single-crystal X-ray structure of [RhCl$_2$([14]aneS$_4$)]$^+$ (Fig. 54) shows *cis*-coordination of the Cl$^-$ ligands, Rh–Cl = 2.3836(12) Å, with the macrocycle folded about octahedral Rh(III), Rh–S = 2.2870(12), 2.3275(12) Å (*51*). As in the isoelectronic Ru(II) complex, *cis*-[RuCl$_2$([14]aneS$_4$)] (*132*), the M–S bonds *trans* to Cl$^-$ are shorter than those *trans* to S (*51*). Whereas the complexes [RhCl$_2$(L)]$^+$ (L = [12]aneS$_4$, [14]aneS$_4$) have been assigned as *cis* isomers (*51, 134, 210*), the single-crystal X-ray structure of [RhCl$_2$([16]aneS$_4$)]$^+$ (Fig. 55) shows it to be a *trans* complex: Rh–Cl = 2.3391(22) Å, Rh–S = 2.3483(25) Å; this is consistent with

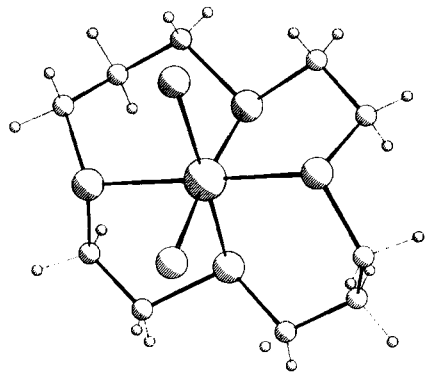

FIG. 54. *cis*-[$RhCl_2$([14]$aneS_4$)]$^+$.

the increased hole-size of the 16-membered ring macrocycle compared to the 12- and 14-membered ring species (*51*).

Reaction of *mer*-$RhCl_3(EEt_2Ph)_3$] (E = P, As) with [12]$aneS_4$ affords the complexes *cis*-[$RhCl(EEt_2Ph)$([12]$aneS_4$)]$^{2+}$. The structure of *cis*-[$RhCl(PEt_2Ph)$([12]$aneS_4$)]$^{2+}$ (Fig. 56) shows Rh–S(*trans* to Cl^-) = 2.2869(16) Å; Rh–S(*trans* to P) = 2.3825(17) Å; Rh–S = 2.3402(17), 2.3505(17) Å; Rh–Cl = 2.3567(19) Å; Rh–P = 2.3494(17) Å (*49*).

Ring-opening reactions of [12]$aneS_4$ species are discussed in Section III,E.

The complexes [$RhCl_2$(L)]$^+$ (L = [12]$aneS_4$, [14]$aneS_4$, [16]$aneS_4$) show irreversible reductions by cyclic voltammetry in CH_3CN near −1.1 V vs. Fc^+/Fc. Electrochemical reduction of these complexes occurs

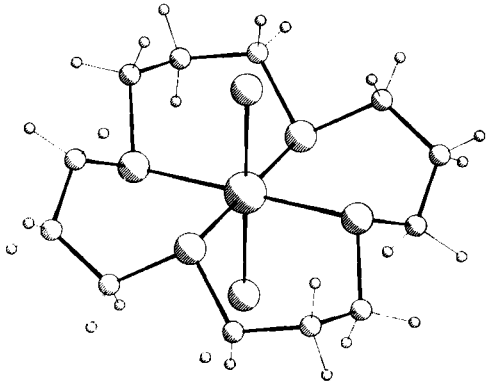

FIG. 55. *trans*-[$RhCl_2$([16]$aneS_4$)]$^+$.

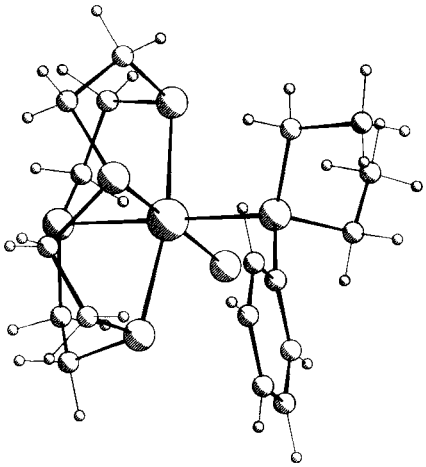

FIG. 56. *cis*-[RhCl(PEt$_2$Ph)([12]aneS$_4$)]$^{2+}$.

via intermediate Rh(II) species with loss of Cl^- (*51*, *134*). The single-crystal X-ray structure of [Rh([14]aneS$_4$)]$^+$ (Fig. 57) shows a dimeric structure with each Rh(I) bound to four thioether donors of one macrocycle, Rh–S = 2.285(4), 2.282(5), 2.261(3), 2.264(6) Å. The Rh atom is displaced 0.133(2) Å out of the least-squares S_4 plane toward a second [Rh([14]aneS$_4$)]$^+$ moiety: Rh···Rh = 3.313(1) Å, Rh···S = 3.697(9)–3.822(3) Å (*231*).

The Rh(I) complexes [Rh(L)]$^+$ [L = [14]aneS$_4$ (*134*, *231*), Me$_4$[14]aneS$_4$ (*231*), Bz[15]aneS$_4$ (*134*)] are strong nucleophiles and

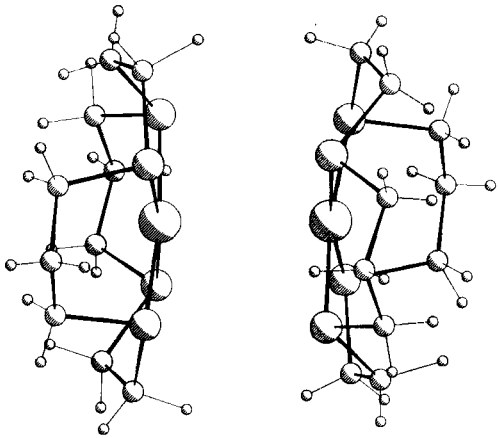

FIG. 57. [Rh([14]aneS$_4$)]$^+$.

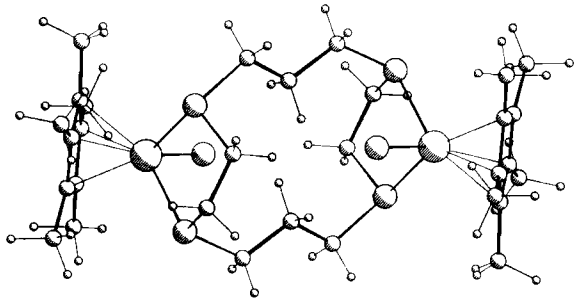

FIG. 58. $[Rh_2(C_5Me_5)_2Cl_2([14]aneS_4)]^{2+}$.

undergo oxidative addition reactions with CH_2Cl_2 (*231*), CH_3I, $C_6H_5CH_2Br$, and CH_3COCl (*134*). In addition, $[Rh([14]aneS_4)]^+$ combines with electrophiles such as SO_2, BF_3, NO^+, O_2, tcne, and H^+ (*134*). Reaction of $[Rh[14]aneS_4)]^+$ with trace amounts of O_2 in CH_3CN affords a blue solution of a Rh(II) product (*134*), which may correspond to a metal-metal bonded dimeric Rh(II)/(II) species.

Treatment of $[Rh_2(C_5Me_5)_2Cl_4]$ with $[14]aneS_4$ yields the dimeric species $[Rh_2(C_5Me_5)_2Cl_2([14]aneS_4)]^{2+}$ (Fig. 58), which shows Rh–Cl = 2.401(3) Å; Rh–S = 2.363(3), 2.389(3) Å (*14, 188*).

Reaction of $IrCl_3$ with $[14]aneS_4$ affords *cis*-$[IrCl_2([14]aneS_4)]^+$, which shows (Fig. 59) Ir–Cl = 2.389(5), 2.385(5) Å; Ir–S = 2.268(4), 2.277(4) (*trans* to Cl^-), 2.287(5), 2.343(5) Å (*50*). This complex exhibits an irreversible reduction at −1.82 V vs. Fc^+/Fc (*50*).

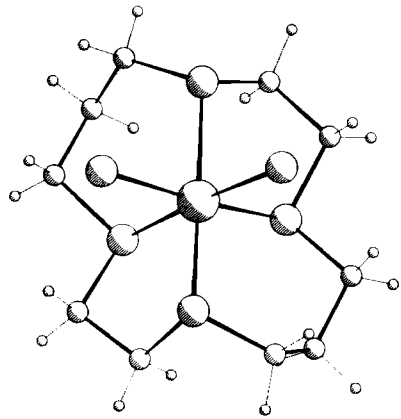

FIG. 59. *cis*-$[IrCl_2([14]aneS_4)]^+$.

H. Nickel, Palladium, and Platinum

A range of square planar Ni(II) complexes incorporating tetrathia macrocycles has been synthesized (*82, 135, 140, 182, 183*). The single-crystal X-ray structure of $[Ni([14]aneS_4)]^{2+}$ (Fig. 60) shows square planar coordination at Ni(II): Ni–S = 2.177(1), 2.175(1) Å (*82*). The formation of paramagnetic octahedral complexes $[NiX_2([14]aneS_4)]^{2+}$ has been monitored and equilibrium constants for the addition of I^- measured [Eq. (3) and (4)] (*182, 183*).

$$[NiI_2(L)] \rightleftharpoons [NiI(L)]^+ + I^- \qquad K = 6.3 \times 10^{-2} \tag{3}$$

$$[NiI(L)]^+ \rightleftharpoons [Ni(L)]^{2+} + I^- \qquad K = 2.5 \times 10^{-4} \tag{4}$$

Reaction of $Ni(BF_4)_2$ with the small-ring macrocycles L in the presence of acetic anhydride affords the violet or blue binuclear species $[Ni_2(L)_3]^{4+}$ (L = [12]aneS$_4$, [13]aneS$_4$) (*184*). Reaction of $NiCl_2$ with L affords the chloro-bridged dimers $[Ni_2Cl_2(L)_2]^{2+}$ (L = [12]aneS$_4$, [14]aneS$_4$, [16]aneS$_4$) (*38*). All three complexes have been characterized crystallographically and show the same type of chloro-bridged, octahedral coordination at the Ni(II) centers. For $[Ni_2Cl_2([12]aneS_4)_2]^{2+}$ (Fig. 61) Ni–S = 2.412(3) (*trans* to Cl), 2.373(3) (*trans* to Cl′), 2.4144(25) Å; Ni–Cl = 2.411(3) Å; Ni–Cl′ = 2.382(3) Å. For $[Ni_2Cl_2([16]aneS_4)_2]^{2+}$, Ni–S = 2.4166(23)–2.4388(25) Å; Ni–Cl = 2.4118(22), 2.4182(23) Å (*38*). Interestingly, the structure of $[Ni_2Cl_2([14]aneS_4)_2]^{2+}$ exhibits the shortest Ni–S distances: Ni–S = 2.3694(22)–2.3798(21) Å,

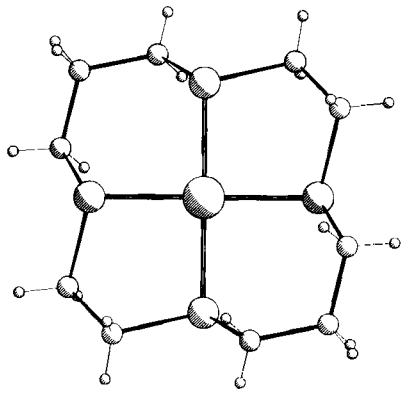

Fig. 60. $[Ni([14]aneS_4)]^{2+}$.

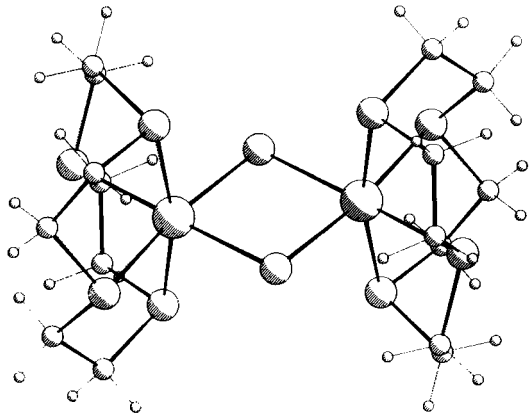

FIG. 61. $[Ni_2Cl_2([12]aneS_4)_2]^{2+}$.

Ni–Cl = 2.4416(20), 2.4252(20) Å. This suggests a better hole-size fit between Ni(II) and [14]aneS$_4$ (*38*). All of the Ni(II) tetrathioether macrocyclic complexes hydrolyze rapidly in water to give aquated Ni(II) and free ligand (*38*).

The extraction of Ni(II) and Pd(II) salts by tetrathioether macrocycles has been described (*68, 190*). Pd(II) can be extracted either as a 1 : 1 or 1 : 2 Pd:[14]aneS$_4$ species (*190*).

Insertion of Pd(II) into [12]-, [14]-, and [16]aneS$_4$ has been achieved (*45, 176*). The single-crystal X-ray structures of these complexes all show square planar coordination about Pd(II). For $[Pd([12]aneS_4)]^{2+}$ (Fig. 62), Pd–S = 2.280(4), 2.307(4) Å with the Pd atom displaced 0.3116 Å out of the least-squares S_4 plane, consistent with poor size-match between the Pd(II) ion and the small-ring macrocycle. For $[Pd([14]aneS_4)]^{2+}$ (Fig. 63), Pd–S = 2.253(10)–2.296(8) Å with the Pd atom lying 0.0381 Å out of the least squares S_4 plane. This contrasts with the structure of $[Pd([16]aneS_4)]^{2+}$ (Fig. 64), which shows the Pd

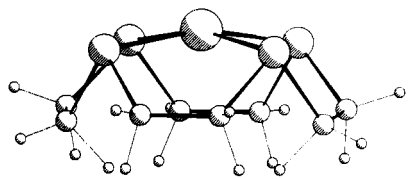

FIG. 62. $[Pd([12]aneS_4)]^{2+}$.

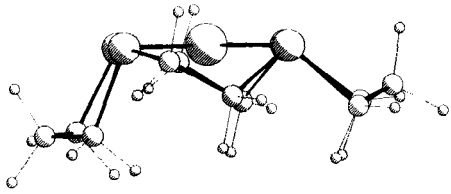

FIG. 63. $[Pd([14]aneS_4)]^{2+}$.

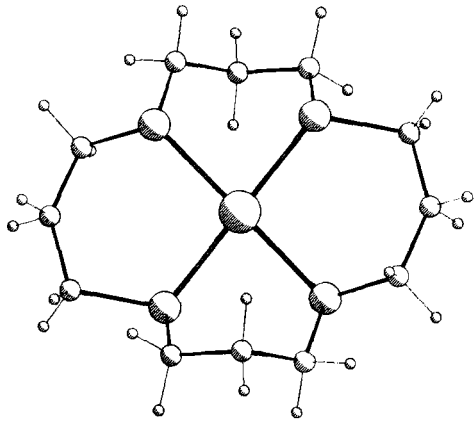

FIG. 64. $[Pd([16]aneS_4)]^{2+}$.

atom precisely in the plane of the four thioether donors: Pd–S = 2.300(10)–2.315(9) Å (*45, 176*). Reduction of the complexes $[Pd(L)]^{2+}$ (L = [12]aneS$_4$, [14]aneS$_4$, [16]aneS$_4$) by one electron affords diamagnetic species tentatively assigned as Pd(I)/(I) metal-metal bonded dimers (*45, 176*).

Variable temperature ^{1}H and ^{13}C NMR spectroscopy has shown that the Pt(IV) complex $[PtMe_3([12]aneS_4)]^+$ undergoes a novel ligand commutation in which the metal exchanges between coordinated and uncoordinated S-atoms of [12]aneS$_4$ (*1, 2*).

I. Copper and Silver

The extraction of Cu(II) and Cu(I) salts by [14]aneS$_4$ and related tetrathia ligands has been studied (*68, 186, 187, 189*). Extraction occurs via the formation of a Cu(I) complex of stoichiometry $[Cu(L)]^+$ (*68, 186*). The single-crystal X-ray structure of $[Cu([14]aneS_4)]^+$ (Fig. 65) shows

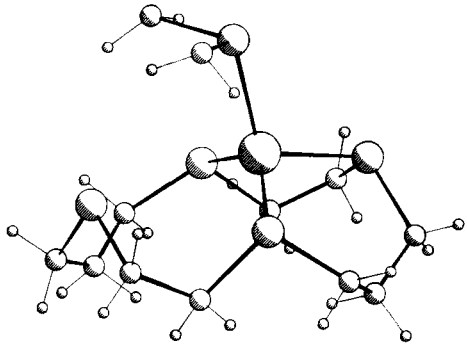

FIG. 65. $[Cu([14]aneS_4)]^+$, part of polymer.

tetrahedral coordination at Cu(I) with the metal ion bound to three S-donors of one [14]aneS$_4$, Cu–S = 2.260(4), 2.327(4), 2.338(4) Å, and to one S-donor of a second [14]aneS$_4$, Cu–S = 2.342(3) Å, generating a polymeric chain (*91, 94*).

The structure of the corresponding Cu(II) complex $[Cu(ClO_3)_2([14]aneS_4)]$ shows octahedral coordination about the metal center with the macrocycle bound equatorially through four S-atoms, Cu–S = 2.297(1), 2.308(1) Å, and two apically-bound ClO_4^- ions, Cu–O = 2.652(4) Å (*103*). Reaction of $CuCl_2$ with [16]aneS$_4$ affords the dimeric species $[Cu_2Cl_4([16]aneS_4)]$; monomeric complexes of Cu(II) and Cu(I) with [16]aneS$_4$ have also been isolated (*107;* see also *226*).

Rorabacher and co-workers have reported a series of elegant studies on the complexation of Cu(II) and Cu(I) by polythia macrocyclic ligands (*91, 92, 94, 95, 99, 103, 121, 122, 163, 180, 181, 207, 232*). Values of the Cu(II)/(I) redox couple, thermodynamic parameters, rates of complex formation and dissociation, rates of electron transfer, and rates of substitution reactions have been related to stereochemical, steric, hole-size, and configurational effects of the polythia ligands. Formation rate constants for Cu(II) complexes of thioether macrocycles and open-chain ligands range from 6.5×10^3 sec^{-1} for [12]aneS$_4$ to 4×10^6 $M^{-1}sec^{-1}$ for the least sterically hindered open-chain ligands (*92*). Formation of the second Cu–S bond was proposed as the rate-determining step for all the cyclic ligands. Ring-size and macrocyclic effects are associated with the final steps of complex formation and parallel the dissociation rate constants, which vary from 2.6 for [12]aneS$_4$ to $4.5 \times 10^4 sec^{-1}$ for open-chain ligands (*92*). The relationship between these Cu-thioether complexes and the blue copper proteins has been discussed (*12, 95, 99, 121, 181*).

The ESR spectrum of $[Ni([14]aneS_4)]^{2+}$ doped with ^{63}Cu shows $g_{\parallel} = 2.087, g_{\perp} = 2.026$ with $A_{\parallel} = 172 \times 10^{-4}, A_{\perp} = 45 \times 10^{-4}$ cm^{-1} (*82*). The complexation of Cu(II) by water-soluble hydroxy-functionalized thioether macrocycles has also been reported (*163*).

The solvent extraction of Ag(I) by [14]aneS$_4$ and related ligands has been described (*68, 155, 186, 187, 189, 190, 199, 203, 204, 205*); in organic media, the formation of $[Ag([14]aneS_4)]^+$ and $[Ag([14]aneS_4)_2]^+$ has been proposed (*205*). Complexes of stoichiometry $[Ag([14]aneS_4)]^+$ and $[Ag_2([14]aneS_4)]^+$ have been isolated (*203, 205*). Successful extraction of Ag(I) from binary and quaternary mixtures of Ag(I) and other metal ions has been achieved except for mixtures containing Hg(II) (*155*); in addition, silver was extracted from copper ore with 80% recovery (*155*).

The synthesis and structure of the Cu(I) complex $[Cu(L^1)_2]^+$ (L^1 = 2, 5, 8-trithia[9](2, 5)thiophenophane (see Fig. 2) has been reported (*138*). The complex shows that each macrocycle acts as a bidentate ligand to a tetrahedral Cu(I) center, Cu–S = 2.359(3), 2.307(3) Å, and 2.392(3), 2.301(3) Å, and that the thiophene S-donors remain nonbonding (*138*). The related Cu(II) complex $[CuCl_2(L^1)]_2$ is dimeric with two bridging Cl$^-$ ions: Cu–Cl = 2.321(3), 2.702(3) Å. Each Cu(II) center is octahedral and is bound to two thioether donors, Cu–S = 2.349(3), 2.358(3) Å; one thiophene S-donor, Cu–S = 3.014(4) Å; and a terminal Cl$^-$, Cu–Cl = 2.234(3) Å (*139*). A series of related Ag(I) and Au(I) complexes have been prepared (*137*).

J. Zinc, Cadmium, and Mercury

The extraction of Cd(II) (*190*) and Hg(II) (*68, 155, 186, 190, 199, 203, 204*) using tetrathia macrocycles has been achieved. The extraction of Hg(II) with [14]aneS$_4$ was found to be particularly efficient with 89.5% recovery; recoveries of Cd(II) and Zn(II) were much smaller: 0.8% and 0.5%, respectively (*68*). Corresponding values for extraction of Cu(I), Cu(II), Ag(I), and Pd(II) were measured as 99.4, 5.9, 99.9, and 14.3%, respectively; the recovery of Class a and Class ab metal ions such as Na(I), Mg(II), Mn(II), Co(II), Ni(II), Zn(II), or Tl(I) was less than 1% in each case (*68*). The formation constant of $[Hg([14]aneS_4)]^{2+}$ has been measured polarographically as log K = 9.8; this is much smaller than the log K values of 25.5 and 26.4 for the formation of $[Hg(tmc)]^{2+}$ and $[Hg(cyclam)]^{2+}$, respectively (*116*).

Reaction of $HgCl_2$ with [14]aneS$_4$ in CH_3NO_2 affords the dimeric complex $[Hg_2Cl_4([14]aneS_4)]$, the single-crystal X-ray structure of which shows (Fig. 66) two tetrahedral Hg(II) centers each bound to two

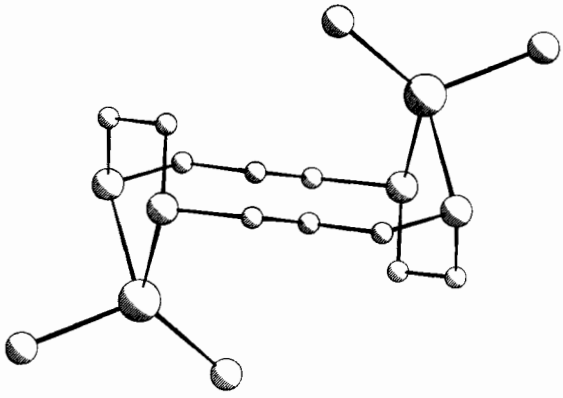

FIG. 66. $[Hg_2Cl_4([14]aneS_4)]$.

Cl^- ions, Hg–Cl = 2.407(3), 2.419(3) Å, and to two S-donors of the macrocycle, Hg–S = 2.580(2), 2.699(2) Å (*6*, *7*). The mononuclear complex $[Hg(OH_2)([14]aneS_4)]^{2+}$ (Fig. 67) shows a square pyramidal stereochemistry with all four S-donors of the macrocycle bound to Hg(II), Hg–S = 2.51(5)–2.71(4), Hg–O = 2.35(4) Å (*7*).

The single-crystal X-ray structure of $[HgI_2([14]aneS_4)]$ shows HgI_2 units bridging $[14]aneS_4$ molecules to give a chain structure. The $[14]aneS_4$ rings act as double, monodentate ligands with the tetrahedral Hg(II) centers bound to two I^- and two thioether S-donors: Hg–S = 2.752(3) Å, Hg–I = 2.653(2), 2.669(2) Å (*100*).

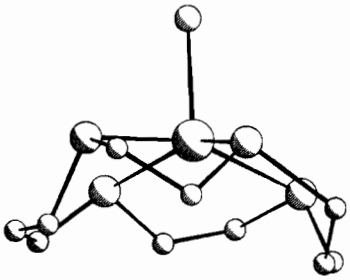

FIG. 67. $[Hg(OH_2)([14]aneS_4)]^{2+}$.

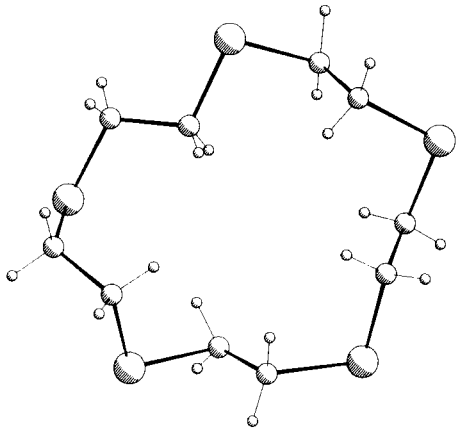

FIG. 68. [15]aneS$_5$.

V. [15]aneS$_5$ and Related Pentathia Ligands

A. FREE LIGANDS

The single-crystal X-ray structure of [15]aneS$_5$ (Fig. 68) shows the molecule to adopt an *exo* conformation with the S-atoms pointing out of the macrocyclic ring (*224*).

The template synthesis of Bz[15]aneS$_5$ about a [Fe(CO)$_2$] fragment has been described (*192*).

The single-crystal X-ray structure of L^3 (L^3 = 2, 5, 9, 12-tetrathia[13](2, 5)thiophenophane (see Fig. 2) shows all the S-donors to lie in exocyclic positions. Thus, although the cavity of L^3 is relatively large (ca. 4.8 × 8.0 Å), coordination of metal ions in an *endo* manner appears to be inhibited (*139*). Complexation of metal ions by L^3 even in an *exo* manner occurs via conformational change of the ligand (*139*).

B. RHENIUM

Reaction of [ReBr(CO)$_5$] with [15]aneS$_5$ affords the neutral complex [ReBr(CO)$_3$([15]aneS$_5$)] (Fig. 69) in which [15]aneS$_5$ is bidentate to the Re(I) center: Re–S = 2.477(4), 2.493(4) Å; Re–Br = 2.602(2) Å; Re–C = 1.900(14), 1.916(15), 1.928(15) Å (*36*).

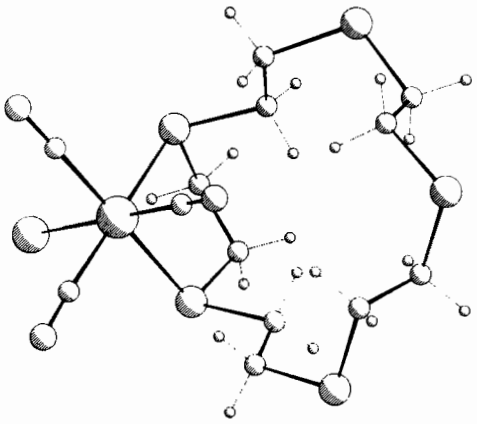

FIG. 69. $[ReBr(CO)_3([15]aneS_5)]$.

C. PALLADIUM AND PLATINUM

Reaction of $[15]aneS_5$ with MCl_2 affords the complexes $[M([15]aneS_5)]^{2+}$ [M = Pd (*27*), Pt (*28*)]. The single-crystal X-ray structure of $[Pd([15]aneS_5)]^{2+}$ shows (Fig. 70) a distorted trigonal bipyramidal stereochemistry: Pd–S = 2.278(8), 2.294(12), 2.336(11), 2.532(11), 2.540(11) Å (*27*). In contrast, the coordination in $[Pt([15]aneS_5)]^{2+}$ (Fig. 71) is closer to square-based pyramidal: Pt–S_{eq} = 2.283(7), 2.301(8), 2.306(7), 2.309(7) Å; Pt···S_{ap} = 2.894(9) Å (*28*).

Ring-opening reactions of $[Pd([15]aneS_5)]^{2+}$ are discussed in Section III,E.

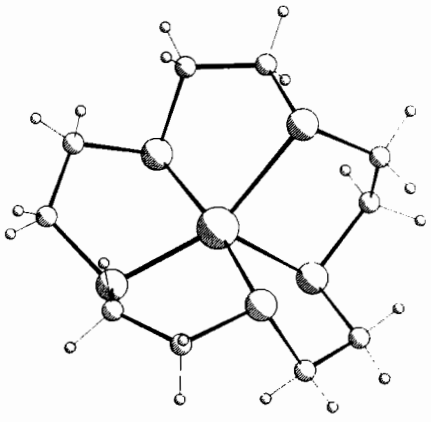

FIG. 70. $[Pd([15]aneS_5)]^{2+}$.

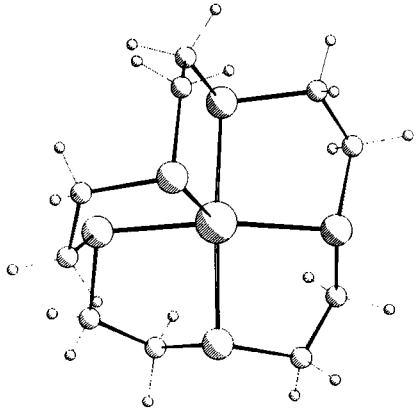

FIG. 71. $[Pt([15]aneS_5)]^{2+}$.

D. COPPER

The complexation of Cu(II) and Cu(I) with $[15]aneS_5$ has been investigated (*76, 95, 180, 181*). The single-crystal X-ray structure of $[Cu([15]aneS_5)]^{2+}$ (Fig. 72) shows a square-based pyramidal stereochemistry, $Cu–S_{eq}$ = 2.289(2), 2.315(2), 2.331(2), 2.338(2) Å; $Cu–S_{ap}$ = 2.398(2) Å, with the Cu atom 0.41 Å out of the basal plane (*76*).

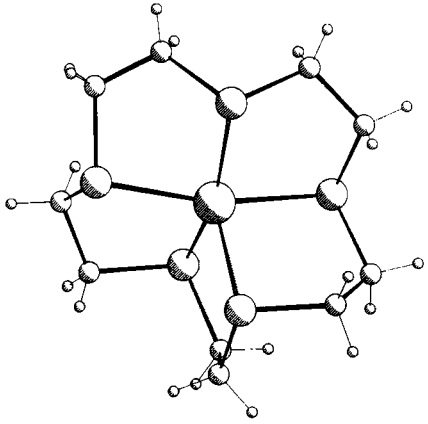

FIG. 72. $[Cu([15]aneS_5)]^{2+}$.

The Cu(II) complex $[Cu([15]aneS_5)]^{2+}$ is highly redox-labile, affording $[Cu([15]aneS_5)]^{+}$ (Fig. 73) in which the Cu(I) center has a distorted tetrahedral geometry: Cu–S = 2.243(5), 2.245(5), 2.317(5), 2.338(5) Å; the fifth S-donor is nonbonding and is disordered over two sites in the solid-state structure, Cu···S = 3.442(12) and 3.560(11) Å (*76*).

The self-exchange electron-transfer rate constant for $[Cu([15]aneS_5)]^{2+/+}$ has been determined as 3×10^4 $M^{-1}sec^{-1}$, which is the largest value determined for any low molecular weight Cu(II)/(I) system apart from $[CuCl_4]^{2-/3-}$ (*76*).

Formation and dissociation rate constants for $[Cu([15]aneS_5)]^{2+}$ have been measured and compared to related tetrathia macrocyclic complexes (*92, 180, 207, 232*). The effect of $[15]aneS_5$ on the configurational stability and reactivity of a cyclopropylcopper complex has been monitored (*215*).

The synthesis and single-crystal X-ray structure of $[CuCl_2(L^3)]_2$ (L^3 = 2, 5, 9, 12-tetrathia[13](2, 5)thiophenophane) (see Fig. 2) shows a trigonal bipyramidal stereochemistry at each Cu(II) center. The Cu(II) ions are bridged by two Cl^- ions, Cu–Cl = 2.661(4), 2.277(4) Å; two thioether donors of L^3, Cu–S = 2.355(5), 2.358(4) Å, and a terminal Cl^-, Cu–Cl = 2.265(4) Å, complete the coordination at the metal centers (*139*). Significantly, the thiophene S-donors are nonbonding; this contrasts with the structure of $[CuCl_2(L^1)]_2$, which shows bonding thiophene S-donors to distorted octahedral Cu(II) centers (*139*).

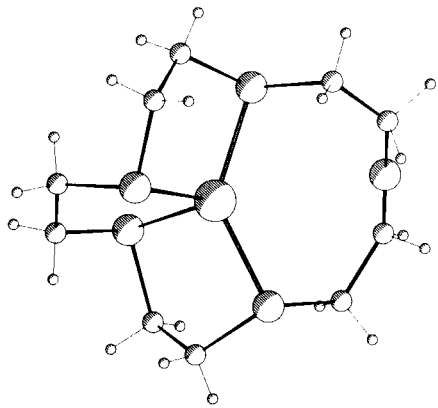

FIG. 73. $[Cu([15]aneS_5)]^{+}$.

VI. [18]aneS$_6$ and Related Hexathia Ligands

A. Free Ligands

The single-crystal X-ray structure of [18]aneS$_6$ (Fig. 74) shows four of the six S atoms *exo*dentate and the remaining two *endo*dentate (*114, 224*). This contrasts with the structures of smaller ring homoleptic thioether macrocycles (apart from [9]aneS$_3$), which show exclusively *exo*dentate S atoms. All the C–S bonds in [18]aneS$_6$ adopt gauche configurations; in contrast, 10 of the 12 C–O bonds in [18]aneO$_6$ lie in anti placements (*224*). The difference in 1, 4-interactions in C–C–X–C and X–C–C–X (X = O, S) is an important factor in controlling the configuration of metal-free cyclic thioethers and oxyethers (*224*).

[18]aneS$_6$ shows antioxidant properties in the stabilization of natural rubber and is a better deactivator than [14]aneS$_4$ (*105*).

Sellmann and co-workers have reported the template synthesis of Bz$_2$[18]aneS$_6$ (*191, 192*) (see Scheme 5, Section II). The structure of the metal-free ligand (Fig. 75) shows all the S-donors lying *exo* to the macrocyclic ring, and four out of 12 C–S bonds in anti configurations (*192*).

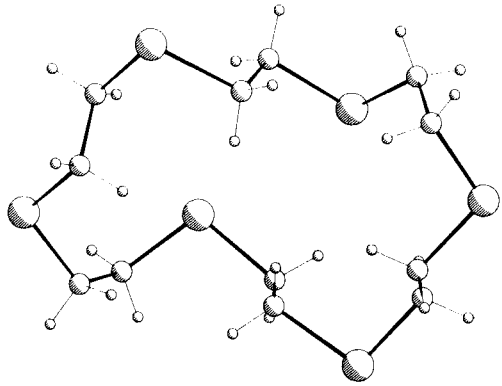

FIG. 74. [18]aneS$_6$.

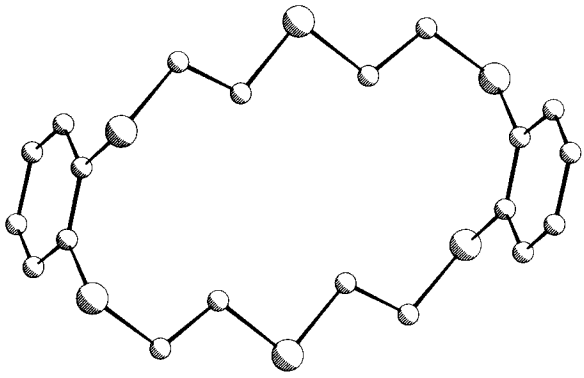

FIG. 75. $Bz_2[18]aneS_6$.

B. NIOBIUM

Reaction of $[NbCl_5]$ with $[24]aneS_6$ affords products of stoichiometry $[(NbCl_5)_x][24]aneS_6$ ($x = 3, 6$) (*89*).

C. MOLYBDENUM AND TUNGSTEN

Reaction of $[M(CO)_6]$ (M = Mo, W) with $[18]aneS_6$ affords the complexes $[Mo(CO)_3([18]aneS_6)]$, $[Mo(CO)_3]_2[18]aneS_6$, and $[W(CO)_4]_2[18]aneS_6$. Oxidation of $[Mo(CO)_3([18]aneS_6)]$ or $[Mo(CO)_3]_2[18]aneS_6$ with I_2 affords $[MoI_2(CO)_3]_2[18]aneS_6$ (*200*). Reaction of $[MoCl_3(THF)_3]$ with $[18]aneS_6$ gives the Mo(III) species $[MoCl_3([18]aneS_6)]$; ring-opening reactions of the coordinated hexathia ligand to form coordinated vinyl thioether products were proposed (*202*). In addition, the high-valent Mo(VI)/(V)/(IV) complexes $[MoO_2Cl_2]_2[18]aneS_6$, $[MoOCl_3]_2[18]aneS_6$, and $[MoCl_4]_2[18]aneS_6$ have been isolated (*201*).

D. IRON, RUTHENIUM, AND OSMIUM

Sellman and co-workers have synthesized $Bz_2[18]aneS_6$ *via* template synthesis around Fe(II) (see Scheme 5, Section II) (*191, 192*).

Reaction of $RuCl_3 \cdot 3H_2O$ with $[18]aneS_6$ in DMF/methanol affords $[Ru([18]aneS_6)]^{2+}$, the single-crystal X-ray structure of which shows (Fig. 76) a *meso* configuration with hexathia coordination at Ru(II),

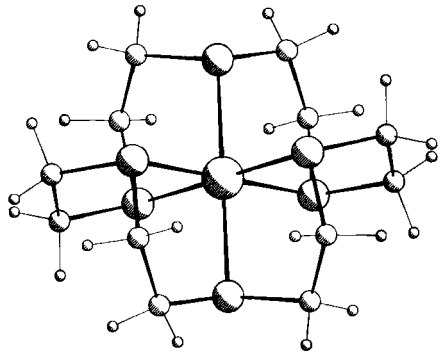

FIG. 76. $[Ru([18]aneS_6)]^{2+}$.

Ru–S = 2.3222(23), 2.3326(25), 2.3373(23) Å (*17*). Reaction of $[Ru(Me_2SO)_6]^{2+}$ with $[20]aneS_6$ affords $[Ru([20]aneS_6)]^{2+}$ (*172*).

Reaction of $[MCl_2(arene)]_2$ with $[18]aneS_6$ affords the binuclear complexes $[M_2Cl_2(arene)([18]aneS_6)]^{2+}$ (M = Ru, arene = C_6H_6, C_6Me_6, 4-$MeC_6H_4{}^iPr$; M = Os, arene = 4-$MeC_6H_4{}^iPr$), in which $[18]aneS_6$ acts as a bridging ligand, bidentate to each Ru(II) center (*14, 188*).

E. COBALT, RHODIUM, AND IRIDIUM

Black and McLean reported the synthesis of $[M([18]aneS_6)]^{2+}$ (M = Co, Ni) in 1969 (*21, 22*). The single-crystal X-ray structure of $[Co([18]aneS_6)]^{2+}$ shows (Fig. 77) a tetragonally elongated octahedral stereochemistry, Co–S = 2.251(1), 2.292(1), 2.479(1) Å (*112, 113*). The complex is a low-spin Co(II) species, μ_{eff} = 1.8 BM, and shows an ESR

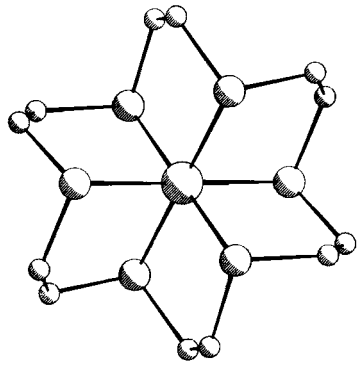

FIG. 77. $[Co([18]aneS_6)]^{2+}$.

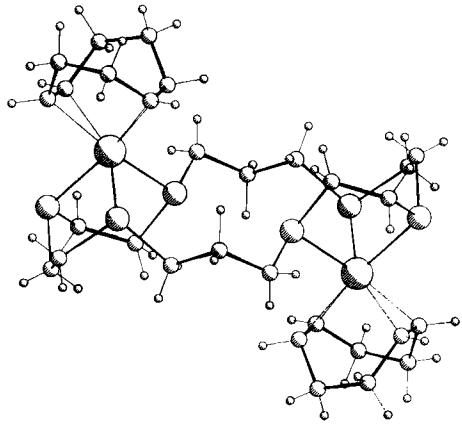

FIG. 78. $[Rh_2(COD)_2([20]aneS_6)]^{2+}$.

spectrum with $g_{\parallel} = 2.05$, $g_{\perp} = 2.14$, $A_{\perp} = 0.70$ cm^{-1} as a frozen glass at 77 K in nitromethane/toluene (*112, 113*). The $[Co([18]aneS_6)]^{2+/3+}$ couple is observed at $E_{1/2} = +0.844$ V vs. NHE, compared to a value of $E_{1/2} = +0.680$ V vs. NHE for the $[Co([9]aneS_3)_2]^{2+/3+}$ couple, indicating an increased stabilization of Co(II) with [18]aneS$_6$ (*113*).

Reaction of $RhCl_3$ with [18]aneS$_6$ affords a product assigned as $[RhCl_2([18]aneS_6)]^+$ (*51*). Treatment of $[RhCl(COD)]_2$ with [20]aneS$_6$ affords an unusual dimeric complex $[Rh_2(COD)_2([20]aneS_6)]^{2+}$ (Fig. 78), which shows *exo* coordination of three thioether donors to each Rh(I) center, Rh–S = 2.320(1), 2.462(1), 2.482(1) Å (*177*).

Reaction of $[M(C_5Me_5)Cl_2]_2$ (M = Rh, Ir) with [18]aneS$_6$ affords the binuclear complexes $[M_2(C_5Me_5)_2Cl_2([18]aneS_6)]^{2+}$; the single-crystal structure of $[Rh_2(C_5Me_5)_2Cl_2([18]aneS_6)]^{2+}$ shows (Fig. 79) [18]aneS$_6$

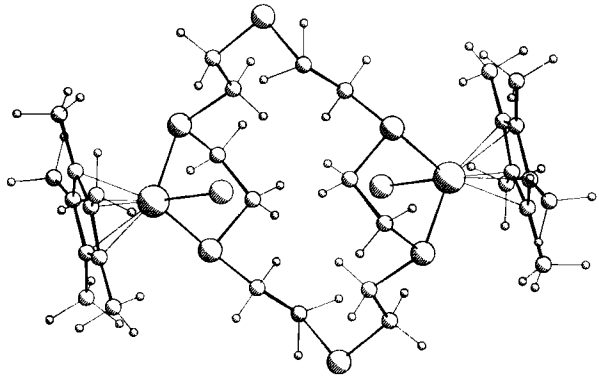

FIG. 79. $[(Rh_2(C_5Me_5)_2Cl_2([18]aneS_6)]^{2+}$.

bridging two $[RhCl(C_5Me_5)]^+$ moieties with two S-donors bound to each Rh(III) center: Rh–S = 2.3645(9), 2.3766(9) Å; Rh–Cl = 2.3869(9) Å (*14, 19, 188*).

Ring-opening reactions to form $[Rh([18]aneS_6\text{-}H)]^{2+}$ have been observed (*176*).

F. Nickel, Palladium, and Platinum

Reaction of Ni(II) salts with L [L = $[18]aneS_6$ (*21, 22, 75, 115*), $[24]aneS_6$ (*75, 171*)] affords the complexes $[Ni(L)]^{2+}$. The single-crystal X-ray structure of the centrosymmetric cation $[Ni([18]aneS_6)]^{2+}$ shows (Fig. 80) a *meso* configuration with hexathia coordination at Ni(II): Ni–S = 2.377(1), 2.389(1), 2.397(1) Å (*75, 115*). In contrast, the structure of $[Ni([24]aneS_6)]^{2+}$ shows (Fig. 81) a *rac* configuration with increased Ni–S bond lengths: Ni–S = 2.413(1), 2.437(1), 2.443(1) Å (*75, 171*). For $[Ni([18]aneS_6)]^{2+}$ $10Dq$ = 12, 290 cm^{-1}; for $[Ni([24]aneS_6)]^{2+}$ $10Dq$ = 11,050 cm^{-1} (*75*).

Insertion of Pd(II) into $[18]aneS_6$ gives the diamagnetic complex cation $[Pd([18]aneS_6)]^{2+}$ (*33*). The single-crystal X-ray structure of brown $[Pd([18]aneS_6)](BPh_4)_2$ shows (Fig. 82) equatorial coordination of four thioether donors, $Pd\text{–}S_{eq}$ = 2.3067(15), 2.3114(14) Å, with the two remaining thioether donors involved in long-range interactions with Pd(II) at apical positions, $Pd\cdots S_{ap}$ = 3.2730(17) Å (*33*). Interestingly, $[Pd([18]aneS_6)](PF_6)_2$ (Fig. 83) is green in the solid state and shows a different structure to the BPh_4^- salt with $Pd\text{–}S_{eq}$ = 2.3347(18) Å, $Pd\cdots S_{ap}$ = 3.0154(25) Å (*27*). Another important difference between the two structures is that in $[Pd([18]aneS_6)](PF_6)_2$ the methylene chains are mutually eclipsed, whereas in $[Pd([18]aneS_6)](BPh_4)_2$ these chains are staggered (*27*).

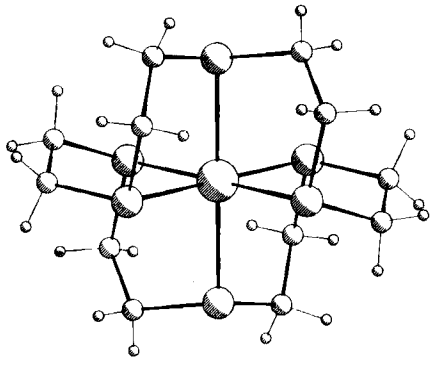

FIG. 80. $[Ni([18]aneS_6)]^{2+}$.

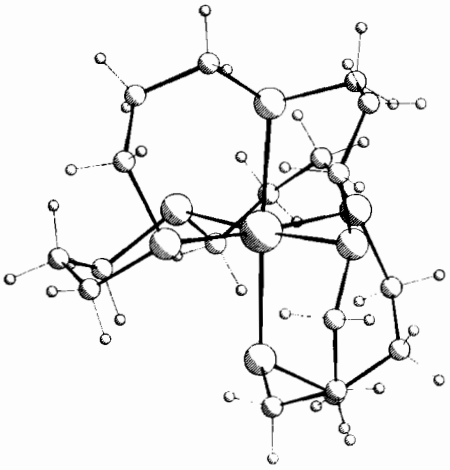

FIG. 81. $[Ni([24]aneS_6)]^{2+}$.

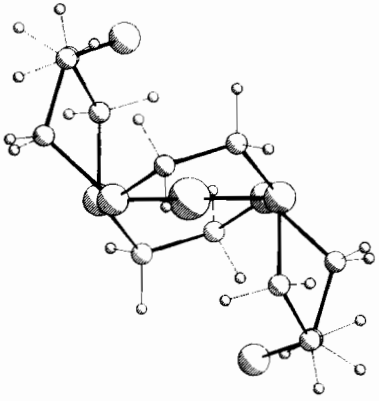

FIG. 82. $[Pd([18]aneS_6)]^{2+}$ as found in brown BPh_4^- salt.

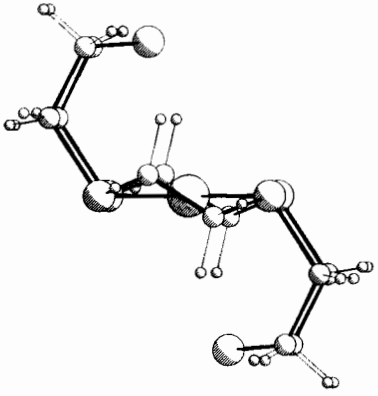

FIG. 83. $[Pd([18]aneS_6)]^{2+}$ as found in green PF_6^- salt.

Unlike $[Pd([9]aneS_3)_2]^{2+}$, $[Pd([18]aneS_6)]^{2+}$ does not show any clear oxidative process by cyclic voltammetry in CH_3CN. However, $[Pd([18]aneS_6)]^{2+}$ can be oxidized *slowly* using chemical oxidants to afford the mononuclear, paramagnetic Pd(III) complex, $[Pd([18]aneS_6)]^{3+}$ (Fig. 84), which shows a tetragonally elongated octahedral stereochemistry: $Pd-S_{eq}$ = 2.3506(23), 2.3593(23) Å; $Pd-S_{ap}$ = 2.5229(24) Å (*27*); therefore, on going from $[Pd([18]aneS_6)]^{2+}$ to $[Pd([18]aneS_6)]^{3+}$ the $Pd-S_{ap}$ distances shorten from 3.0154(25) to 2.5229(24) Å, consistent with the increase in nuclear charge at the metal center and the preferred stereochemistry for d^7 metal centers. The bond lengths for $[Pd([18]aneS_6)]^{3+}$ are marginally shorter than in the related $[Pd([9]aneS_3)_2]^{3+}$ cation, which shows $Pd-S_{eq}$ = 2.3558(14), 2.3692(15) Å; $Pd-S_{ap}$ = 2.5448(15) Å (*27, 42*).

Liquid-liquid extraction of Pd(II) with $[18]aneS_6$ has been reported (*120, 189*).

The single-crystal X-ray structure of $[Pt([18]aneS_6)](BPh_4)_2$ shows a coordination geometry similar to $[Pd([18]aneS_6)](BPh_4)_2$: $Pt-S_{eq}$ = 2.2948(24), 2.2980(25) Å; $Pt\cdots S_{ap}$ = 3.380(3) Å (*28, 33*).

Ring-opening reactions of $[M([18]aneS_6)]^{2+}$ (M = Pd, Pt) are discussed in Section III,E.

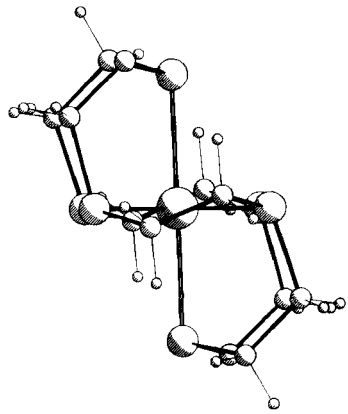

FIG. 84. $[Pd([18]aneS_6)]^{3+}$.

G. Copper and Silver

Insertion of Cu(II) into [18]aneS$_6$ affords the hexathia species [Cu([18]aneS$_6$)]$^{2+}$, the single-crystal X-ray structure of which shows (Fig. 85) a *meso* configuration for the complex with a tetragonally elongated octahedral stereochemistry, Cu–S = 2.323(1), 2.402(1), 2.635(1) Å (*111*). The ESR spectrum of [Cu([18]aneS$_6$)]$^{2+}$ shows $g_x = 2.028$, $g_y = 2.035$, $g_z = 2.119$, $A_{\parallel} = 0.0153\ cm^{-1}$, $A\perp = 0.0019\ cm^{-1}$ as a frozen glass in nitromethane/toluene at 77 K. The [Cu([18]aneS$_6$)]$^{2+/+}$ couple is observed at $E_{1/2} = +0.72$ V vs. SCE in CH_3NO_2; the related [Cu([9]aneS$_3$)$_2$]$^{2+/+}$ couple is observed at $E_{1/2} = +0.61$ V. vs. SCE under the same conditions (*111*).

Reduction of [Cu([18]aneS$_6$)]$^{2+}$ affords the corresponding Cu(I) complex [Cu([18]aneS$_6$)]$^{+}$, the single-crystal X-ray structure of which confirms (Fig. 86) a distorted tetrahedral stereochemistry at the metal center, Cu–S = 2.245(2), 2.253(2), 2.358(2), 2.360(2) Å (*111*). The two remaining S-donors are not bound to the Cu(I) center. The interconversion of Cu(II) and Cu(I) within the coordination sphere of [18]aneS$_6$ occurs, therefore, *via* rapid Cu–S bond-breaking and -making between six- and four-coordinate complexes (*111*); related redox/stereochemical interconversion between [Cu([15]aneS$_5$)]$^{2+/+}$ has been observed (*76*).

The binuclear Cu(I) complex [Cu$_2$(NCCH$_3$)$_2$([18]aneS$_6$)]$^{2+}$ has been prepared (*108*); the single-crystal X-ray structure of this complex shows (Fig. 87) each tetrahedral Cu(I) center bound to three S-donors of the macrocycle, Cu–S = 2.3200(15), 2.3250(15), 2.3415(16) Å; and to one

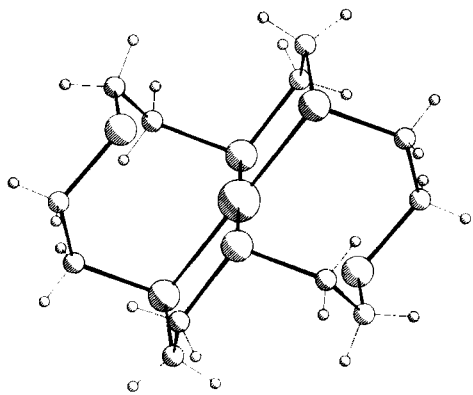

Fig. 85. [Cu([18]aneS$_6$)]$^{2+}$.

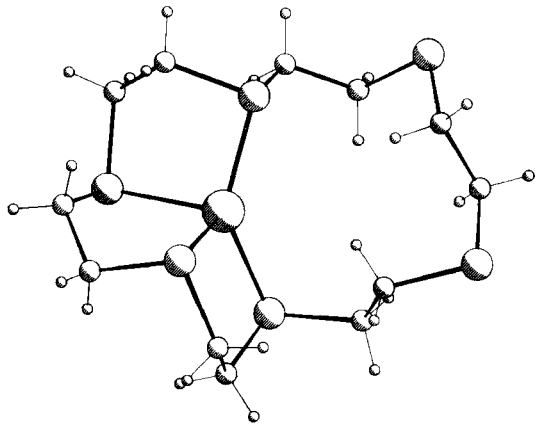

FIG. 86. $[Cu([18]aneS_6)]^+$.

$NCCH_3$ molecule, Cu–N = 1.939(5) Å (*108*). The Cu···Cu distance is 4.25 Å. A long-range interaction with a fourth S-donor, Cu···S = 3.32 Å, distorts the coordination at Cu(I) toward trigonal bipyramidal (*32, 108*).

The extraction of Cu(II) and Cu(I) with $[18]aneS_6$ has been reported (*189*), and the effect of $[18]aneS_6$ on the configurational stability and reactivity of a cyclopropylcopper complex has been monitored (*215*).

Reaction of $AgNO_3$ with $[18]aneS_6$ affords $[Ag([18]aneS_6)]^+$, which shows (Fig. 88) Ag(I) bound to six thioether donors of $[18]aneS_6$ in a tetragonally compressed stereochemistry, Ag–S = 2.6665(12),

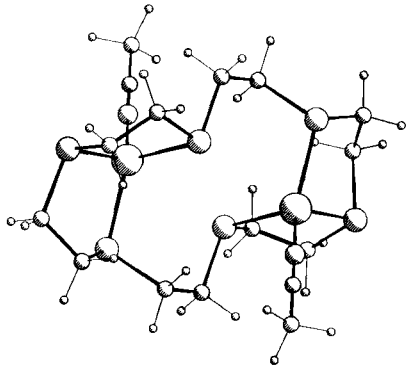

FIG. 87. $[Cu_2(NCCH_3)_2([18]aneS_6)]^{2+}$.

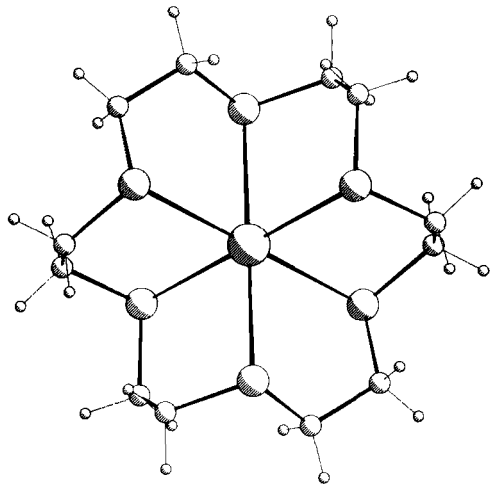

FIG. 88. $[Ag([18]aneS_6)]^+$.

2.7813(10) Å (*31*). Oxidation of this species affords an Ag(II) species that is stabilized under acidic conditions (*31*). The extraction of Ag(I) with [18]aneS$_6$ has been achieved (*119, 203, 206*); species incorporating Ag : [18]aneS$_6$ ratios of 1 : 1 (*189, 206*), 2 : 1, and 3 : 1 (*203, 206*) have been isolated.

H. MERCURY

The extraction of Hg(II) with [18]aneS$_6$ has been reported; complexes incorporating Hg : [18]aneS$_6$ ratios of 1 : 1 and 2 : 1 have been isolated (*203, 206*).

I. LEAD

The extraction of Pb(II) with [18]aneS$_6$ has been investigated (*119*).

VII. [24]aneS$_8$, [28]aneS$_8$, and Related Octathia Ligands

Very little coordination chemistry of these large-ring ligands has been reported. Products incorporating Nb(V) (*89*), Ni(II) (*209*), Pd(II) (*209*), Cu(II) (*61*), Ag(I) (*186, 205*), and Hg(II) (*186*) have been described;

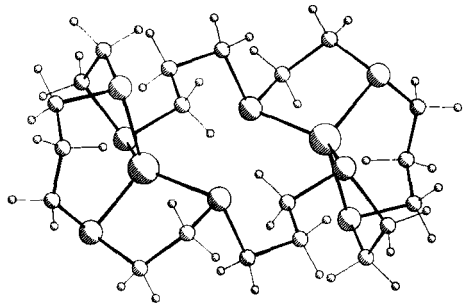

FIG. 89. $[Cu_2([28]aneS_8)]^{2+}$.

however, none of these complexes have been characterized unambiguously.

Recently, the reaction of $[Cu(NCCH_3)_4]^+$ with $[28]aneS_8$ has been shown to afford the binuclear Cu(I) complex $[Cu_2([28]aneS_8)]^{2+}$ (Fig. 89), in which each Cu(I) is bound tetrahedrally to four S-donors of the macrocycle Cu–S = 2.268(5), 2.278(5), 2.328(5), 2.333(5) Å, with a Cu···Cu separation of 6.454(4) Å (*53*).

VIII. Abbreviations

$[9]aneS_3$: 1, 4, 7-trithiacyclononane
$[12]aneS_3$: 1, 5, 9-trithiacyclododecane
$[12]aneS_4$: 1, 4, 7, 10-tetrathiacyclododecane
$[13]aneS_4$: 1, 4, 7, 10-tetrathiacyclotridecane
$[14]aneS_4$: 1, 4, 8, 11-tetrathiacyclotetradecane
$[15]aneS_4$: 1, 4, 8, 12-tetrathiacyclopentadecane
$[16]aneS_4$: 1, 5, 9, 13-tetrathiacyclohexadecane
$[15]aneS_5$: 1, 4, 7, 10, 13-pentathiacyclopentadecane
$[18]aneS_6$: 1, 4, 7, 10, 13, 16-hexathiacyclooctadecane
$[20]aneS_6$: 1, 4, 7, 11, 14, 17-hexathiacycloeicosane
$[24]aneS_6$: 1, 5, 9, 13, 17, 21-hexathiacyclotetracosane
$[24]aneS_8$: 1, 4, 7, 10, 13, 16, 19, 22-octathiacyclotetracosane
$[28]aneS_8$: 1, 4, 8, 11, 15, 18, 22, 25-octathiacyclooctacosane
$Bz[9]aneS_3$: 2, 3-benzo-1, 4, 7-trithia-2-cyclononaene
$Bz_2[18]aneS_6$: 2, 3, 11, 12-dibenzo-1, 4, 7, 10, 13, 16-hexathia-2, 11-cyclooctadecadiene

ACKNOWLEDGMENTS

We are most grateful to Michael N. Bell, Robert M. Christie, John A. Greig, Malcolm A. Halcrow, Alan J. Holder, Timothy I. Hyde, Aidan J. Lavery, Gillian Reid, Yvonne V. Roberts, Ramesh C. Sharma, and Anne Taylor for their work and dedication. We thank Dr. Robert O. Gould for his invaluable help with numerous crystallographic disorder models. We also thank Professor Karl Wieghardt for many fruitful discussions.

REFERENCES

1. Abel, E. W., Beer, P. D., Moss, I., Orrell, K. G., Sik, V., Bates, P. A., and Hursthouse, M. B., *J. Chem. Soc., Chem. Commun.* 978 (1987).
2. Abel, E. W., Beer, P. D., Moss, I., Orrell, K. G., Sik, V., Bates, P. A., and Hursthouse, M. B., *J. Organomet. Chem.* **341,** 559 (1988).
3. Adachi, T., Sasaki, N., Ueda, T., Kaminaka, M., and Yoshida, T., *J. Chem. Soc., Chem. Commun.* 1320 (1989).
4. Adman, E. T., Stenkamp, R. E., Sieker, L. C., and Jensen, L. H., *J. Mol. Biol.* **123,** 35 (1978).
5. Alberts, A. H., Annunziata, R., and Lehn, J. M., *J. Am. Chem. Soc.* **99,** 8502 (1977).
6. Alcock, N. W., Herron, N., and Moore, P., *J. Chem. Soc., Chem. Commun.* 886 (1976).
7. Alcock, N.W., Herron N., and Moore, P., *J. Chem. Soc., Dalton Trans.* 394 (1978).
8. Ali, R., Higgins, S. J., and Levason, W., *Inorg. Chim. Acta* **84,** 65 (1984).
9. Ashby, M. T., Enemark, J. H., Lichtenberger, D. L., and Ortega, R. B., *Inorg. Chem.* **25,** 3154 (1986).
10. Ashby, M. T., and Lichtenberger, D. L., *Inorg. Chem.* **24,** 636 (1985).
11. Asmus, K-D., Gillis, H. A., and Teather, G. G., *J. Phys. Chem.* **82,** 2677 (1978).
12. Augustin, M. A., Yandell, J. K., Addison, A. W., and Karlin, K. D., *Inorg. Chim. Acta* **55,** L35 (1981).
13. Beinert, H., *Coord. Chem. Rev.* **33,** 55 (1980).
14. Bell, M. N., Ph.D. Thesis, University of Edinburgh, 1987.
15. Bell, M. N., Blake, A. J., Christie, R. M., Holder, A. J., Hyde, T. I., Schröder, M., and Yellowlees, L. J., unpublished results.
16. Bell, M. N., Blake, A. J., Holder, A. J., Hyde, T. I., Lavery, A. J., Reid, G., and Schröder, M., *J. Inclusion Phenomena* **5,** 169 (1987).
17. Bell, M. N., Blake, A. J., Holder, A. J., Hyde, T. I., and Schröder, M., *J. Chem. Soc., Dalton Trans.*, submitted.
18. Bell, M. N., Blake, A. J., Küppers, H-J., Schröder, M., and Wieghardt, K., *Angew. Chem.* **99,** 253 (1987); *Angew. Chem. Int. Ed. Engl.* **26,** 250 (1987).
19. Bell, M. N., Blake, A. J., Schröder, M., and Stephenson, T. A., *J. Chem. Soc., Chem. Commun.* 471 (1986).
20. Bjerrum, M. J., Gajheda, M., Larsen, E., and Springborg, J., *Inorg. Chem.* **27,** 3960 (1988).
21. Black, D.St.C., and McLean, I. A., *Tetrahedron Lett.* 3961 (1969).
22. Black, D.St.C., and McLean, I. A., *Aust. J. Chem.* **24,** 1401 (1971).
23. Blake, A. J., Christie, R. M., Hyde, T. I., Schröder, M., and Yellowlees, L. J., unpublished results.

24. Blake, A. J., Crofts, R. D., Reid, G., and Schröder, M., *J. Organomet. Chem.* **357,** 371 (1989).
25. Blake, A. J., Gordon, L. M., Holder, A. J., Hyde, T. I., Reid, G., and Schröder, M., *J. Chem. Soc., Chem. Commun.* 1452 (1988).
26. Blake, A. J., Gould, R. O., Greig, J. A., Holder, A. J., Hyde, T. I., and Schröder, M., *J. Chem. Soc., Chem. Commun.* 876 (1989).
27. Blake, A. J., Gould, R. O., Holder, A. J., Hyde, T. I., Lavery, A. J., Reid, G., and Schröder, M., *J. Chem. Soc., Dalton Trans.*, submitted.
28. Blake, A. J., Gould, R. O., Holder, A. J., Hyde, T. I., Lavery, A. J., Reid, G., and Schröder, M. *J. Chem. Soc., Dalton Trans.*, submitted.
29. Blake, A. J., Gould, R. O., Holder, A. J., Hyde, T. I., Odulate, M. O., Lavery, A. J., and Schröder, M., *J. Chem. Soc., Chem. Commun.* 118 (1987).
30. Blake, A. J., Gould, R. O., Holder, A. J., Hyde, T. I., and Schröder, M., *J. Chem. Soc., Dalton Trans.* 1861 (1988).
31. Blake, A. J., Gould, R. O., Holder, A. J., Hyde, T. I., and Schröder, M., *Polyhedron* **8,** 513 (1989).
32. Blake, A. J., Gould, R. O., Holder, A. J., Lavery, A. J., and Schröder, M., *Polyhedron.*, submitted.
33. Blake, A. J., Gould, R. O., Lavery, A. J., and Schröder, M., *Angew. Chem.* **98,** 282 (1986); *Angew. Chem. Int. Ed. Engl.* **25,** 274 (1986).
34. Blake, A. J., Greig, J. A., Holder, A. J., Hyde, T. I., Taylor, A., and Schröder, M., *Angew. Chem.*, in press.
35. Blake, A. J., Greig, J. A., and Schröder, M., *J. Chem. Soc., Dalton Trans.*, submitted.
36. Blake, A. J., Greig, J. A., and Schröder, M., unpublished results.
37. Blake, A. J., Halcrow, M. A., and Schröder, M., unpublished results.
38. Blake, A. J., Halcrow, M. A., and Schröder, M., unpublished results.
39. Blake, A. J., Holder, A. J., Hyde, T. I., Küppers, H-J., Schröder, M., Stötzel, S., and Wieghardt, K., *J. Chem. Soc., Chem. Commun.* 1600 (1989).
40. Blake, A. J., Holder, A. J., Hyde, T. I., Reid, G., and Schröder, M., *Polyhedron* **8,** 2041 (1989).
41. Blake, A. J., Holder, A. J., Hyde, T. I., Roberts, Y. V., Lavery, A. J., and Schröder, M., *J. Organomet. Chem.* **323,** 261 (1987).
42. Blake, A. J., Holder, A. J., Hyde, T. I., and Schröder, M., *J. Chem. Soc., Chem. Commun.* 987 (1987).
43. Blake, A. J., Holder, A. J., Hyde, T. I., and Schröder, M., *J. Chem. Soc., Chem. Commun.* 1433 (1989).
44. Blake, A. J., Holder, A. J., Hyde, T. I., Reid, G., and Schröder, M., *J. Chem. Soc., Dalton Trans.*, in press.
45. Blake, A. J., Holder, A. J., Reid, G., and Schröder, M., unpublished results.
46. Blake, A. J., Holder, A. J., Roberts, Y. V., and Schröder, M., *Acta Crystallogr., Sect. C* **44,** 360 (1988).
47. Blake, A. J., Holder, A. J., Roberts, Y. V., and Schröder, M., unpublished results.
48. Blake, A. J., Holder, A. J., Taylor, A., and Schröder, M., *J. Chem. Soc., Chem. Commun.*, submitted.
49. Blake, A. J., Hyde, T. I., and Schröder, M., unpublished work.
50. Blake, A. J., Gould, R. O., Reid, G., and Schröder, M., *J. Organomet. Chem.* **356,** 389 (1988).
51. Blake, A. J., Reid, G., and Schröder, M., *J. Chem. Soc., Dalton Trans.* 1675 (1989).
52. Blake, A. J., Roberts, Y. V., and Schröder, M., unpublished results.
53. Blake, A. J., Taylor, A., and Schröder, M., unpublished results.

54. Blower, P. J., and Cooper, S. R., *Inorg. Chem.* **26,** 2009 (1987).
55. Boeyens, J. C. A., Forbes, A. G. S., Hancock, R. D., and Wieghardt, K., *Inorg. Chem.* **24,** 2926 (1985).
56. Borgen, G., Dale, J., Anet, F. A. L., and Krone, J., *J. Chem. Soc., Chem. Commun.* 243 (1974).
57. Bradshaw, J. S., and Hui, J. Y., *J. Heterocycl. Chem.* **11,** 649 (1974).
58. Bradshaw, J. S., Hui, J. Y., Haymore, B. L., Izatt, R. M., and Christensen, J. J., *J. Heterocycl. Chem.* **10,** 1 (1973).
59. Bradshaw, J. S., Hui, J. Y., Haymore, B. L., Izatt, R. M., and Christensen, J. J., *J. Heterocycl. Chem.* **11,** 45 (1974).
60. Bradshaw, J. S., and Stott, P. E., *Tetrahedron* **36,** 461 (1980).
61. Braithwaite, A. C., Rickard, C. E. F., and Waters, T. N., *Aust. J. Chem.* **34,** 2665 (1981).
62. Buter, J., and Kellogg, R. M., *J. Chem. Soc., Chem. Commun.* **466** (1980).
63. Buter, J., and Kellogg, R. M., *J. Org. Chem.* **46,** 4481 (1981).
64. Carothers, W. H., *J. Amer. Chem. Soc.* **51,** 2458, 2560 (1929).
65. Carothers, W. H., *J. Amer. Chem. Soc.* **52,** 314, 711, 3292 (1930).
66. Carothers, W. H., *J. Amer. Chem. Soc.* **55,** 5023, 5031 (1933).
67. Chaudhuri, P., and Wieghardt, K., "Progress in Inorganic Chemistry," (S. J. Lippard, ed.) vol. 35, p. 329. Wiley, New York, 1987.
68. Chayama, K., and Sekido, E., *Anal. Sci.* **3,** 535 (1987).
69. Chen, B., Li, Y., Yang, J., and Peng, Q., *Huaxue Xuebao* **42,** 701; *Chemical Abstracts,* **101,** 183147z (1984).
70. Christie, R. M., Ph.D. Thesis, University of Edinburgh, 1989.
71. Clarkson, J. A., Yagbasan, R., Blower, P. J., and Cooper, S. C., *J. Chem. Soc., Chem. Commun.* 1244 (1989).
72. Clarkson, J. A., Yagbasan, R., Blower, P. J., Rawle, S. C., and Cooper, S. R., *J. Chem. Soc., Chem. Commun.* 950 (1987).
73. Collman, P. M., Freeman, H. C., Guss, J. M., Murata, V. A., Norris, V. A., Ramshaw, J. A. M., and Venkatappa, M. P., *Nature* (London) **272,** 319 (1978).
74. Cooper, S. R., *Acc. Chem. Res.* **21,** 141 (1988).
75. Cooper, S. R., Rawle, S. C., Hartman, J. R., Hintsa, E. J., and Admans, G. A., *Inorg. Chem.* **27,** 1209 (1988).
76. Corfield, P. W. R., Ceccarelli, C., Glick, M. D., Moy, I. W-Y., Ochrymovycz, L. A., and Rorabacher, D. B., *J. Am. Chem. Soc.* **107,** 2399 (1985).
77. Cragel J. Jr., Pett, V. B., Glick, M. D., and DeSimone, R. E., *Inorg. Chem.* **17,** 2885 (1978).
78. Crumbie, R. L., and Ridley, D. D., *Aust. J. Chem.* **32,** 2777 (1979).
79. Dabrowiak, J. C., Merrell, P. H., Stone, J. A., and Busch, D. H., *J. Am. Chem. Soc.* **95,** 6613 (1973).
80. For definition of nomenclature see: Dale, J., *Acta Chem. Scand.* **27,** 1115 (1973).
81. Dalley, N. K., Smith, J. S., Larson, S. B., Matheson, K. L., Christensen, J. J., and Izatt, R. M., *J. Chem. Soc., Chem. Commun.* 84 (1975).
82. Davis, P. H., White, P. L., and Bedford, R. L., *Inorg. Chem.* **14,** 1753 (1975).
83. DeSimone, R. E., Albright, M. J., Kennedy, W. J., and Ochrymovycz, L. A., *Org. Magn. Res.* **6,** 583 (1974).
84. DeSimone, R. E., Cragel J. Jr., Ilsley, W. H., and Glick, M. D., *J. Coord. Chem.* **9,** 167 (1979).
85. DeSimone, R. E., and Glick, M. D., *J. Am. Chem. Soc.* **97,** 942 (1975).
86. DeSimone, R. E., and Glick, M. D., *J. Am. Chem. Soc.* **98,** 762 (1976).

87. DeSimone, R. E., and Glick, M. D., *J. Coord. Chem.* **5,** 181 (1976).
88. DeSimone, R. E., and Glick, M. D., *Inorg. Chem.* **17,** 3574 (1978).
89. DeSimone, R. E., and Tighe, T. M., *J. Inorg. Nucl. Chem.* **38,** 1623 (1976).
90. Deutsch, E., Libson, K., Jurisson, S., and Lindoy, L. F., *Progr. Inorg. Chem.* **30,** 75 (1983).
91. Diaddario, L. L., Jr., Dockal, E. R., Glick, M. D., Ochrymowycz, L. A., and Rorabacher, D. B., *Inorg. Chem.* **24,** 356 (1985).
92. Diaddario, L. L., Zimmer, L. L., Jones, T. E., Sokol, L. S. W. L., Cruz, R. B., Yee, E. L., Ochrymowycz, L. A., and Rorabacher, D. B., *J. Am. Chem. Soc.* **101,** 3511 (1979).
93. Dietrich, B., Lehn, J. M., and Sauvage, J. P., *J. Chem. Soc., Chem. Commun.* 1055 (1970).
94. Dockal, E. R., Diaddario, L. L., Glick, M. D., and Rorabacher, D. B., *J. Am. Chem. Soc.* **99,** 4530 (1977).
95. Dockal, E. R., Jones, T. E., Sokol, W. F., Engerer, R. J., and Rorabacher, D. B., *J. Am. Chem. Soc.* **98,** 4322 (1976).
96. Down, J. L., Lewis, J., Moore, B., and Wilkinson, G., *J. Chem. Soc.* 3767 (1959).
97. Dunitz, J. D., and Shearer, H. M. M., *Helv. Chim. Acta* **43,** 18 (1960).
98. Elias, H., Schmidt, G., Küppers, H-J., Saher, M., Wieghardt, K., Nuber, B., and Weiss, J., *Inorg. Chem.* **28,** 3021 (1989).
99. Ferris, N. S., Woodruff, W. H., Rorabacher, D. B., Jones, T. E., and Ochrymowycz, L. A., *J. Am. Chem. Soc.* **100,** 5939 (1978).
100. Galešić, N., Herceg, M., and Sevdić, D., *Acta Crystallogr., Sect. C.* **C42,** 565 (1986).
101. Gerber, D., Chongsawangvirod, P., Leung, A. K., and Ochrymowycz, L. A., *J. Org. Chem.* **42,** 2644 (1977).
102. Glass, R. S., Wilson, G. S., and Setzer, W. N., *J. Am. Chem. Soc.* **102,** 5068 (1980).
103. Glick, M. D., Gavel, D. P., Diaddario, L. L., and Rorabacher, D. B., *Inorg. Chem.* **15,** 1190 (1976).
104. Goh, S. H., *Polym. Degred. Stab.* **8,** 123 (1984).
105. Goh, S. H., Lee, S. Y., and Seah, C. L., *Thermochimica Acta* **126,** 149 (1988).
106. Gokel, G. W., and Korzeniowski, S. H., "Macrocyclic Polyether Syntheses," Springer-Verlag, Berlin, 1982.
107. Gorewit, B. V., and Murker, W. K., *J. Coord. Chem.* **5,** 67 (1976).
108. Gould, R. O., Lavery, A. J., and Schröder, M., *J. Chem. Soc., Chem. Commun.* 1492 (1985).
109. Guss, J. M., and Freeman, H. C., *J. Mol. Biol.* **169,** 521 (1983).
110. Hancock, R. D., and Martell, A. E., *Comments Inorg. Chem.* **6,** 237 (1988).
111. Hartman, J. R., and Cooper, S. R., *J. Am. Chem. Soc.* **108,** 1202 (1986).
112. Hartman, J. R., Hintsa, E. J., and Cooper, S. R., *J. Chem. Soc., Chem. Commun.* 386 (1984).
113. Hartman, J. A., Hintsa, E. J., and Cooper, S. R., *J. Am. Chem. Soc.* **108,** 1208 (1986).
114. Hartman, J. R., Wolf, R. E., Foxman, B. M., and Cooper, S. R., *J. Am. Chem. Soc.* **105,** 131 (1983).
115. Hintsa, E. J., Hartman, J. R., and Cooper, S. R., *J. Am. Chem. Soc.* **105,** 3738 (1983).
116. Hojo, M., Hagiwara, M., Nagai, H., and Imai, Y., *J. Electroanal. Chem.* **234,** 251 (1987).
117. Holder, A. J., Ph.D. Thesis, University of Edinburgh, 1987.
118. Holder, A. J., Schröder, M., and Stephenson, T. A., *Polyhedron* **6,** 461 (1987).
119. Izatt, R. M., Clark, G. A., and Christensen, J. J., *Sep. Sci. Technol.* **21,** 865 (1986).

120. Izatt, R. M., Eblerhardt, L., Clark, G. A., Bruening, R. L., Bradshaw, J. S., Cho, M. H., and Christensen. J. J., *Sep. Sci. Technol.* **22,** 701 (1987).
121. Jones, T. E., Rorabacher, D. B., and Ochrymowycz, L. A., *J. Am. Chem. Soc.* **97,** 7485 (1975).
122. Jones, T. E., Zimmer, L. L., Diaddario, L. L., Rorabacher, D. B., and Ochrymowycz, L. A., *J. Am. Chem. Soc.* **97,** 7163 (1975).
123. Kahn, O., Morgenstern-Badaru, I., Audiere, J. P., and Lehn, J. P., *J. Am. Chem. Soc.* **102,** 5935 (1980).
124. Karlin, K. D., and Zubieta, J., *Inorg. Perspect. Biol. Med.* **2,** 127 (1979).
125. Kuehn, C. G., and Isied, S. S., *Prog. Inorg. Chem.* **27,** 153 (1980).
126. Küppers, H-J., and Wieghardt, K., *Polyhedron* 8, 1770 (1989).
127. Küppers, H-J., Neves, A., Pomp, C., Ventur, D., Wieghardt, K., Nuber, B., and Weiss, J., *Inorg. Chem.* **25,** 2400 (1986).
128. Küppers, H-J., Wieghardt, K., Nuber, B., and Weiss, J., *Z. Anorg. Allg. Chem.* In press (1989).
129. Küppers, H-J., Wieghardt, K., Nuber, B., Weiss, J., Bill, E., and Trautwein, A. X., *Inorg. Chem.* **26,** 3762 (1987).
130. Küppers, H-J., Wieghardt, K., Steenken, S., Nuber, B., and Weiss, J., *Z. Anorg. Allgem. Chem.*, in press.
131. Küppers, H-J., Wieghardt, K., Tsay, Y-H., Krüger, C., Nuber, B., and Weiss, J., *Angew. Chem.* **99,** 583 (1987); *Angew. Chem. Int. Ed. Engl.* **26,** 575 (1987).
132. Lai, T-F., and Poon, C-K., *J. Chem. Soc., Dalton Trans.* 1465 (1982).
133. Lancaster, J. R., Ed. "The Bioinorganic Chemistry of Nickel," VCH Publishers, New York, 1988.
134. Lemke, W. D., Travis, K. E., Takvoryan, N. E., and Busch, D. H., *Adv. Chem. Ser.* **150,** 358 (1977).
135. Leszczynski, J., Nowek, A., and Koziol, J., *Seventh School on Biophysics of Membrane Transport* **2,** 267, Poland (May 4–13, 1984).
136. Li, Y., Wang, D., Wu, L., Luo, S., and Yang, J., *Huaxue Xuebao* **42,** 313 (1984).; *Chemical Abstracts* **101,** 72076f (1984).
137. Lucas, C. M., and Shuang, L., Third American Congress of North America, Toronto, posters INOR 308 and 536, June 1988.
138. Lucas, C. M., Shuang, L., Newlands, M. J., Charland, J-P., and Gabe, E. J., *Can. J. Chem.* **66,** 1506 (1988).
139. Lucas, C. M., Shuang, L., Newlands, M. J., Charland, J-P., and Gabe, E. J., *Can. J. Chem.* **66,** 639 (1989).
140. Margerum, D. W., and Smith, G. F., *J. Chem. Soc., Chem. Commun.* 807 (1975).
141. McAuley, A., Whitcombe, T. W., and Hunter, G., *Inorg. Chem.* **27,** 2634 (1988).
142. McAuliffe, C. A., *in* "Comprehensive Co-ordination Chemistry" (G. Wilkinson, R. D. Gillard, and J. A. McCleverty, eds.) Vol. 2, pp. 989–1066. Pergamon Press, Oxford, 1987.
143. McAuliffe, C. A., and Levason, W., "Phosphine, Arsine and Stibine Complexes of Transition Elements." Elsevier, Amsterdam, 1979.
144. McAuliffe, C. A., Werfali, A., Hill, W. E., and Minahan, D. M. A., *Inorg. Chim. Acta* **60,** 87 (1982).
145. McCormick, D. B., Griesser, R., and Sigel, H., *Met. Ions Biol. Syst.* **1,** 213 (1973).
146. Meadow, J. R., and Reid, E. E., *J. Am. Chem. Soc.* **56,** 2177 (1934).
147. Montaudo, G., Scamporrino, E., Puglisi, C., and Vitalini, D., *J. Polym. Sci. Polym. Symp.* **74,** 285 (1986).
148. Müller, A., and Diemann, E., *in* "Comprehensive Co-ordination Chemistry" (G.

Wilkinson, R. D. Gillard, and J. A. McCleverty, eds.), Vol. 2, pp. 551–558. Pergamon Press, Oxford, 1987.
149. Murray, S. G., and Hartley, F. R., *Chem. Rev.* **81,** 365 (1981).
150. Newkome, G. R., Sauer, J. D., Roper, J. M., and Hager, D. C., *Chem. Rev.* **77,** 513 (1977).
151. Ochrymowycz, L. A., Mak, C-K., and Mincha, J. D., *J. Org. Chem.* **14,** 2079 (1974).
152. Okazaki, R., Takai, H., O-oka, M., and Inamato, T. L., *Tetrahedron Letts.* **23,** 4973 (1982).
153. Olmstead, M. M., Kessler, R. M., Hope, H., Yanuck, M. D., and Musker, W. K., *Acta Crystallogr., Sect. C* **43,** 1890 (1987).
154. Orpen, A. G., and Connelly, N. G., *J. Chem. Soc., Chem. Commun.* 1310 (1985).
155. Oue, M., Kimura, K., and Shono, T., *Analytica Chim. Acta* **194,** 293 (1987).
156. Pauling, L., "The Nature of the Chemical Bond," 3rd ed. pp. 260. Cornell University Press, Ithaca, New York, 1960.
157. Pedersen, C. J., *J. Am. Chem. Soc.* **89,** 2495 (1967).
158. Pedersen, C. J., *J. Am. Chem. Soc.* **89,** 7071 (1967).
159. Pedersen, C. J., *J. Am. Chem. Soc.* **92,** 386 (1970).
160. Pedersen, C. J., *J. Am. Chem. Soc.* **92,** 391 (1970).
161. Pedersen, C. J., *J. Org. Chem.* **36,** 254 (1971).
162. Pedersen, C. J., *J. Org. Chem.* **36,** 1690 (1971).
163. Pett, V. B., Leggett, G. H., Cooper, T. H., Reed, P. R., Situmeang, D., Ochrymowycz, L. A., and Rorabacher, D. B., *Inorg. Chem.* **27,** 2164 (1988).
164. Pomp, C., Drüeke, S., Küppers, H-J., Wieghardt, K., Krüger, C., Nuber, B., and Weiss, J., *Z. Naturforsch. B.* **43,** 299 (1988).
165. Poon, C-K., and Che, C-M., *J. Chem. Soc., Dalton Trans.* 756 (1980).
166. Poon, C-K., and Che, C. M., *J. Chem. Soc., Dalton Trans.* 495 (1981).
167. Poon, C-K., Kwong, S-S., Che, C-M., and Kon, Y-P., *J. Chem. Soc., Dalton Trans.* 1457 (1982).
168. Poonia, N. S., *J. Am. Chem. Soc.* **96,** 1012 (1974).
169. Rawle, S. C., Admans, G. A., and Cooper, S. R. *J. Chem. Soc., Dalton Trans.* 93 (1988).
170. Rawle, S. C., and Cooper, S. R., *J. Chem. Soc., Chem. Commun.* 308 (1987).
171. Rawle, S. C., Hartman, J. R., Watkins, D. J., and Cooper, S. R., *J. Chem. Soc., Chem. Commun.* 1083 (1986).
172. Rawle, S. C., Sewell, T. J., and Cooper, S. R., *Inorg. Chem.,* **26,** 3769 (1987).
173. Rawle, S. C., Yagbasan, R., Prout, K., and Cooper, S. R., *J. Am. Chem. Soc.* **109,** 6181 (1987).
174. Ray, P. C., *J. Chem. Soc.* **123,** 2174 (1923).
175. Reinen, D., Ozarowski, A., Jakob, B., Pebler, J., Stratemeier, H., Wieghardt, K., and Tolksdorf, I., *Inorg. Chem.* **26,** 4010 (1987).
176. Reid, G., Ph.D. Thesis, University of Edinburgh, 1989.
177. Riley, D. P., and Oliver, J. D., *Inorg. Chem.* **22,** 3361 (1983).
178. Robinson, G. H., and Sangokoya, S. A., *J. Am. Chem. Soc.* **110,** 1494 (1988).
179. Robinson, G. H., Zhang, H., and Atwood, J. L., *Organometallics,* **6,** 887 (1987).
180. Rorabacher, D. B., Bernado, M. M., Vande Linde, A. M. Q., Leggett, G. H., Westerby, B. C., Martin, M. J., and Ochrymowycz, L. A., *Pure Appl. Chem.* **60,** 501 (1988).
181. Rorabacher, D. B., Martin, M. J., Koenigbauer, M. J., Malik, M., Schroeder, R. R., Endicott, J. F., and Ochrymowycz, L. A., *in* "Copper Co-ordination Chemistry: Biochemical and Inorganic Perspectives" (K. D. Karlin and J. Zubieta, eds.). p. 167. Adenine Press, New York, 1983.
182. Rosen, W., and Busch, D. H., *J. Chem. Soc., Chem. Commun.* 148 (1969).

183. Rosen, W., and Busch, D. H., *J. Am. Chem. Soc.* **91,** 4694 (1969).
184. Rosen, W., and Busch, D. H., *Inorg. Chem.* **9,** 262 (1970).
185. Rydel, L., and Lundgren, J. O., *Nature (London)* **261,** 344 (1976).
186. Saito, K., Masudo, Y., and Sekido, E., *Anal. Chim. Acta* **151,** 447 (1983).
187. Saito, K., Masuda, Y., and Sekido, E., *Bull. Chem. Soc. Jpn.* **57,** 189 (1984).
188. Schröder, M., *Pure Appl. Chem.* **60,** 517 (1988).
189. Sekido, E., Kawahara, H., and Tsuji, K., *Bull. Chem. Soc. Jpn.* **61,** 1587 (1988).
190. Sekido, E., Saito, K., Naganuma, Y., and Kumazaki, H., *Anal. Sci.* **1,** 363 (1985).
191. Sellmann, D., and Frank, P., *Angew. Chem.* **98,** 1115 (1986); *Angew. Chem. Int. Ed. Engl.* **25,** 1107 (1986).
192. Sellmann, D., Frank, P., and Knoch, F., *J. Organomet. Chem.* **339,** 345 (1988).
193. Sellmann, D., Knoch, F., and Wronna, C., *Angew. Chem.* **100,** 710 (1988); *Angew. Chem. Int. Ed. Engl.* **27,** 691 (1988).
194. Sellmann, D., and Zapf, L., *Angew. Chem.* **96,** 799 (1984); *Angew. Chem. Int. Ed. Engl.* **23,** 807 (1984).
195. Sellmann, D., and Zapf, L., *J. Organomet. Chem.* **289,** 57 (1985).
196. Sellmann, D., Zapf, L., Keller, J., and Moll, M., *J. Organomet. Chem.* **289,** 71 (1985).
197. Setzer, W. N., Coleman, B. R., Wilson, G. S., and Glass, R. S., *Tetrahedron* **37,** 2743 (1981).
198. Setzer, W. N., Ogle, C. A., Wilson, G. S., and Glass, R. S., *Inorg. Chem.* **22,** 266 (1983).
199. Sevdić, D., *Proc. Int. Solvent Extr. Conf.* **1974 3,** 2733 (1974).
200. Sevdić, D., Curić, M., and Tušek-Božić, Lj., *Polyhedron* **8,** 505 (1989).
201. Sevdić, D., and Fekete, L., *Inorg. Chim. Acta* **57,** 111 (1982).
202. Sevdić, D., and Fekete, L., *Polyhedron* **4,** 1371 (1985).
203. Sevdić, D., Fekete, L., and Meider, H., *J. Inorg. Nucl. Chem.* **42,** 885 (1980).
204. Sevdić, D., Jovanovac, Lj., and Meider-Gorican, H., *Mikrochim. Acta* **2,** 235 (1975).
205. Sevdić, D., and Meider, H., *J. Inorg. Nucl. Chem.* **39,** 1403 (1977).
206. Sevdić, D., and Meider, H., *J. Inorg. Nucl. Chem.* **43,** 153 (1981).
207. Sokol, L. S. W. L., Ochrymowycz, L. A., and Rorabacher, D. B., *Inorg. Chem.* **20,** 3189 (1981).
208. Solomon, E. I., Penfield, K. W., and Wilcox, D. E., *Struct. Bonding (Berlin)* **53,** 1 (1983).
209. Travis, K., and Busch, D. H., *J. Chem. Soc., Chem. Commun.* 1041 (1970).
210. Travis, K., and Busch, D. H., *Inorg. Chem.* **13,** 2591 (1974).
211. Tucker, N. B., and Reid, E. E., *J. Amer. Chem. Soc.* **55,** 775 (1933).
212. Vallee, B. L., and Williams, R. J. P., *Biochemistry* **59,** 498 (1986).
213. Vögtle, F., and Neumann, P., *Synthesis* 85 (1978).
214. Vögtle, E., and Weber, F., "Host Guest Complex Chemistry: Macrocycles." Springer-Verlag, Berlin, 1985.
215. Walborsky, H. M., and Periasamy, M. P., *J. Organomet. Chem.* **179,** 81 (1979).
216. Wieghardt, K., Kleine-Boymann, M., Nuber, B., and Weiss, J., *Inorg. Chem.* **25,** 1309 (1986).
217. Wieghardt, K., Kleine-Boymann, M., Nuber, B., and Weiss, J., *Inorg. Chem.* **25,** 1654 (1986).
218. Wieghardt, K., Küppers, H-J., Raabe, E., and Krüger, C., *Angew. Chem.* **98,** 1136 (1986); *Angew. Chem. Int. Ed. Engl.* **25,** 1101 (1986).
219. Wieghardt, K., Küppers, H-J., and Weiss, J., *Inorg. Chem.* **24,** 3067 (1985).
220. Wieghardt, K., Schmidt, W., Herrman, W., and Küppers, H-J., *Inorg. Chem.* **22,** 2953 (1983).
221. Williams, R. J. P., *J. Mol. Cat.* 1 (1986).

222. Wilson, G. S., Swanson, D. D., and Glass, R. S., *Inorg. Chem.* **25,** 3827 (1986).
223. Wolf, R. E. Jr., Hartman, J. R., Ochrymowycz, L. A., and Cooper, S. R., *Inorg. Synth.*, in press.
224. Wolf, R. E., Hartman, J. R., Storey, J. M. E., Foxman, B. M., and Cooper, S. R., *J. Am. Chem. Soc.* **109,** 4328 (1987) and references therein.
225. Yang, R., and Zompa, L. J., *Inorg. Chem.* **15,** 1499 (1976).
226. Yatsimirskii, K. B., Pavlishchuk, V. V., and Strizhak, P. E., *Zh. Obshch. Khim.* **57,** 2750 (1987); *Chemical Abstracts* **109,** 128976j (1988).
227. Yoshida, T., Adachi, T., Kaminaka, M., Ueda, T., and Higuchi, T., *J. Am. Chem. Soc.* **110,** 4872 (1988).
228. Yoshida, T., Adachi, T., and Ueda, T., *14th International Symposium on Macrocyclic Compounds,* Abstract P77/M, Townsville, Australia, July 1989.
229. Yoshida, T., Adachi, T., Ueda, T., Kaminaka, M., Sasaki, N., Higuchi, T., Aoshima, T., Mega, I., Mizobe, Y., and Hidai, M., *Angew. Chem.* **101,** 1053 (1989); *Angew. Chem. Int. Ed. Engl.* **28,** 1040 (1989).
230. Yoshida, T., Adachi, T., Ueda, T., Watanabe, M., Kaminaka, M., and Higuchi, T., *Angew. Chem.* **99,** 1182 (1987); *Angew. Chem. Int. Ed. Engl.* **26,** 1171 (1987).
231. Yoshida, T., Ueda, T., Adachi, T., Yamamoto, K., Higuchi, T., *J. Chem. Soc., Chem. Commun.* 1137 (1985).
232. Young, I. R., Ochrymowycz, L. A., Rorabacher, D. B., *Inorg. Chem.* **25,** 2576 (1986).